UC Riverside

UC Riverside Electronic Theses and Dissertations

Title

The Role of Locus Coeruleus in Sensory-Related Behaviors

Permalink

https://escholarship.org/uc/item/7j02n291

Author

McBurney-Lin, Jim

Publication Date

2022

Copyright Information

Peer reviewed|Thesis/dissertation

UNIVERSITY OF CALIFORNIA
RIVERSIDE

The Role of Locus Coeruleus in Sensory-Related Behaviors

A Dissertation submitted in partial satisfaction
of the requirements for the degree of

Doctor of Philosophy

in

Neuroscience

by

Jim McBurney-Lin

March 2022

Dissertation Committee:
      Dr. Hongdian Yang, Chairperson
      Dr. Megan Peters
      Dr. Edward Zagha

The Dissertation of Jim McBurney-Lin is approved:

_____

_____

_____

Committee Chairperson

University of California, Riverside

ABSTRACT OF THE DISSERTATION

The Role of Locus Coeruleus in Sensory-Related Behaviors

by

Jim McBurney-Lin

Doctor of Philosophy, Graduate Program in Neuroscience
University of California, Riverside, March 2022
Dr. Hongdian Yang, Chairperson

The locus coeruleus (LC) is a small nucleus situated in the pons of the brainstem,
comprised of less than 20,000 neurons in the adult human brain. Neurons in the LC
broadly innervate the brain and release the neuromodulator norepinephrine (NE) at their
terminal field. NE, a neurotransmitter commonly associated with stress, acts on both
post- and pre-synaptic adrenergic receptors to alter cellular and circuit function. LC
neurons also exhibit distinct morphological and neurochemical differences that contribute
to a heterogeneous cellular distribution within the nucleus. Notably, this heterogeneity in
the LC, as well as heterogeneity in adrenergic receptor distribution, suggests that the LC-
NE system is capable of differential modulation of downstream areas. Accordingly, the
LC-NE system has long been recognized as critical in mediating a wide spectrum of brain
functions ranging from sleep-wake transitions and arousal to higher-order processes such

as attention and learning. Clinically, this modulatory system is implicated in attention-, stress- and anxiety-related disorders, including attention-deficit hyperactivity disorder (ADHD) and post-traumatic stress disorder (PTSD). Decades of research have made tremendous progress toward revealing LC-NE functions, but our knowledge of the fundamental neurobiology underlying how the LC-NE system affects the activity of downstream neurons and modulates behavioral states and cognition is still incomplete.

To bridge these gaps, we present three distinct research questions focused on the role of LC in sensory related behaviors and on the LC-pupil relationship. First, we explore how LC affects whisker sensory perception through bidirectional perturbations of the nucleus during a sensory behavior task. We then assess how LC contributes to behavioral flexibility using electrophysiology and optogenetic perturbations in a novel behavior task. Finally, we test the relationship between LC and pupil diameter, to determine the extent to which pupil can be used as a non-invasive measure of LC spiking in real-time. Together, these research studies help elucidate the involvement of LC in various sensory-related behavioral processes. It is our hope that these findings will further our understanding of the LC, as well as the diseases and disorders associated with this neuromodulatory nucleus.

Acknowledgements

Table of Contents

List of Tables

Chapter 1 - Bidirectional Pharmacological Perturbations of the Noradrenergic System Differentially Affect Tactile Detection

List of Figures

Chapter 1 - Bidirectional Pharmacological Perturbations of the Noradrenergic System Differentially Affect Tactile Detection

Abbreviations:

Adrenergic Receptor (AR)

Afterhyperpolarization (AHP)

Area Under the Curve (AUC)

Attention-Deficit Hyperactivity Disorder (ADHD)

Adrenergic Receptor (AR)

Central Nervous System (CNS)

Channelrhodopsin-2 (ChR2)

Correct Rejection (CR)

Criterion (c)

Detection sensitivity (d')

Dopamine (DA)

Dopamine Beta Hydroxylase (DBH)

False Alarm Rate (FAR)

Hit Rate (HR)

Impulsive (IS)

Intracerebroventricular (i.c.v.)

Intraperitoneal (i.p.)

Locus Coeruleus (LC)

Methylphenidate (MPH)

Norepinephrine/Noradrenergic (NE/NA)

Phopholipase C (PLC)

Prefrontal Cortex (PFC)

Protein Kinase C (PKC)

Reaction Time (RT)

Signal to Noise Ratio (SNR)

Tyrosine Hydroxylase (TH)

Ventral Posteromedial Nucleus (VPM)

General Introduction

The locus coeruleus (LC), translating literally to 'blue spot', was first discovered in the early 1800s. Since then, this small nucleus, numbering in the range of thousands of neurons (~1500 in mice, ~20,000 in humans), has been shown to exhibit a broad, diffuse projection system that releases the majority of norepinephrine (NE) within the central nervous system. Given its broad connectivity, unsurprisingly the LC has also been implicated in a diverse array of CNS functions, including arousal, sensory processing, and attention and goal-directed tasks (Foote et al., 1983; Berridge and Waterhouse, 2003; Waterhouse and Navarra, 2018; Chandler et al., 2019). Correspondingly the LC is also associated with a diverse spectrum of diseases and disorders related to dysfunctions in these cognitive processes (Atzori et al., 2016). Often, interventions for LC-related disorders target the LC-NE system (e.g., attention deficit hyperactive disorder (ADHD), and methylphenidate (MPH), an NE reuptake inhibitor and highly effective ADHD treatment; Arnsten and Dudley, 2005). Additionally, pupil diameter, often used as an indirect readout of LC activity, has recently been utilized as an early indicator of risk for Alzheimer's disease (Kremen et al., 2019). A more complete understanding of this small nucleus will not only pave the way for future research directions, but may also lead to more effective interventions for ailments associated with LC dysfunctions. Although, for the purposes of this dissertation, the scope will be limited primarily towards the LC and its association with the somatosensory system and somatosensory behaviors.

Theories of LC function

It has been suggested that the LC-NE system plays key roles in sensory signal processing to facilitate downstream processes such as decision making and motor response (Foote et al., 1983; Berridge and Waterhouse, 2003; Waterhouse and Navarra, 2018). The adaptive gain theory proposes that the LC is more involved in higher brain functions in such a way that LC phasic activity acts as an attentional filter to selectively promote task-relevant behavior within a given task, and LC tonic activity promotes disengagement from the current task and facilitates exploring alternative behaviors (Aston-Jones and Cohen, 2005). While not mutually exclusive, it has also been suggested that LC phasic responses reorganize the functional network of downstream neurons to allow rapid behavior adaptation and cognitive shifts (Bouret and Sara, 2005; Sara, 2009). Together, these theories largely represent the prevailing view on LC-NE function: *The LC-NE system assists in regulating signal processing to drive behavioral orienting and reorienting to behaviorally relevant stimuli in complex, changing environments.* It is likely that LC executes these functions by interacting with both the bottom-up stream that directly conveys sensory information and the top-down control signals (Sara and Bouret, 2012).

The molecular and anatomical organization of the LC

Early views on LC function proposed that the neuromodulatory system served primarily as a global arousal circuit. This idea stemmed from the observation that LC neurons classically exhibited the broad connectivity, but also due to the small size and

synchronous nature of the nucleus. However, recent works have uncovered evidence that suggests that LC is a heterogeneous neuromodulatory system.

Molecularly, although LC neurons all synthesize and release norepinephrine, there are subpopulations within the nucleus that express a diverse range of receptors and neuropeptides (Schwarz and Luo, 2015; Poe et al., 2020). Additionally, cellular morphologies are not uniform; There are two identified cell types: the larger monopolar and smaller fusiform cells, which exhibit a biased distribution across LC (Swanson, 1976). Anatomically, on the other hand, some LC neurons appear to be organized according to their output target (Simpson et al., 1997; Chandler et al., 2014; Schwarz and Luo, 2015; Schwarz et al., 2015). Accordingly, tracing studies have shown that individual LC neurons may target multiple functionally related areas (Simpson et al., 1997). This, along with the observation that LC neurons projecting to distinct areas exhibit unique phenotypical and electrophysiological characteristics, suggests that subpopulations of LC neurons are responsible for independent functions (Chandler et al., 2014; Schwarz and Luo, 2015; Uematsu et al., 2017; Poe et al., 2020).

A brief overview of adrenergic receptors and NE synaptic effects

There are three main types of adrenergic receptors (AR) in the brain: α_1, α_2 and β, with several subtypes in each family. α_2 ARs have the highest affinity to NE. Presynaptic α_2 functions as an autoreceptor. α_2 ARs are linked to the G_i protein and inhibit the production of cyclic adenosine monophosphate (cAM P). Activating α_2 may increase K^+ conductance and inhibit Ca^{2+} channels. α_1 ARs have a lower affinity to NE, and activate

the G_q pathway to promote phospholipase C (PLC), protein kinase C (PKC) and Ca^{2+} release, and to decrease K^+ conductance. β ARs have the lowest affinity to NE. They activate adenylate cyclase via the G_s pathway. Activating β ARs may decrease K^+ conductance, increase cAMP, enhance hyperpolarization-activated currents and Ca^{2+} currents (Ramos and Arnsten, 2007; Marzo et al., 2009).

The intracellular mechanisms of NE-mediated effects have been mainly examined *in vitro* (McCormick and Prince, 1988; Nicoll et al., 1990; McCormick, 1992a, 1992b). NE can induce both excitatory and inhibitory effects on neuronal activity. The inhibitory hyperpolarization effect is mainly mediated by $α_2$ ARs, due to an increase in K^+ conductance and a decrease in Ca^{2+} currents. NE may cause a small hyperpolarization and block the slow afterhyperpolarization (AHP) through β ARs. Activating β ARs can also depolarize neurons by decreasing K^+ conductance or activating adenylate cyclase. The primary excitatory effect of NE is a slow depolarization via $α_1$-mediated decrease of K^+ currents. Depending on NE concentration, brain regions, cortical layers and AR types, NE mediates diverse effects of glutamatergic and GABAergic signaling (Salgado et al., 2016).

LC-NE modulation of the somatosensory system

In the somatosensory cortex of rats and cats, most studies generally agree that LC-NE activation facilitates the representation of sensory signals by inhibiting spontaneous activity more than sensory-evoked responses, thus effectively enhancing the signal-to-noise ratio (SNR) at the population level. Specifically, local NE administration

(Waterhouse and Woodward, 1980; Waterhouse et al., 1980, 1981; Armstrong-James and Fox, 1983; Warren and Dykes, 1996; Castro-Alamancos and Gulati, 2014) or LC stimulation (Lecas, 2001; Devilbiss and Waterhouse, 2004) inhibits both spontaneous activity and periphery stimuli-evoked responses of the majority of somatosensory cortex neurons (50-80% of sampled population). A smaller population, though, show increased firing rate (10-40%). LC-NE also potentiates sensory- or artificially-evoked inhibitory responses (Waterhouse and Woodward, 1980; Waterhouse et al., 1980). If the evoked activity has a phasic-tonic temporal profile, NE tends to differentially enhance the initial transient phasic component and inhibit the following long-lasting tonic component (Waterhouse and Woodward, 1980; Warren and Dykes, 1996; Waterhouse et al., 1998; Lecas, 2004). In addition, LC-NE activation has been shown to enhance the fidelity of stimulus representation by reducing response latency and jitter (Lecas, 2001, 2004; Devilbiss and Waterhouse, 2004), and making previously unresponsive neurons fire action potentials in the presence of sensory stimuli (sensory gating, Waterhouse et al., 1988; Devilbiss and Waterhouse, 2004, 2011; Vazey et al., 2018). Vazey and colleagues further showed that phasic, but not tonic LC activation facilitates cortical representation of sensory inputs (Vazey et al., 2018), consistent with the idea that LC tonic and phasic activity patterns serve different functions (Berridge and Waterhouse, 2003; Aston-Jones and Cohen, 2005; Bouret and Sara, 2005).

LC-NE modulatory effects vary across different layers of the somatosensory cortex. The general consensus is that inhibition dominates all cortical layers (Waterhouse and Woodward, 1980; Armstrong-James and Fox, 1983; Devilbiss and Waterhouse,

2004), and facilitation is restricted mainly to layer (L) 5 and 6 (Waterhouse and Woodward, 1980; Warren and Dykes, 1996; Waterhouse et al., 1998; Devilbiss and Waterhouse, 2011). However, an overwhelming facilitation in superficial layers and suppression in L4 of cats have been reported (Warren and Dykes, 1996). We think that the documented layer-specific, dose-dependent effects could help understand such differences: facilitation occurs during iontophoresis of low concentrations of NE ([NE], Armstrong-James and Fox, 1983a; Warren and Dykes, 1996), and increasing [NE] either switches the facilitating effect to inhibition, or further potentiates the existing inhibitory action. Armstrong-James and Fox also demonstrated that about 30% of deeper layer neurons can be excited by low [NE] (applying small iontophoretic currents) which readily inhibits superficial layers, and higher [NE] suppresses the majority of neurons located in superficial as well as deeper layers (Armstrong-James and Fox, 1983). In light of these findings, most studies that reported a predominantly inhibitory effect employed high [NE] of 0.5-1.0 M for iontophoresis (e.g., Waterhouse and Woodward, 1980; Waterhouse et al., 1980, 1981). In comparison, facilitation occurs during 0.1 M [NE] administration (e.g., Armstrong-James and Fox, 1983).

Few studies have investigated the role of LC-NE in modulating subcortical regions of the somatosensory pathway. Limited data reveal that local NE microdialysis inhibits both spontaneous activity and whisker-evoked neuronal spiking in the whisker-responsive intermediate layers of the superior colliculus (Bezdudnaya and Castro-Alamancos, 2014). In the whisker-representing ventral posteromedial nucleus (VPM) of the thalamus, LC-NE inhibits spontaneous activity of most neurons (Hirata et al., 2006),

but the primary effect on sensory response is a facilitation (Devilbiss and Waterhouse, 2004; Devilbiss et al., 2006a; Hirata et al., 2006; Devilbiss and Waterhouse, 2011): the net effect is an SNR enhancement, similar to the situation in the cortex. A recent work (Rodenkirch et al., 2019) reported that LC stimulation improves thalamic information transmission in both anesthetized and awake rats, and provided evidence to suggest that this is likely due to LC-NE modulation of the interactions between VPM and the reticular nucleus. By systematically varying LC stimulation parameters, Devilbiss and colleagues found that both the firing rate of individual VPM neurons and their pairwise correlation change non-monotonically with stimulation frequency, despite significant heterogeneity (Devilbiss and Waterhouse, 2004; Devilbiss et al., 2006). They also showed that LC tonic and phasic activation mediate diverse modulatory effects at single-cell, pairwise and ensemble levels in both somatosensory thalamus and cortex (Devilbiss and Waterhouse, 2011). LC phasic stimulation preferentially enhances stronger sensory inputs and produces larger changes in functional connectivity compared with tonic stimulation. Interestingly, when LC is activated by stress-related corticotropin-releasing factor, spontaneous activity is enhanced and evoked response suppressed (Devilbiss et al., 2012), suggesting that abnormally activated LC-NE signaling likely engages different pathways and impairs information processing.

LC-NE modulation of somatosensory-related behavior

Given that LC-NE affects neuronal activity from single-cell to population levels, it is natural to expect that behavioral effects would ensue. For example, if LC-NE

7

specifically facilitates neuronal responses to weak stimuli, it would enhance an animal's ability to perceive peri-threshold sensory inputs. However, to our knowledge only a few studies directly tested LC-NE effects on sensory-related behaviors, and even fewer attempted to link the modulation of neuronal responses to behavioral effects.

One major avenue of investigation is how LC contributes directly to somatosensory perception. In one recent work, rats were trained to perform a Go/NoGo tactile discrimination task, where the Go stimulus is an 8 Hz whisker deflection, and NoGo stimulus is 4 or 6 Hz (Rodenkirch et al., 2019). Optogenetic LC stimulation significantly improves rats' perceptual sensitivity *d'*. Interestingly, LC stimulation produces a larger improvement when the NoGo stimulus is more perceptually similar to the Go stimulus (NoGo vs. Go, 6 vs. 8 Hz, compared with 4 vs. 8 Hz). Behavioral enhancement was abolished by locally blocking NE in the VPM during LC stimulation, in agreement with the electrophysiological findings that LC-NE actions on somatosensory thalamus facilitates information transmission. Yet, the literature still lacks a comprehensive understanding on how bidirectional perturbations contribute to somatosensory perception.

Another key avenue involves the role of locus coeruleus in behavioral flexibility. That is, how the locus coeruleus affects an individual's ability to adapt to environmental changes. As discussed above, the adaptive gain theory posits that LC may be promoting task-relevant behavior. In line with this idea, early evidence demonstrated that LC activity in non-human primates increases when there is a shift in the task rule (i.e. the initial target visual stimulus was replaced with a new target visual stimulus; Aston-Jones

et al., 1997). In more recent work, rats were trained to an initial set of auditory cues, and then their ability to switch to a reversed set of auditory cues was quantified. Pairing the presentation of the reversed cues with optogenetic LC stimulation resulted in a more rapid behavioral switch to adopt the new task-rule (Glennon et al., 2018). Together, these works highlight the role of LC in the sensory cue-behavioral response relationship. However, evidence that directly links LC activity to the magnitude of changes in behavioral response following task-rule changes is lacking.

A brief primer on the LC-pupil relationship

Primarily in human research, pupil diameter has been often used to index LC activity (e.g., Beatty, 1982; Aston-Jones and Cohen, 2005). Pupil diameter has also been found to co-fluctuate with brain states, task performance and sensory neuron activity (Reimer et al., 2014; McGinley et al., 2015a, 2015b; Vinck et al., 2015; Lee and Margolis, 2016; Schriver et al., 2018). Thus, pupil diameter is also widely used to monitor brain states and the underlying neural substrates. A plethora of work has demonstrated that the LC-NE system also closely tracks brain states (e.g., Foote et al., 1980; Berridge and Foote, 1991; Carter et al., 2010; Takahashi et al., 2010; Fazlali et al., 2016), but not until recently had we begun to rigorously test the correlative or even casual relationship between LC activity and pupil dilation (Murphy et al., 2014; Joshi et al., 2016; Reimer et al., 2016; Liu et al., 2017). Unfortunately, how accurately it can be used to directly index LC activity in real-time is not known.

Summary

Over the past decades, significant progress has been made to understand LC-NE functions in intact animal models under anesthesia, during wakefulness, or even in behaving conditions. Nevertheless, very few studies attempt to directly link the modulatory effects at cellular and circuit levels to behavior. As a result, our knowledge of the fundamental neurobiology underlying how the LC-NE system modulates the activity of downstream neurons to affect behavioral states and cognitive processes remains incomplete. To address this, we pair in-vivo electrophysiology, targeted perturbations of LC neurons, and well-controlled whisker-based behavior tasks to establish both correlative and causal relationships between the LC and sensory-related behaviors.

In Chapter 1, we explore how the LC affects whisker sensory perception. We demonstrate that bidirectional perturbations of LC activity differentially alter sensory task performance. Chapter 2 assesses how LC contributes to behavioral flexibility in a novel behavior task. LC spiking exhibits a strong relationship with flexible task performance and activating the LC is sufficient to improve flexible task performance. Finally, in Chapter 3, we test the relationship between the LC and pupil diameter, to determine the extent to which pupil can be used as a non-invasive measure of LC spiking in real-time. We conclude that pupil diameter is only capable of recapitulating the strong, but infrequent bouts of LC spiking. The results from this dissertation will contribute to a more comprehensive understanding of the fundamental neurobiology of the LC.

References

Armstrong-James M, Fox K (1983a) Effects of Ionophoresed Noradrenaline on the Spontaneous Activity of Neurones in Rat Primary Somatosensory Cortex. :541–558.

Armstrong-James M, Fox K (1983b) Effects of ionophoresed noradrenaline on the spontaneous activity of neurones in rat primary somatosensory cortex. J Physiol 335:427–447.

Arnsten AFT, Dudley AG (2005) Methylphenidate improves prefrontal cortical cognitive function through α2 adrenoceptor and dopamine D1 receptor actions: Relevance to therapeutic effects in Attention Deficit Hyperactivity Disorder. Behav Brain Funct 1:1–9.

Aston-Jones G, Cohen JD (2005) AN INTEGRATIVE THEORY OF LOCUS COERULEUS-NOREPINEPHRINE FUNCTION: Adaptive Gain and Optimal Performance. Annu Rev Neurosci 28:403–450

Aston-Jones G, Rajkowski J, Kubiak P (1997) Conditioned responses of monkey locus coeruleus neurons anticipate acquisition of discriminative behavior in a vigilance task. Neuroscience 80:697–715.

Atzori M, Cuevas-olguin R, Esquivel-rendon E, Garcia-oscos F, Salgado-delgado RC, Saderi N, Miranda-morales M, Treviño M, Pineda JC, Salgado H (2016) Locus Ceruleus Norepinephrine Release : A Central Regulator of CNS. 8.

Beatty J (1982) Task-evoked pupillary responses, processing load, and the structure of processing resources. Psychol Bull 91:276–292.

Berridge CW, Foote SL (1991) Effects of Locus Coeruleus Activation on Electroencephalographic Activity in Neocortex and Hippocampus. 385:22–29.

Berridge CW, Waterhouse BD (2003) The locus coeruleus-noradrenergic system: Modulation of behavioral state and state-dependent cognitive processes. Brain Res Rev 42:33–84.

Bezdudnaya T, Castro-Alamancos MA (2014) Neuromodulation of Whisking Related Neural Activity in Superior Colliculus. J Neurosci 34:7683–7695

Bouret S, Sara SJ (2005) Network reset: A simplified overarching theory of locus coeruleus noradrenaline function. Trends Neurosci 28:574–582.

Carter ME, Yizhar O, Chikahisa S, Nguyen H, Adamantidis A, Nishino S, Deisseroth K, de Lecea L (2010) Tuning arousal with optogenetic modulation of locus coeruleus neurons. Nat Neurosci 13:1526–1533

Castro-Alamancos MA, Gulati T (2014) Neuromodulators Produce Distinct Activated States in Neocortex. J Neurosci 34:12353–12367 Available at: http://www.jneurosci.org/cgi/doi/10.1523/JNEUROSCI.1858-14.2014.

Chandler DJ, Gao W-J, Waterhouse BD (2014) Heterogeneous organization of the locus coeruleus projections to prefrontal and motor cortices. Proc Natl Acad Sci 111:6816–6821 Available at: http://www.pnas.org/cgi/doi/10.1073/pnas.1320827111.

Chandler DJ, Jensen P, McCall JG, Pickering AE, Schwarz LA, Totah NK (2019) Redefining Noradrenergic Neuromodulation of Behavior: Impacts of a Modular Locus Coeruleus Architecture. J Neurosci 39:8239–8249.

Devilbiss DM, Page ME, Waterhouse BD (2006a) Locus ceruleus regulates sensory encoding by neurons and networks in waking animals. J Neurosci 26:9860–9872.

Devilbiss DM, Page ME, Waterhouse BD (2006b) Locus Ceruleus Regulates Sensory Encoding by Neurons and Networks in Waking Animals. J Neurosci 26:9860–9872 Available at: http://www.jneurosci.org/cgi/doi/10.1523/JNEUROSCI.1776-06.2006.

Devilbiss DM, Waterhouse BD (2004) The Effects of Tonic Locus Ceruleus Output on Sensory-Evoked Responses of Ventral Posterior Medial Thalamic and Barrel Field Cortical Neurons in the Awake Rat. J Neurosci 24:10773–10785 Available at: http://www.jneurosci.org/cgi/doi/10.1523/JNEUROSCI.1573-04.2004.

Devilbiss DM, Waterhouse BD (2011) Phasic and Tonic Patterns of Locus Coeruleus Output Differentially Modulate Sensory Network Function in the Awake Rat. J Neurophysiol 105:69–87.

Devilbiss DM, Waterhouse BD, Berridge CW, Valentino R (2012) Corticotropin-releasing factor acting at the locus coeruleus disrupts thalamic and cortical sensory-evoked responses. Neuropsychopharmacology 37:2020–2030 Available at: http://dx.doi.org/10.1038/npp.2012.50.

Fazlali Z, Ranjbar-Slamloo Y, Adibi M, Arabzadeh E (2016) Correlation between Cortical State and Locus Coeruleus Activity: Implications for Sensory Coding in Rat Barrel Cortex. Front Neural Circuits 10:1–16 Available at: http://journal.frontiersin.org/Article/10.3389/fncir.2016.00014/abstract.

Foote SL, Aston-Jones G, Bloom FE (1980) Impulse activity of locus coeruleus neurons in awake rats and monkeys is a function of sensory stimulation and arousal (norepinephrine/sleep/neurotransmitters/electrophysiology). Neurobiology 77:3033–3037 Available at: http://www.pnas.org/content/pnas/77/5/3033.full.pdf.

Foote SL, Bloom FE, Aston-Jones G (1983) Nucleus locus ceruleus: new evidence of anatomical and physiological specificity. Physiol Rev 63:844–914.

Glennon E, Carcea I, Martins ARO, Multani J, Shehu I, Svirsky MA, Froemke RC (2018) Locus coeruleus activation accelerates perceptual learning. Brain Res 1709:39–49 Available at: https://doi.org/10.1016/j.brainres.2018.05.048.

Hirata A, Aguilar J, Castro-Alamancos MA (2006) Noradrenergic Activation Amplifies Bottom-Up and Top-Down Signal-to-Noise Ratios in Sensory Thalamus. J Neurosci 26:4426–4436 Available at: http://www.jneurosci.org/cgi/doi/10.1523/JNEUROSCI.5298-05.2006.

Joshi S, Li Y, Kalwani RM, Gold JI (2016) Relationships between Pupil Diameter and Neuronal Activity in the Locus Coeruleus, Colliculi, and Cingulate Cortex. Neuron 89:221–234 Available at: http://dx.doi.org/10.1016/j.neuron.2015.11.028.

Kremen WS, Panizzon MS, Elman JA, Granholm EL, Andreassen OA, Dale AM, Gillespie NA, Gustavson DE, Logue MW, Lyons MJ, Neale MC, Reynolds CA, Whitsel N, Franz CE (2019) Pupillary dilation responses as a midlife indicator of risk for Alzheimer's disease: association with Alzheimer's disease polygenic risk. Neurobiol Aging 83:114–121

Lecas JC (2001) Noradrenergic modulation of tactile responses in rat cortex. Current source-density and unit analyses. Comptes Rendus l'Academie des Sci - Ser III 324:33–44.

Lecas JC (2004) Locus coeruleus activation shortens synaptic drive while decreasing spike latency and jitter in sensorimotor cortex. Implications for neuronal integration. Eur J Neurosci 19:2519–2530.

Lee CR, Margolis DJ (2016) Pupil Dynamics Reflect Behavioral Choice and Learning in a Go/NoGo Tactile Decision-Making Task in Mice. Front Behav Neurosci 10:1–14.

Liu Y, Rodenkirch C, Moskowitz N, Schriver B, Wang Q (2017) Dynamic Lateralization of Pupil Dilation Evoked by Locus Coeruleus Activation Results from Sympathetic, Not Parasympathetic, Contributions. Cell Rep 20:3099–3112 Available at: https://doi.org/10.1016/j.celrep.2017.08.094.

Marzo A, Bai J, Otani S (2009) Neuroplasticity Regulation by Noradrenaline in Mammalian Brain. Curr Neuropharmacol 7:286–295

McCormick DA (1992a) Cellular mechanisms underlying cholinergic and noradrenergic modulation of neuronal firing mode in the cat and guinea pig dorsal lateral geniculate nucleus. J Neurosci 12:278–289.

McCormick DA, Prince D (1988) Noradrenergic modulation of firing pattern in guinea pig and cat thalamic neurons, in vitro. J Neurophysiol 59:978–996.

McCormick DA (1992b) Neurotransmitter actions in the thalamus and cerebral cortex. [Review] [75 refs]. J Clin Neurophysiol 9:212–223.

McGinley MJ, David S V., McCormick DA (2015a) Cortical Membrane Potential Signature of Optimal States for Sensory Signal Detection. Neuron 87:179–192 Available at: http://dx.doi.org/10.1016/j.neuron.2015.05.038.

McGinley MJ, Vinck M, Reimer J, Batista-Brito R, Zagha E, Cadwell CR, Tolias AS, Cardin JA, McCormick DA (2015b) Waking State: Rapid Variations Modulate Neural and Behavioral Responses. Neuron 87:1143–1161 Available at: http://dx.doi.org/10.1016/j.neuron.2015.09.012.

Murphy PR, O'Connell RG, O'Sullivan M, Robertson IH, Balsters JH (2014) Pupil diameter covaries with BOLD activity in human locus coeruleus. Hum Brain Mapp 35:4140–4154.

Nicoll RA, Malenka RC, Kauer JA (1990) Functional comparison of neurotransmitter receptor subtypes in mammalian central nervous system. Physiol Rev 70:513–565.

Poe GR, Foote S, Eschenko O, Johanson JP, Bouret S, Aston- G, Harley CW, Manahan-vaughn D, Weinshenker D, Valentino R, Chandler D, Waterhouse B, Sara SJ (2020) Locus Coeruleus : A New Look at the Blue Spot Anatomy of the LC and its Terminal Fields. Nat Rev Neurosci Available at: http://dx.doi.org/10.1038/s41583-020-0360-9.

Ramos BP, Arnsten AFT (2007) Adrenergic Pharmacology and Cognition: Focus on the Prefrontal Cortex. Pharmacol Ther 113:523–536.

Reimer J, Froudarakis E, Cadwell CR, Yatsenko D, Denfield GH, Tolias AS (2014) Pupil Fluctuations Track Fast Switching of Cortical States during Quiet Wakefulness. Neuron 84:355–362 Available at: http://dx.doi.org/10.1016/j.neuron.2014.09.033.

Reimer J, McGinley MJ, Liu Y, Rodenkirch C, Wang Q, McCormick DA, Tolias AS (2016) Pupil fluctuations track rapid changes in adrenergic and cholinergic activity in cortex. Nat Commun 7:1–7 Available at: http://dx.doi.org/10.1038/ncomms13289.

Rodenkirch C, Liu Y, Schriver BJ, Wang Q (2019) Locus coeruleus activation enhances thalamic feature selectivity via norepinephrine regulation of intrathalamic circuit dynamics. Nat Neurosci 22:120–133 Available at: http://www.nature.com/articles/s41593-018-0283-1.

Salgado H, Treviño M, Atzori M (2016) Layer- and area-specific actions of norepinephrine on cortical synaptic transmission. Brain Res 1641:163–176.

Sara SJ (2009) The locus coeruleus and noradrenergic modulation of cognition. Nat Rev Neurosci 10:211–223.

Sara SJ, Bouret S (2012) Orienting and Reorienting: The Locus Coeruleus Mediates Cognition through Arousal. Neuron 76:130–141 Available at: http://dx.doi.org/10.1016/j.neuron.2012.09.011.

Schriver BJ, Bagdasarov S, Wang Q (2018) Pupil-linked arousal modulates behavior in rats performing a whisker deflection direction discrimination task. J Neurophysiol 120:1655–1670.

Schwarz LA, Luo L (2015) Organization of the locus coeruleus-norepinephrine system. Curr Biol 25.

Schwarz LA, Miyamichi K, Gao XJ, Beier KT, Weissbourd B, Deloach KE, Ren J, Ibanes S, Malenka RC, Kremer EJ, Luo L (2015) Viral-genetic tracing of the input-output organization of a central noradrenaline circuit. Nature 524:88–92.

Simpson KL, Altman DW, Wang L, Kirifides ML, Lin RCS, Waterhouse BD (1997) Lateralization and functional organization of the locus coeruleus projection to the trigeminal somatosensory pathway in rat. J Comp Neurol 385:135–147.

Swanson LW (1976) The locus coeruleus: A cytoarchitectonic, golgi and immunohistochemical study in the albino rat. Brain Res 110:39–56.

Takahashi K, Kayama Y, Lin JS (2010) Locus coeruleus neuronal activity during the sleep-waking cycle in mice. Neuroscience 169:1115–1126

Uematsu A, Tan BZ, Ycu EA, Cuevas JS, Koivumaa J, Junyent F, Kremer EJ, Witten IB, Deisseroth K, Johansen JP (2017) Modular organization of the brainstem noradrenaline system coordinates opposing learning states. Nat Neurosci

Vazey EM, Moorman DE, Aston-Jones G (2018) Phasic locus coeruleus activity regulates cortical encoding of salience information. Proc Natl Acad Sci 115:E9439–E9448 Available at: http://www.pnas.org/lookup/doi/10.1073/pnas.1803716115.

Vinck M, Batista-Brito R, Knoblich U, Cardin JA (2015) Arousal and Locomotion Make Distinct Contributions to Cortical Activity Patterns and Visual Encoding. Neuron 86:740–754 Available at: http://dx.doi.org/10.1016/j.neuron.2015.03.028.

Warren RA, Dykes RW (1996a) Transient and long-lasting effects of iontophoretically

administered norepinephrine on somatosensory cortical neurons in halothane-anesthetized cats. Can J Physiol Pharmacol 74:38–57.

Warren RA, Dykes RW (1996b) Transient and long-lasting effects of iontophoretically administered norepinephrine on somatosensory cortical neurons in halothane-anesthetized cats. Can J Physiol Pharmacol 74:38–57

Waterhouse BD, Moises HC, Woodward DJ (1981a) Alpha receptor-mediated facilitation of somatosensory cortical neuronal responses to excitatory synaptic inputs and iontophoretically applied acetylcholine. Methods 20:907–920.

Waterhouse BD, Moises HC, Woodward DJ (1980) Noradrenergic modulation of somatosensory cortical neuronal responses to lontophoretically applied putative neurotransmitters. Exp Neurol 69:30–49.

Waterhouse BD, Moises HC, Woodward DJ (1981b) Alpha-receptor-mediated facilitation of somatosensory cortical neuronal responses to excitatory synaptic inputs and iontophoretically applied acetylcholine. Neuropharmacology 20:907–920.

Waterhouse BD, Moises HC, Woodward DJ (1998) Phasic activation of the locus coeruleus enhances responses of primary sensory cortical neurons to peripheral receptive field stimulation. Brain Res 790:33–44.

Waterhouse BD, Navarra RL (2018) The locus coeruleus-norepinephrine system and sensory signal processing : A historical review and current perspectives. Brain Res:1–15 Available at: https://doi.org/10.1016/j.brainres.2018.08.032.

Waterhouse BD, Sessler FM, Cheng JT, Woodward DJ, Azizi SA, Moises HC (1988) New evidence for a gating action of norepinephrine in central neuronal circuits of mammalian brain. Brain Res Bull 21:425–432.

Waterhouse BD, Woodward DJ (1980) Interaction of norepinephrine with cerebrocortical activity evoked by stimulation of somatosensory afferent pathways in the rat. Exp Neurol 67:11–34.

Chapter 1 - Bidirectional Pharmacological Perturbations of the Noradrenergic System Differentially Affect Tactile Detection

Jim McBurney-Lin [a,b*], Yina Sun[b*], Lucas S. Tortorelli[b], Quynh Anh T. Nguyen[a,b],

Sachiko Haga-Yamanaka[a,b], Hongdian Yang[a,b]

[a] Neuroscience Graduate Program,

[b] Department of Molecular, Cell and Systems Biology,

University of California, Riverside, CA 92521, USA

* Equal contributions

Abstract

The brain neuromodulatory systems heavily influence behavioral and cognitive processes. Previous work has shown that norepinephrine (NE), a classic neuromodulator mainly derived from the locus coeruleus (LC), enhances neuronal responses to sensory stimuli. However, the role of the LC-NE system in modulating perceptual task performance is not well understood. In addition, systemic perturbation of NE signaling has often been proposed to specifically target the LC in functional studies, yet the assumption that localized (specific) and systemic (non-specific) perturbations of LC-NE have the same behavioral impact remains largely untested.

In this study, we trained mice to perform a head-fixed, quantitative tactile detection task, and administered an α2 adrenergic receptor agonist or antagonist to pharmacologically down- or up-regulate LC-NE activity, respectively. We addressed the outstanding question of how bidirectional perturbations of LC-NE activity affect tactile detection, and tested whether localized and systemic drug treatments exert the same behavioral effects. We found that both localized and systemic suppression of LC-NE

impaired tactile detection by reducing motivation. Surprisingly, while locally activating

LC-NE enabled mice to perform in a near-optimal regime, systemic activation impaired

behavior by promoting impulsivity. Our results demonstrate that localized silencing and

activation of LC-NE differentially affect tactile detection, and that localized and systemic

NE activation induce distinct behavioral changes.

Introduction

The locus coeruleus (LC) is a major source of the neuromodulator norepinephrine

(NE) in mammalian brains. With profuse projections across the central nervous system,

this modulatory circuit has been hypothesized to be critical in mediating a variety of brain

functions and behavior, including sleep-wake transitions, perception, attention, and

learning. The dysfunction of the LC-NE circuit has also been thought to be involved in

several neurological disorders (Arnsten, 2000; Berridge and Waterhouse, 2003; Aston-

Jones and Cohen, 2005; Sara, 2009; Sara and Bouret, 2012; Waterhouse and Navarra,

2018).

We recently proposed that understanding how LC-NE modulates sensory

perception offers a stepping stone toward unraveling its roles in higher cognitive

functions (McBurney-Lin et al., 2019). LC neurons extensively innervate sensory cortical

and subcortical regions, and LC- NE signaling modulates sensory neuron responses to

external stimuli (e.g., Foote et al., 1975; Waterhouse et al., 1980; Heggelund, 1982;

Morrison and Foote, 1986; Simpson et al., 1997; Devilbiss and Waterhouse, 2004;

Manella et al., 2017; Navarra et al., 2017; Rho et al., 2018). LC-NE may also affect

sensory perception through modulating motivation or attention (Berridge and

Waterhouse, 2003; Lee and Dan, 2012; Sara and Bouret, 2012; Thiele and Bellgrove,

2018). To our knowledge, only a limited number of studies have examined LC-NE

influence on perception-related behavior (Doucette et al., 2007; Escanilla et al., 2010;

Martins and Froemke, 2015; Navarra et al., 2017; Rodenkirch et al., 2019). It remains

poorly understood how bidirectional perturbations of LC-NE activity affect perceptual

task performance.

To examine the causal role of a neural circuit, such as the LC-NE, in regulating

behavior, one would perturb this system and assess the subsequent behavioral changes.

Traditional lesion approaches may induce compensatory plasticity changes (Acheson et

al., 1980; Harik et al., 1981; Valentini et al., 2004) and mask the effects specific to LC-

NE. More recent studies employed acute, reversible perturbations including

pharmacological, electrical, chemogenetic, and optogenetic stimulations. Among these

approaches, pharmacology facilitates translational comparison between animal and

human studies. The inhibitory α2 adrenergic receptors (ARs) are highly expressed in the

LC, but only sparsely expressed, if at all, in neighboring brainstem regions (McCune et

al., 1993; Nicholas et al., 1993). Targeting α2 ARs is considered a specific manner to

perturb LC-NE activity (e.g., Neves et al., 2018). Agonizing α2 ARs suppresses LC-NE

signaling by hyperpolarizing LC neurons and reducing NE release in downstream areas

(Cedarbaum and Aghajanian, 1977; Aghajanian and Vandermaelen, 1982; Abercrombie

and Jacobs, 1987; Aghajanian and Wang, 1987; Adams and Foote, 1988; Berridge et al.,

1993; Kalwani et al., 2014). Conversely, antagonists acting on α2 ARs increase LC

neuron excitability and spiking response to stimuli as well as NE release (Cedarbaum and

Aghajanian, 1976; Aghajanian and Vandermaelen, 1982; Raiteri et al., 1983; Rasmussen

and Jacobs, 1986; Simson and Weiss, 1987; Adams and Foote, 1988; Herr et al., 2012).

Human studies have reported that systemically up- or down-regulating NE

signaling (mainly through targeting α2 ARs) affected subjects performing perception-

related tasks (Halliday et al., 1989; Turetsky and Fein, 2002; Gelbard-Sagiv et al., 2018).

Targeting α2 ARs non-specifically (e.g., intraperitoneal – i.p. or intracerebroventricular –

i.c.v., hereafter referred to as "systemic") or specifically (e.g., intra- or peri-LC, hereafter

referred to as "localized") exerts similar changes on LC activity (Aghajanian and

Vandermaelen, 1982; Adams and Foote, 1988; Berridge et al., 1993). However, systemic

perturbations of α2 ARs could induce physiological and behavioral effects that are

different from localized perturbation. Systemic α2 perturbation would likely affect

noradrenergic neurons in the nucleus of the solitary tract (Van Bockstaele et al., 1999;

Kirouac, 2015), as well as many α2-expressing regions in the nervous system (McCune et

al., 1993; Nicholas et al., 1993; Robertson et al., 2013). It should also be noted that α2

ARs are expressed both presynaptically (auto-receptors) and postsynaptically in terminal

fields. Agonizing or antagonizing presynaptic α2 ARs suppresses or enhances NE release,

respectively, and the post- synaptic effects would depend on the specific types of

postsynaptic adrenergic receptors that are activated in terminal fields. In contrast,

agonizing or antagonizing postsynaptic α2 ARs exerts direct inhibitory or excitatory

postsynaptic effects, respectively.

Head-fixed behavior facilitates stimulus control and movement measurement, and allows reliable quantification of different components of perceptual behavior, including detection, discrimination, impulsivity and motivation (Schwarz et al., 2010; Guo et al., 2014). To our knowledge, using well-controlled, quantitative perceptual behavior to examine the effects of localized (specific) and systemic (non-specific) perturbations of LC-NE is lacking.

In the current study, we trained mice to perform a head-fixed, quantitative tactile detection task. We administered an α2 agonist or antagonist to pharmacologically down- or up-regulate LC activity, respectively. We addressed the outstanding question of how bidirectional perturbations of LC activity affect tactile detection, and tested whether localized and systemic drug treatments exert the same behavioral effects.

Results

Mouse behavior fluctuates within single sessions

Mice were trained to perform a head-fixed, Go/NoGo single-whisker detection task, in which mice reported whether they perceived a brief deflection to the right C2 whisker by licking or withholding licking (Figure 1.1a). The performance of well-trained mice fluctuated during single behavior sessions, as reported by others recently (Berditchevskaia et al., 2016). A typical behavior session started with mice licking indiscriminately, resulting in high Hit rate (fraction of Hit trials among Go trials), high Impulsive rate (IS rate, fraction of IS trials among all trials), and low Correct Rejection rate (CR rate, fraction of CR trials among NoGo trials). As the session

proceeded, Hit rate remained high while mice better withheld licking in NoGo trials, increasing Correct Rejection rate. Towards session end, mice licked less in all trials, and Hit and Impulsive rates reached a minimum and Correct Rejection rate reached a maximum (Figure 1.1b). Within sessions, the fluctuations of Impulsive rate were positively correlated with Hit rate, and highly anti-correlated with Correct Rejection rate (Figure 1.2). Using signal detection theory (Green and Swets, 1966), we found that decision bias/criterion (c) increased over time, while detection sensitivity/discriminability (d') exhibited an inverted-U profile (Figure 1.1c). Toward session end, reaction time (RT, latency from stimulus onset to the time of first licking response) increased and lick frequency declined (Figure 1.1e, Figure 1.3). As demonstrated in previous work (e.g., Dickinson and Balleine, 1995; Mayrhofer et al., 2013; Berditchevskaia et al., 2016), these behavioral changes reflect a systematic shift of the motivational states of the mice. To illustrate this shift, we constructed a trajectory of motivational states based on Hit rate and Correct Rejection rate (Figure 1.1g): mice started with an over-motivated/impulsive state (high Hit and Impulsive rates, low Correct Rejection rate and decision bias, and short reaction time), potentially due to being water restricted. As the behavior session progressed, their performance transitioned to a near-optimal regime (high Hit rate, intermediate Correct Rejection rate, high detection sensitivity, and short reaction time). Eventually, mice were much less motivated to perform the task and often disengaged (low Hit and Impulsive rates, high Correct Rejection rate and decision bias, and long reaction time), potentially due to satiety (Figure 1.1f). The collective changes of Hit and Correct Rejection rates led to an inverted-U trajectory of overall performance (Fraction

Correct, Figure 1.1d), which peaked in the middle of a session and declined toward session start and session end. Interestingly, this inverted-U relationship resembles how LC-NE has been hypothesized to modulate task performance (Aston-Jones and Cohen, 2005).

Localized and systemic clonidine treatments similarly impair detection performance

To assess the behavioral effects of suppressing LC activity, we implanted drug delivery cannulas unilaterally in the left LC (contralateral to whisker stimulation) of 6 mice to locally infuse an α2 agonist clonidine (300 nL, 10 mM, 60 nL/min, Figure 1.4a). Cannula placement was verified post-hoc to ensure targeted drug administration to the LC (Figure 1.4b). Clonidine infusion suppressed LC activity, as it reduced c-fos expression in LC neurons (Figure 1.4c). On average, c-fos expression was ~40% lower in the clonidine side compared with the contralateral control side (12.7% vs. 19.5%). This reduction was also significant in individual mice ($p < 0.01$ in 3 out of 4 mice, permutation test; Table 1.1). Saline infusions did not significantly change c-fos expression in the LC ($p > 0.05$ in 2 mice, permutation test. Table 1.3). Drug spread was estimated to be ~400 μm (Figure 1.5, St. Peters et al., 2011). Following clonidine treatments, mice licked less in all trials. As a result, Hit and Impulsive (IS) rates decreased and Correct Rejection (CR) rate increased (Figure 1.4d and e). Later in the session, mice showed a tendency of behavioral recovery and re-engaged in the task (Figure 1.4d, Figure 1.6). Since a typical behavior session in our study lasts 40–50 min, this time course is consistent with diminished clonidine effects after ~30 min (Abercrombie and Jacobs, 1987; Adams and

Foote, 1988; Kalwani et al., 2014). Saline infusions had no effects on behavior (Figure 1.7 and Figure 1.8). In addition, in mice where the drug infusion was outside of LC, we observed minimal behavioral changes (Figure 1.9). 5 mM clonidine did not have a significant influence on tactile detection, but the trend is consistent with a dose-dependent effect (Figure 1.10). Overall, localized clonidine infusions decreased Hit rate, Impulsive rate and detection sensitivity (d'), elevated Correct Rejection rate, reaction time (RT) and decision bias (c), and impaired task performance (Figure 1.4e–g, Figure 1.7). Clonidine treated mice behaved as if they were at the end of normal behavior sessions (Figure 1.4h). Decreased Impulsive rate, increased reaction time and increased decision bias (changes in c are greater than changes in d', 1.20 ± 0.15 vs. 0.61 ± 0.10, P = 0.002, n = 10) are all indicative of a motivational shift (Dickinson and Balleine, 1995; Schwarz et al., 2010; Mayrhofer et al., 2013; Berditchevskaia et al., 2016). Thus, we conclude that reduced motivation is the main factor underlying impaired behavior during localized clonidine treatment.

To compare the behavioral effects of localized and systemic drug treatments, we injected clonidine via i.p. (0.05–0.1 mg/kg, Marzo et al., 2014; Devilbiss, 2018) in an additional 3 mice. Although systemic drug treatment may affect other areas in the nervous system, the observed behavioral changes resembled localized infusion (reduced Hit rate, Impulsive rate and detection sensitivity, elevated Correct Rejection rate, reaction time and decision bias, Figure 1.11a–c). Saline i.p. injections did not affect behavior (Figure 1.12).

To conclude, we found that both localized and systemic clonidine treatments (decreasing LC activity) impaired task performance in a similar fashion, i.e., by reducing motivation (Figure 1.4h and Figure 1.11d).

Localized and systemic yohimbine treatments differently affect detection performance

Next, to assess the behavioral effects of enhancing LC activity, we locally infused an α2 antagonist yohimbine (300 nL, 10 mM, 60 nL/ min) via cannulas implanted in the left LC of 7 mice. Localized yohimbine administration enhanced LC activity as it increased c-fos expression in LC neurons (Figure 1.13a). On average, c-fos expression was ~100% higher in the yohimbine side compared with the contralateral control side (38.6% vs. 19.9%). This effect was significant in individual mice ($P < 1e-5$ in all 5 mice, permutation test. Table 1.2). Interestingly, we did not observe any changes in Hit rate after yohimbine infusion, but Correct Rejection (CR) rate was significantly increased, accompanied with a reduction of Impulsive (IS) rate (Figure 1.13b, c, Figure 1.14). We note that later in the session, the Correct Rejection rate returned to baseline levels (after ~30 min, Figure 1.13b), consistent with the time course of diminished yohimbine effects (Andén et al., 1982). However, it has also been reported that elevated LC baseline firing could be sustained up to 60 min upon yohimbine administration (Rasmussen and Jacobs, 1986). Saline treatments did not affect behavior (Figure 1.14 and Figure 1.15). 20 mM yohimbine had a similar influence on behavior as 10 mM, and the trend is consistent with a dose-dependent effect (Figure 1.16). However, 20 mM yohimbine appeared to induce transient behavioral arrests during the initial 50–100 trials (data not shown), implying

that this dose over-activates LC (Carter et al., 2010). Overall, the primary behavioral effect of localized yohimbine treatment was an improvement of task performance as mice could better withhold licking in NoGo trials and were less prone to False Alarms (Figure 1.13b–d, Figure 1.14), resembling their peak performance in the middle of normal behavior sessions (Figure 1.13f). Yohimbine did not affect decision bias but significantly increased detection sensitivity (Figure 1.13e, Figure 1.14), which suggests that the behavioral improvement is not simply a result of an overall increase of arousal (which would be reflected by significant decreases in decision bias, Gelbard-Sagiv et al., 2018), but more specifically of enhanced sensory processing (e.g., increased signal-to-noise ratio).

To compare the behavioral effects of localized and systemic drug treatments, we injected yohimbine via i.p. in 5 mice (2 mg/kg, Rasmussen and Jacobs, 1986). Contrary to localized infusion, systemically treated mice were less capable of withholding licks during the waiting periods as well as in NoGo trials, resulting in increased Impulsive rate and reduced Correct Rejection rate, decision bias and detection sensitivity (Figure 1.17a–c). These behavioral changes are consistent with an increase of impulsivity, and mice behaved as if they were at the beginning of normal behavior sessions (Figure 1.17d).

To conclude, we found that localized and systemic yohimbine treatments (increasing LC activity) exerted opposing behavioral effects. Localized infusion improved tactile detection, and mice achieved near-optimal performance (Figure 1.13f). In contrast, systemic treatment impaired performance by promoting impulsivity (Figure 1.17d).

Discussion

The current study is one of the first to investigate how bidirectional perturbations of LC-NE affect quantitative perceptual task performance. We found that localized and systemic pharmacological suppression of LC-NE similarly impaired tactile detection (decreased Hit and Impulsive rates, elevated Correct Rejection rate and decision bias, and prolonged reaction time), suggesting that a major site of action during systemic clonidine treatment is the LC.

Our results support previous findings that suppressing LC-NE signaling decreases arousal, promotes sleep, and slows down reaction time (De Sarro et al., 1987; Halliday et al., 1989; Berridge et al., 1993; Turetsky and Fein, 2002; Hou et al., 2005; Carter et al., 2010). Given that the main effect of suppressing LC-NE is to reduce arousal/motivation, the behavioral impairment is likely to be task-independent. A recent study showed that systemic clonidine did not affect decision bias (Gelbard-Sagiv et al., 2018). In this study human subjects were instructed to adjust their preparedness before initiating a new trial, which possibly engaged other arousal-promoting circuits (e.g., the cholinergic system, McGaughy et al., 1996) to compensate the clonidine-induced decline of arousal/motivation (Thiele and Bellgrove, 2018).

In terms of activation, we found that localized yohimbine infusion in the LC improved tactile detection (increased Correct Rejection rate and detection sensitivity, and reduced Impulsive rate), while systemic yohimbine treatment impaired behavior (increased Impulsive rate, and decreased Correct Rejection rate, decision bias and detection sensitivity). Our findings are consistent with others showing that systemic

yohimbine increased impulsivity (Swann et al., 2005, 2013; Sun et al., 2010). The different behavioral effects between localized and systemic treatments suggest that increased impulsivity is likely due to yohimbine acting on presynaptic and postsynaptic α2 ARs (Starke et al., 1975; Szemeredi et al., 1991; Arnsten and Cai, 1993) in "off-target" α2-expressing regions, such as the peripheral nervous system (Liu et al., 2017), the noradrenergic neurons in the nucleus of the solitary tract (Van Bockstaele et al., 1999; Kirouac, 2015), and the prefrontal cortex (Solanto, 1998; Arnsten, 2000; Ramos and Arnsten, 2007; Sun et al., 2010; Janitzky et al., 2015). It should be noted that yohimbine also has pronounced affinity to 5-HT1 receptors and dopamine D2 receptors (Millan et al., 2000). In addition, activating LC via localized or systemic administration of corticotropin-releasing factors differently affected rats performing an attention set shifting task (Snyder et al., 2012). Together, these findings strongly suggest that systemic yohimbine treatment, or in general non-specific NE activation, cannot be interpreted as specific manipulation of the LC-NE circuit.

Importantly, whether systemic (non-specific) NE activation impairs or improves task performance likely depends on the brain regions, the receptors (adrenergic and non-adrenergic), and the type of the behavior task involved. For example, during systemic administration of the psychostimulant methylphenidate (MPH, an NE-DA reuptake inhibitor), enhanced NE release acting on α1 ARs in the prefrontal cortex was reasoned to underlie the dose-dependent changes in rats performing a sustained attention task (Berridge et al., 2006, 2012; Andrzejewski et al., 2014; Spencer et al., 2015; Berridge and Spencer, 2016). On the other hand, the activation of prefrontal α2 ARs and dopamine D1

receptors during MPH administration contributed to improved performance in a spatial working memory task (e.g., Arnsten and Dudley, 2005; Berridge et al., 2006).

Our study could have implications for several neurological disorders, including attention-deficit hyperactivity disorder (ADHD), for which one of the major diagnostic criteria is impulsive behavior (Castellanos and Tannock, 2002). In children performing a Go/NoGo learning task, those diagnosed with ADHD had a higher False Alarm rate than controls (e.g., Iaboni et al., 1995). Mice with ADHD phenotypes also exhibited higher False Alarm and Impulsive rates during Go/ NoGo motor tests (Majdak et al., 2016). Interestingly, this impulsive/ distractible response has been linked to high tonic LC activity (Rajkowski et al., 1994; Usher et al., 1999; Aston-Jones and Cohen, 2005). Consistent with these findings, clonidine, and possibly other α2 agonists, can suppress LC activity and reduce impulsivity (Mangeot et al., 2001; Berridge and Waterhouse, 2003).

We found that unilateral LC perturbation (contralateral to whisker stimulation) is sufficient to produce pronounced behavioral changes. Since unilateral LC suppression mainly reduced arousal/motivation, it suggests that this manipulation affects arousal-related circuits down-stream of LC, such as the basal forebrain cholinergic system and the preoptic area of the hypothalamus (Jones and Moore, 1977; Espana and Berridge, 2008). Thus, we anticipate that the behavioral impairment is laterality independent, i.e., suppressing the LC ipsilateral to whisker stimulation would similarly reduce arousal/motivation. We found that unilateral LC activation improves tactile detection. In our behavior task, the right C2 whisker was stimulated, and yohimbine was infused in the

left LC. In rodents, the ascending whisker information is fully crossed in somatosensory

thalamus and cortex (Diamond et al., 2008), which in turn receive extensive innervations

from the ipsilateral LC (Simpson et al., 1997). Since unilateral LC activation improves

detection sensitivity (d') while leaving decision bias (c) unaffected, our results imply that

activating the left LC enhances the representation of the contralateral (right) whisker

stimulation to improve task performance, potentially through NE modulating the

ipsilateral (left) somatosensory thalamus and/or somatosensory cortex. This interpretation

is in line with previous results showing that enhanced LC-NE signaling improves sensory

processing in somatosensation-related area (e.g., Lecas, 2004; Devilbiss et al., 2006;

Hirata et al., 2006; Vazey et al., 2018). We anticipate that stimulating the right LC

(ipsilateral to whisker stimulation) would not produce similar behavioral effects, and that

the behavioral improvement is laterality- and task-dependent (e.g., perceptual vs. non-

perceptual). However, it remains a possibility that unilateral LC activation could enhance

bilateral LC responses (Marzo et al., 2014), and stimulating the right LC could produce

similar behavioral improvement. Future experiments are needed to test these hypotheses.

Our localized yohimbine results support two recent studies testing how activating

LC-NE affects perceptual task performance. In one, LC was optogenetically activated in

rats performing a tactile frequency discrimination task (Rodenkirch et al., 2019). In

another, LC-NE signaling was enhanced by using a selective NE reuptake inhibitor in

human subjects performing visual detection/discrimination tasks (Gelbard-Sagiv et al.,

2018). Regardless of the differences in species and perturbation methods, activating LC-

NE improves sensitivity (d') and performance, suggesting that the behavioral

enhancement is more specific to LC-NE acting on sensory processing-related areas.

Future work is needed to examine how LC projections in different somatosensory areas

differentially contribute to tactile perception, and how perturbing LC-NE modulates other

types of behavioral tasks.

Methods

Mice

      Both male and female mice were used in this study. All mice were C57BL/6J

except 2 (out of 6) included in the localized clonidine treatment were of mixed B6J/129

background. Mice were housed with reversed light/dark cycle (9A – 9P dark, 9P – 9A

light). Mice of 6–12 weeks were implanted with head posts and/or cannulas. Clonidine

(an α2 agonist, Sigma-Aldrich) was administered locally in 6 mice and systemically in 3

mice. Yohimbine (an α2 antagonist, Sigma-Aldrich) was administered locally in 7 mice

and systemically in 5 mice. Every mouse received corresponding localized or systemic

saline injections as controls. Quantification of localized pharmacological effects on LC

activity was performed by immunostaining for the immediate early gene c-fos in 11 mice.

All procedures were approved by the UC Riverside Animal Care and Use Committee.

Surgery

      Head post surgeries were similar to previously published work (Yang et al.,

2016). In brief, mice were anesthetized (1–2% isoflurane) and affixed to a stereotaxic

instrument (Kopf, RWD). Body temperature was maintained with a heating blanket

(Harvard Apparatus, RWD) throughout the surgical procedures. The scalp over the dorsal surface of the skull was cleaned with betadine and 70% ethanol, then removed. The periosteum was removed and the skull scored with a dental drill. Cyanoacrylate was applied to the border of the skull and scalp. The head post was placed and secured with dental acrylic. A craniotomy of ~1 mm × 1 mm was made over the left hemisphere, centered at 5.2–5.3 mm posterior to bregma and 0.9–1.0 mm lateral to midline. A guide cannula (27G, 3.5 mm long, RWD) with dummy insert was advanced vertically into the brain until a depth of 1.8 mm. Dental acrylic was used to secure the guide cannula and filled in the remaining exposed skull surface. After surgery, mice were single housed and allowed to recover for at least 48 h.

Behavioral task

Following recovery from the surgery, mice were restricted to 1 mL/day water consumption for 7–10 days before behavioral training. The behavior task was adapted from published work (Yang et al., 2016). Briefly, mice were trained to perform a head-fixed, Go/NoGo single-whisker detection task, in which mice reported whether they perceived a brief deflection (200 ms, 25 Hz, ~600 deg/s) to the right C2 whisker by licking or withholding licking. Ambient white noise (1–40 kHz) was played throughout the session. An auditory cue (8 kHz) was presented at the beginning of each trial, 1.5 s prior to the time of possible stimulus onset. Trial outcomes comprised a mixture of successful and failed stimulus detection (Hit and Miss), as well as successful and failed responses to stimulus absence (Correct Rejection and False Alarm). Trials were aborted if

mice licked prematurely during the waiting period between auditory cue and the time of possible stimulus onset (Impulsive). Trials were also considered impulsive when mice licked within the first 100 ms window from stimulus onset (Mayrhofer et al., 2013; Yang et al., 2016). Mice performed one behavior session (300–500 trials) per day. Mice never achieved saturating performance in this task (Yang et al., 2016), indicating that detecting weak single-whisker deflection is perceptually demanding. All aspects of behavioral control were managed by custom Arduino-based hardware and software. Behavioral data were acquired with WaveSurfer (https://www.janelia. org/open-science/wavesurfer).

Pharmacology

All drugs were dissolved in physiological saline. Localized pharmacology was administered during behavior sessions. Drug or saline was loaded into a 1 μL Hamilton syringe, controlled by a syringe pump (Harvard Apparatus). Mice were placed in the behavior chamber and injection cannula (33G, 5 mm long) inserted into the guide cannula. The infusion depth was 3.3 mm. Infusion was initiated within the first 20 behavior trials. 300 nL of drug or saline was infused at a rate of 60 nL/min. At the conclusion of a behavior session, the injection cannula was removed and dummy insert replaced.

Systemic pharmacology was administered just prior to behavior sessions. Mice were briefly anesthetized (< 1 min) with 2–3% isoflurane, during which 50 μL of drug or saline was injected via i.p.. Mice were allowed to recover for 5 min before starting the

behavior session. During baseline behavioral sessions (one day before i.p. treatment), mice were also briefly anesthetized to account for any potential effects from anesthesia.

Histology

At the conclusion of behavioral experiments, mice with cannula implants received localized Fluoro-Gold infusion (0.1–1%, 300 nL) at a rate of 60 nL/min. 40–60 min later, mice were anesthetized with ketamine/xylazine and perfused intracardially with 4% paraformaldehyde, and the brains harvested and post fixed. 100 μM thick coronal sections were cut (Leica, VT1200s). Sections containing LC were incubated with rabbit anti-Tyrosine Hydroxylase (TH) antibody (Thermofisher OPA 1–04050, 1:1000), followed by goat anti-rabbit IgG Alexa Fluor 488 or 594 secondary antibody (Thermofisher A32731 or A32740, 1:1000), and mounted with DAPI mounting media (Vector labs). Co-localization of Fluoro-Gold and TH immunoactivity, as well as the cannula tract, were used to verify cannula placement.

The expression of an immediate early gene, c-fos, was examined to assess the impact of localized drug treatment on LC activity. Infusions were performed in the left LC, with the contralateral (right) LC serving as a control. Clonidine was infused in 4 awake mice. Yohimbine was infused in 5 mice, 2 of which received infusion under anesthesia, with the purpose to reduce basal LC activation and to enhance the contrast between the injected side and the control side. The remaining 3 mice received infusion during wakefulness. Saline was infused in 2 awake mice. All mice were perfused 40–60 min post infusion. Coronal sections containing LC were first incubated with rabbit anti-c-

fos antibody (Cell Signaling 2250S, 1:400), followed by secondary antibody (Thermofisher A32740, 1:400). Sections were then incubated with rabbit IgG isotype control (Thermofisher 31235, 1:17000) to quench non-specific signals, and subsequently stained for TH. Z-stack images were acquired using a confocal microscope (Leica SPE II) and flattened using Fiji (Schindelin et al., 2012)

Data analysis

Behavior data were analyzed off-line with MATLAB. To account for the fact that some mice did not immediately engage in the task, the initial 20–40 trials were removed from behavior analysis. In some sessions, trials toward session end were also removed from analysis when mice appeared to be disengaged from the task (Hit rate dropped below 50%, typically after 300–400 trials). For sessions shown in Figure 1.1, we included an additional 20–50 trials toward session end to demonstrate a near-complete cessation of task performance. Decision bias/ criterion (c) and detection sensitivity (d') were calculated based on Hit rate (HR) and False Alarm rate (FAR): $c = z(HR) - z(FAR)$, $d' = -(z(HR) + z(FAR))/2$, where z is the normal inverse cumulative distribution function.

c-fos expression was analyzed using QuPath (Bankhead et al., 2017). Borders around the LC were manually drawn to identify regions of interest. For each mouse, 2–3 images with the greatest TH and c-fos expressions were used to determine the minimum and maximum cell sizes, as well as the fluorescent intensity threshold. Individual cells

expressing supra-threshold TH or c-fos were detected. Results were manually verified for each image.

Data were reported as mean ± s.e.m. unless otherwise noted. Statistical tests were by two-tailed Wilcoxon signed rank unless otherwise noted.

References

Abercrombie ED, Jacobs BL (1987) Microinjected clonidine inhibits noradrenergic neurons of the locus coeruleus in freely moving cats. Neurosci Lett 76:203–208.

Acheson AL, Zigmond MJ, Stricker EM (1980) Compensatory increase in tyrosine hydroxylase activity in rat brain after intraventricular injections of 6-hydroxydopamine. Science (80-) 207:537–540.

Adams LM, Foote SL (1988) Effects of locally infused pharmacological agents on spontaneous and sensory-evoked activity of locus coeruleus neurons. Brain Res Bull 21:395–400.

Aghajanian GK, Vandermaelen CP (1982) alpha2-Adrenoceptor-Mediated Hyperpolarization of Locus Coeruleus Neurons: Intracellular Studies in vivo. Science (80-) 215:1394–1396.

Aghajanian GK, Wang YY (1987) Common α2- and opiate effector mechanisms in the locus coeruleus: intracellular studies in brain slices. Neuropharmacology 26:793–799.

Andén NE, Pauksens K, Svensson K (1982) Selective blockade of brain α2-autoreceptors by yohimbine: Effects on motor activity and on turnover of noradrenaline and dopamine. J Neural Transm 55:111–120.

Andrzejewski ME, Spencer RC, Harris RL, Feit EC, McKee BL, Berridge CW (2014) The effects of clinically relevant doses of amphetamine and methylphenidate on signal detection and DRL in rats. Neuropharmacology 79:634–641

Arnsten AFT (2000) Through the Looking Glass: Different Noradrenergic Modulation of Prefrontal Cortical Function. Neural Plast 7:133–146.

Arnsten AFT, Cai JX (1993) Postsynaptic alpha-2 receptor stimulation improves memory in aged monkeys: Indirect effects of yohimbine versus direct effects of clonidine. Neurobiol Aging 14:597–603.

Arnsten AFT, Dudley AG (2005) Methylphenidate improves prefrontal cortical cognitive function through α2 adrenoceptor and dopamine D1 receptor actions: Relevance to therapeutic effects in Attention Deficit Hyperactivity Disorder. Behav Brain Funct 1:1–9.

Aston-Jones G, Cohen JD (2005) AN INTEGRATIVE THEORY OF LOCUS COERULEUS-NOREPINEPHRINE FUNCTION: Adaptive Gain and Optimal Performance. Annu Rev Neurosci 28:403–450

Bankhead P, Loughrey MB, Fernández JA, Dombrowski Y, McArt DG, Dunne PD, McQuaid S, Gray RT, Murray LJ, Coleman HG, James JA, Salto-Tellez M, Hamilton PW (2017) QuPath: Open source software for digital pathology image analysis. Sci Rep 7:1–7.

Berditchevskaia A, Cazé RD, Schultz SR (2016) Performance in a GO/NOGO perceptual task reflects a balance between impulsive and instrumental components of behaviour. Sci Rep 6:27389 Available at: http://www.nature.com/articles/srep27389.

Berridge CW, Devilbiss DM, Andrzejewski ME, Arnsten AFT, Kelley AE, Schmeichel B, Hamilton C, Spencer RC (2006) Methylphenidate Preferentially Increases Catecholamine Neurotransmission within the Prefrontal Cortex at Low Doses that Enhance Cognitive Function. Biol Psychiatry 60:1111–1120.

Berridge CW, Page ME, Valentino RJ, Foote SL (1993) Effects of locus coeruleus inactivation on electroencephalographic activity in neocortex and hippocampus. Neuroscience 55:381–393.

Berridge CW, Shumsky JS, Andrzejewski ME, McGaughy JA, Spencer RC, Devilbiss DM, Waterhouse BD (2012) Differential sensitivity to psychostimulants across prefrontal cognitive tasks: Differential involvement of noradrenergic α 1- and α 2-receptors. Biol Psychiatry 71:467–473

Berridge CW, Spencer RC (2016) Differential cognitive actions of norepinephrine a2 and a1 receptor signaling in the prefrontal cortex. Brain Res 1641:189–196 Available at: http://dx.doi.org/10.1016/j.brainres.2015.11.024.

Berridge CW, Waterhouse BD (2003) The locus coeruleus-noradrenergic system: Modulation of behavioral state and state-dependent cognitive processes. Brain Res Rev 42:33–84.

Carter ME, Yizhar O, Chikahisa S, Nguyen H, Adamantidis A, Nishino S, Deisseroth K, de Lecea L (2010) Tuning arousal with optogenetic modulation of locus coeruleus neurons. Nat Neurosci 13:1526–1533

Castellanos FX, Tannock R (2002) Neuroscience of attention-deficit/hyperactivity disorder: The search for endophenotypes. Nat Rev Neurosci 3:617–628.

Cedarbaum JM, Aghajanian GK (1976) Noradrenergic neurons of the locus coeruleus: inhibition by epinephrine and activation by the α-antagonist piperoxane. Brain Res 112:413–419.

Cedarbaum JM, Aghajanian GK (1977) Catecholamine receptors on locus coeruleus neurons: Pharmacological characterization. Eur J Pharmacol 44:375–385.

De Sarro GB, Ascioti C, Froio F, Libri V, Nisticò G (1987) Evidence that locus coeruleus is the site where clonidine and drugs acting at α1- and α2-adrenoceptors affect sleep and arousal mechanisms. Br J Pharmacol 90:675–685.

Devilbiss DM (2018) Consequences of tuning network function by tonic and phasic locus coeruleus output and stress: Regulating detection and discrimination of peripheral stimuli. Brain Res Available at: https://doi.org/10.1016/j.brainres.2018.06.015.

Devilbiss DM, Page ME, Waterhouse BD (2006) Locus Ceruleus Regulates Sensory Encoding by Neurons and Networks in Waking Animals. J Neurosci 26:9860–9872

Devilbiss DM, Waterhouse BD (2004) The Effects of Tonic Locus Ceruleus Output on Sensory-Evoked Responses of Ventral Posterior Medial Thalamic and Barrel Field Cortical Neurons in the Awake Rat. J Neurosci 24:10773–10785

Diamond ME, Von Heimendahl M, Knutsen PM, Kleinfeld D, Ahissar E (2008) "Where" and "what" in the whisker sensorimotor system. Nat Rev Neurosci 9:601–612.

Dickinson A, Balleine B (1995) Motivational Control of Instrumental Action. Curr Dir Psychol Sci 4:162–167.

Doucette W, Milder J, Restrepo D, Doucette W, Milder J, Restrepo D (2007) Adrenergic modulation of olfactory bulb circuitry affects odor discrimination. :539–547.

Escanilla O, Arrellanos A, Karnow A, Ennis M, Linster C (2010) Noradrenergic modulation of behavioral odor detection and discrimination thresholds in the olfactory bulb. Eur J Neurosci 32:458–468.

Espana RA, Berridge CW (2008) Organization of Noradrenergic Efferents to Arousal-Related Basal Forebrain Structures. J Comp Neurol 346:339–346.

Foote SL, Freedman R, Oliver AP (1975) Effects of putative neurotransmitters on neuronal activity in monkey auditory cortex. Brain Res 86:229–242.

Gelbard-Sagiv H, Magidov E, Sharon H, Hendler T, Nir Y (2018) Noradrenaline Modulates Visual Perception and Late Visually Evoked Activity. Curr Biol 28:2239-2249.e6 Available at: https://doi.org/10.1016/j.cub.2018.05.051.

Green DM, Swets JA (1966) Signal Detection Theory and Psychophysics.

Guo Z V., Hires SA, Li N, O'Connor DH, Komiyama T, Ophir E, Huber D, Bonardi C, Morandell K, Gutnisky D, Peron S, Xu NL, Cox J, Svoboda K (2014) Procedures for behavioral experiments in head-fixed mice. PLoS One 9.

Halliday R, Callaway E, Lannon R (1989) The effects of clonidine and yohimbine on human information processing. Psychopharmacology (Berl) 99:563–566.

Harik S, Duckrow R, LaManna J, Rosenthal M, Sharma V, Banerjee S (1981) Cerebral compensation for chronic noradrenergic denervation induced by locus ceruleus lesion: recovery of receptor binding, isoproterenol- induced adenylate cyclase activity, and oxidative metabolism. J Neurosci 1:641–649.

Heggelund TK and P (1982) Single Cell Responses in Cat Visual Cortex to Visual Stimulation During Iontophoresis of Noradrenaline. Exp brain Res 1982:317–327.

Herr NR, Park J, McElligott ZA, Belle AM, Carelli RM, Mark Wightman R (2012) In vivo voltammetry monitoring of electrically evoked extracellular norepinephrine in subregions of the bed nucleus of the stria terminalis. J Neurophysiol 107:1731–1737.

Hirata A, Aguilar J, Castro-Alamancos MA (2006) Noradrenergic Activation Amplifies Bottom-Up and Top-Down Signal-to-Noise Ratios in Sensory Thalamus. J Neurosci 26:4426–4436

Hou RH, Freeman C, Langley RW, Szabadi E, Bradshaw CM (2005) Does modafinil activate the locus coeruleus in man? Comparison of modafinil and clonidine on arousal and autonomic functions in human volunteers. Psychopharmacology (Berl) 181:537–549.

Iaboni F, Douglas VI, Baker AG (1995) Effects of presentation rate of stimuli on response inhibition in ADHD children with and without tics. J Abnorm Psychol 104:232–240.

Janitzky K, Lippert MT, Engelhorn A, Tegtmeier J, Goldschmidt J, Heinze H-J, Ohl FW (2015) Optogenetic silencing of locus coeruleus activity in mice impairs cognitive flexibility in an attentional set-shifting task. Front Behav Neurosci 9:1–8.

Jones BE, Moore RY (1977) Ascending projections of the locus coeruleus in the rat. II. Autoradiographic study. Brain Res 127:23–53.

Kalwani RM, Joshi S, Gold JI (2014) Phasic Activation of Individual Neurons in the Locus Ceruleus/Subceruleus Complex of Monkeys Reflects Rewarded Decisions to Go But Not Stop. J Neurosci 34:13656–13669.

Kirouac GJ (2015) Placing the paraventricular nucleus of the thalamus within the brain circuits that control behavior. Neurosci Biobehav Rev 56:315–329 Available at: http://dx.doi.org/10.1016/j.neubiorev.2015.08.005.

Lecas JC (2004) Locus coeruleus activation shortens synaptic drive while decreasing spike latency and jitter in sensorimotor cortex. Implications for neuronal integration. Eur J Neurosci 19:2519–2530.

Lee SH, Dan Y (2012) Neuromodulation of Brain States. Neuron 76:209–222 Available at: http://dx.doi.org/10.1016/j.neuron.2012.09.012.

Liu Y, Rodenkirch C, Moskowitz N, Schriver B, Wang Q (2017) Dynamic Lateralization of Pupil Dilation Evoked by Locus Coeruleus Activation Results from Sympathetic, Not Parasympathetic, Contributions. Cell Rep 20:3099–3112

Majdak P, Ossyra JR, Ossyra JM, Cobert AJ, Hofmann GC, Tse S, Panozzo B, Grogan EL, Sorokina A, Rhodes JS (2016) A new mouse model of ADHD for medication development. Sci Rep 6:1–18.

Manella LC, Petersen N, Linster C (2017) Stimulation of the locus coeruleus modulates signal-to-noise ratio in the olfactory bulb. J Neurosci 37:11605–11615

Mangeot SD, Miller LJ, McIntosh DN, McGrath-Clarke J, Simon J, Hagerman RJ, Goldson E (2001) Sensory modulation dysfunction in children with attention-deficit hyperactivity disorder. J Dev Behav Pediatr 22:449.

Martins ARO, Froemke RC (2015) Coordinated forms of noradrenergic plasticity in the locus coeruleus and primary auditory cortex. Nat Neurosci 18:1483–1492

Marzo A, Totah NK, Neves RM, Logothetis NK, Eschenko O (2014) Unilateral electrical stimulation of rat locus coeruleus elicits bilateral response of norepinephrine neurons and sustained activation of medial prefrontal cortex. J Neurophysiol 111:2570–2588.

Mayrhofer JM, Skreb V, Von der Behrens W, Musall S, Weber B, Haiss F (2013) Novel two-alternative forced choice paradigm for bilateral vibrotactile whisker frequency discrimination in head-fixed mice and rats. J Neurophysiol 109:273–284.

McBurney-Lin J, Lu J, Zuo Y, Yang H (2019) Locus Coeruleus-Norepinephrine Modulation of Sensory Processing and Perception: A Focused Review. Neurosci Biobehav Rev 105:190–199.

McCune SK, Voigt MM, Hill JM (1993) Expression of multiple alpha adrenergic receptor subtype messenger RNAs in the adult rat brain. Neuroscience 57:143–151.

McGaughy J, Kaiser T, Sarter M (1996) Behavioral vigilance following infusions of 192 IgG-saporin into the basal forebrain: Selectivity of the behavioral impairment and relation to cortical AChE-positive fiber density. Behav Neurosci 110:247–265.

Millan MJ, Newman-Tancredi A, Audinot V, Cussac D, Lejeune F, Nicolas JP, Cogé F, Galizzi JP, Boutin JA, Rivet JM, Dekeyne A, Gobert A (2000) Agonist and antagonist actions of yohimbine as compared to fluparoxan at α2-adrenergic receptors (AR)s, serotonin (5-HT)(1A), 5-HT(1B), 5-HT(1D) and dopamine D2 and D3 receptors. Significance for the modulation of frontocortical monoaminergic transmission. Synapse 35:79–95.

Morrison JH, Foote SL (1986) Noradrenergic and serotoninergic innervation of cortical, thalamic, and tectal visual structures in old and new world monkeys. J Comp Neurol 243:117–138.

Navarra RL, Clark BD, Gargiulo AT, Waterhouse BD (2017) Methylphenidate Enhances Early-Stage Sensory Processing and Rodent Performance of a Visual Signal Detection Task. Neuropsychopharmacology 42:1326–1337

Neves RM, van Keulen S, Yang M, Logothetis NK, Eschenko O (2018) Locus coeruleus phasic discharge is essential for stimulus-induced gamma oscillations in the prefrontal cortex. J Neurophysiol 119:904–920.

Nicholas AP, Pieribone V, Hokfelt T (1993) Distributions of mRNAs for alpha-2 adrenergic receptor subtypes in rat brain: an in situ hybridization study. J Comp Neurol 328:575–594.

Raiteri M, Maura G, Versace P (1983) Functional evidence for two stereochemically different alpha-2 adrenoceptors regulating central norepinephrine and serotonin release. J Pharmacol Exp Ther 224:679–684.

Rajkowski J, Kubiak P, Aston-Jones G (1994) Locus coeruleus activity in monkey: Phasic and tonic changes are associated with altered vigilance. Brain Res Bull 35:607–616.

Ramos BP, Arnsten AFT (2007) Adrenergic Pharmacology and Cognition: Focus on the Prefrontal Cortex. Pharmacol Ther 113:523–536.

Rasmussen K, Jacobs BL (1986) Single unit activity of locus coeruleus neurons in the freely moving cat. II. Conditioning and pharmacologic studies. Brain Res 371:335–344.

Rho HJ, Kim JH, Lee SH (2018) Function of selective neuromodulatory projections in the mammalian cerebral cortex: Comparison between cholinergic and noradrenergic systems. Front Neural Circuits 12:1–13.

Robertson SD, Plummer NW, De Marchena J, Jensen P (2013) Developmental origins of central norepinephrine neuron diversity. Nat Neurosci 16:1016–1023

Rodenkirch C, Liu Y, Schriver BJ, Wang Q (2019) Locus coeruleus activation enhances thalamic feature selectivity via norepinephrine regulation of intrathalamic circuit dynamics. Nat Neurosci 22:120–133 Available at: http://www.nature.com/articles/s41593-018-0283-1.

Sara SJ (2009) The locus coeruleus and noradrenergic modulation of cognition. Nat Rev Neurosci 10:211–223 Available at: http://www.nature.com/doifinder/10.1038/nrn2573.

Sara SJ, Bouret S (2012) Orienting and Reorienting: The Locus Coeruleus Mediates Cognition through Arousal. Neuron 76:130–141 Available at: http://dx.doi.org/10.1016/j.neuron.2012.09.011.

Schindelin J, Arganda-Carreras I, Frise E, Kaynig V, Longair M, Pietzsch T, Preibisch S, Rueden C, Saalfeld S, Schmid B, Tinevez JY, White DJ, Hartenstein V, Eliceiri K, Tomancak P, Cardona A (2012) Fiji: An open-source platform for biological-image analysis. Nat Methods 9:676–682.

Schwarz C, Hentschke H, Butovas S, Haiss F, Stüttgen MC, Gerdjikov T V., Bergner CG, Waiblinger C (2010) The head-fixed behaving rat - Procedures and pitfalls. Somatosens Mot Res 27:131–148.

Simpson KL, Altman DW, Wang L, Kirifides ML, Lin RCS, Waterhouse BD (1997) Lateralization and functional organization of the locus coeruleus projection to the trigeminal somatosensory pathway in rat. J Comp Neurol 385:135–147.

Simson PE, Weiss JM (1987) Alpha-2 receptor blockade increases responsiveness of locus coeruleus neurons to excitatory stimulation. J Neurosci 7:1732–1740.

Snyder K, Wang WW, Han R, McFadden K, Valentino RJ (2012) Corticotropin-releasing factor in the norepinephrine nucleus, locus coeruleus, facilitates behavioral flexibility. Neuropsychopharmacology 37:520–530

Solanto M V. (1998) Neuropsychopharmacological mechanisms of stimulant drug action in attention-deficit hyperactivity disorder: A review and integration. Behav Brain Res 94:127–152.

Spencer RC, Devilbiss DM, Berridge CW (2015) The cognition-enhancing effects of psychostimulants involve direct action in the prefrontal cortex. Biol Psychiatry 77:940–950 Available at: http://dx.doi.org/10.1016/j.biopsych.2014.09.013.

St. Peters M, Demeter E, Lustig C, Bruno JP, Sarter M (2011) Enhanced Control of Attention by Stimulating Mesolimbic-Corticopetal Cholinergic Circuitry. J Neurosci 31:9760–9771

Starke K, Borowski E, Endo T (1975) Preferential blockade of presynaptic α-adrenoceptors by yohimbine. Eur J Pharmacol 34:385–388.

Sun HS, Green TA, Theobald DEH, Birnbaum SG, Graham DL, Zeeb FD, Nestler EJ, Winstanley CA (2010) Yohimbine Increases Impulsivity Through Activation of cAMP Response Element Binding in the Orbitofrontal Cortex. Biol Psychiatry 67:649–656 Available at: http://dx.doi.org/10.1016/j.biopsych.2009.11.030.

Swann AC, Birnbaum D, Jagar AA, Dougherty DM, Moeller FG (2005) Acute yohimbine increases laboratory-measured impulsivity in normal subjects. Biol Psychiatry 57:1209–1211.

Swann AC, Lijffijt M, Lane SD, Cox B, Steinberg JL, Moeller FG (2013) Norepinephrine and impulsivity: Effects of acute yohimbine. Psychopharmacology (Berl) 229:83–94.

Szemeredi K, Komoly S, Kopin IJ, Bagdy G, Keiser HR, Goldstein DS (1991) Simultaneous measurement of plasma and brain extracellular fluid concentrations of catechols after yohimbine administration in rats. Brain Res 542:8–14.

Thiele A, Bellgrove MA (2018) Neuromodulation of Attention. Neuron 97:769–785 Available at: https://doi.org/10.1016/j.neuron.2018.01.008.

Turetsky BI, Fein G (2002) α2-noradrenergic effects on ERP and behavioral indices of auditory information processing. Psychophysiology 39:147–157.

Usher M, Cohen JD, Servan-Schreiber D, Rajkowski J, Aston-Jones G (1999) The role of locus coeruleus in the regulation of cognitive performance. Science (80-) 283:549–554.

Valentini V, Frau R, Di Chiara G (2004) Noradrenaline transporter blockers raise extracellular dopamine in medial prefrontal but not parietal and occipital cortex: Differences with mianserin and clozapine. J Neurochem 88:917–927.

Van Bockstaele EJ, Peoples J, Telegan P (1999) Efferent projections of the nucleus of the solitary tract to peri-Locus coeruleus dendrites in rat brain: Evidence for a monosynaptic pathway. J Comp Neurol 412:410–428.

Vazey EM, Moorman DE, Aston-Jones G (2018) Phasic locus coeruleus activity regulates cortical encoding of salience information. Proc Natl Acad Sci 115:E9439–E9448 Available at: http://www.pnas.org/lookup/doi/10.1073/pnas.1803716115.

Waterhouse BD, Moises HC, Woodward DJ (1980) Noradrenergic modulation of somatosensory cortical neuronal responses to Iontophoretically applied putative neurotransmitters. Exp Neurol 69:30–49.

Waterhouse BD, Navarra RL (2018) The locus coeruleus-norepinephrine system and sensory signal processing : A historical review and current perspectives. Brain Res:1–15 Available at: https://doi.org/10.1016/j.brainres.2018.08.032.

Yang H, Kwon SE, Severson KS, O'Connor DH (2016) Origins of choice-related activity in mouse somatosensory cortex. Nat Neurosci 19:127–134

Figures and Tables
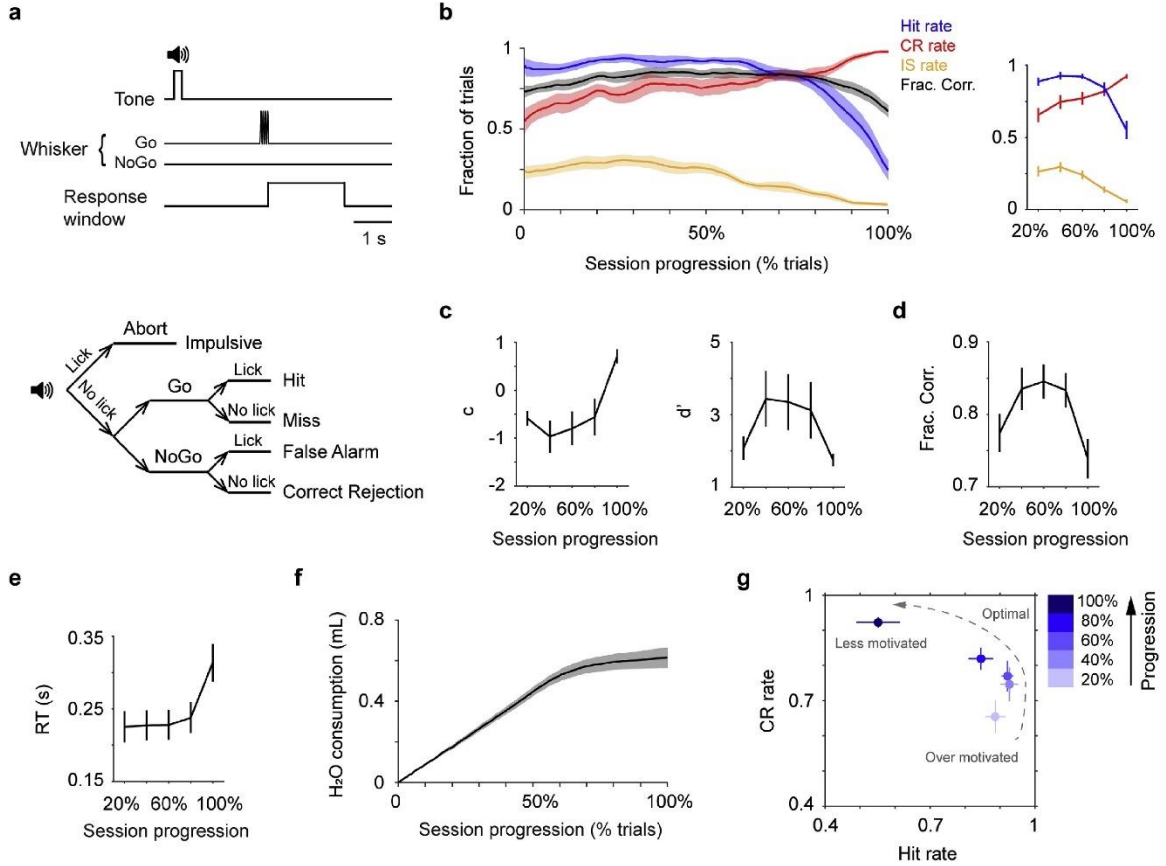
Figure 1.1 Mouse behavior fluctuates within single sessions.
(a) Trial structure (top) and the five possible trial types (bottom). (b) Left: Mean single-session trajectories of Hit rate, CR rate, IS rate and overall performance (± s.e.m.). Behavioral sessions of different lengths (348 ± 20 trials, mean ± s.e.m., n = 13) are normalized using % total number of trials (session progression). Trajectories are smoothed using a moving window of 30 trials. Right: Trajectories of Hit, CR and IS rates averaged every 20% progression. (c) Trajectories of decision bias (c) and detection sensitivity (d'), based on Hit and CR rates in b. (d) Trajectory of overall performance (Fraction Correct shown in b, averaged every 20% progression) illustrates an inverted-U shape. (e) Mean single-session trajectory of RT (± s.e.m.), averaged every 20% progression. (f) Mean single-session trajectory of cumulated water consumption (± s.e.m.), based on an estimate of 5 μL dispense per Hit trial. g. CR rate vs. Hit rate trajectory, based on values in b.

46

a

Slope = 0.34
R = 0.24
P = 3.36 e-5

IS rate

0.6
0.3
0

0   0.5   1
Hit rate

b

Slope = -0.66
R = 0.66
P = 2.84 e-16

IS rate

0.6
0.3
0

0   0.5   1
CR rate
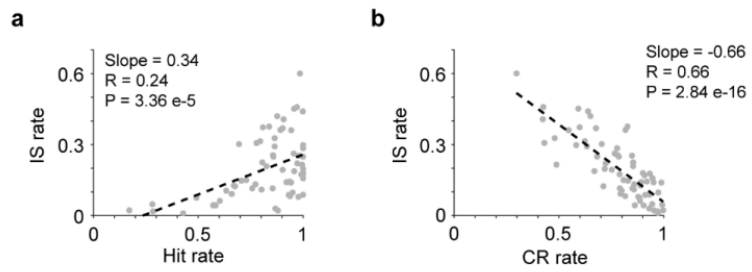
Figure 1.2 IS rate was positively correlated with Hit rate (a), and negatively correlated with CR rate (b).
Dashed lines: linear fitting.
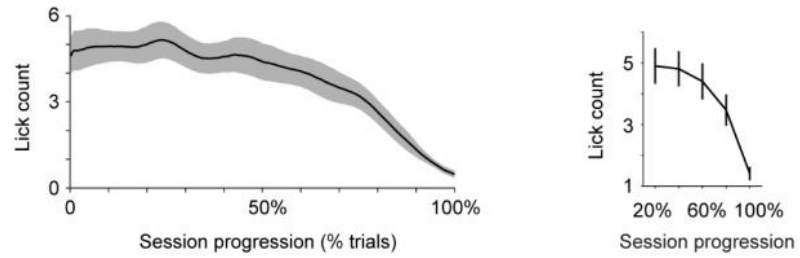
Figure 1.3 Lick count decreased as task progressed within sessions.
Left: normalized single session trajectory of lick count, mean ± s.e.m. Right: averaged every 20% progression. Lick count is defined as the total number of licks emitted in each trial.
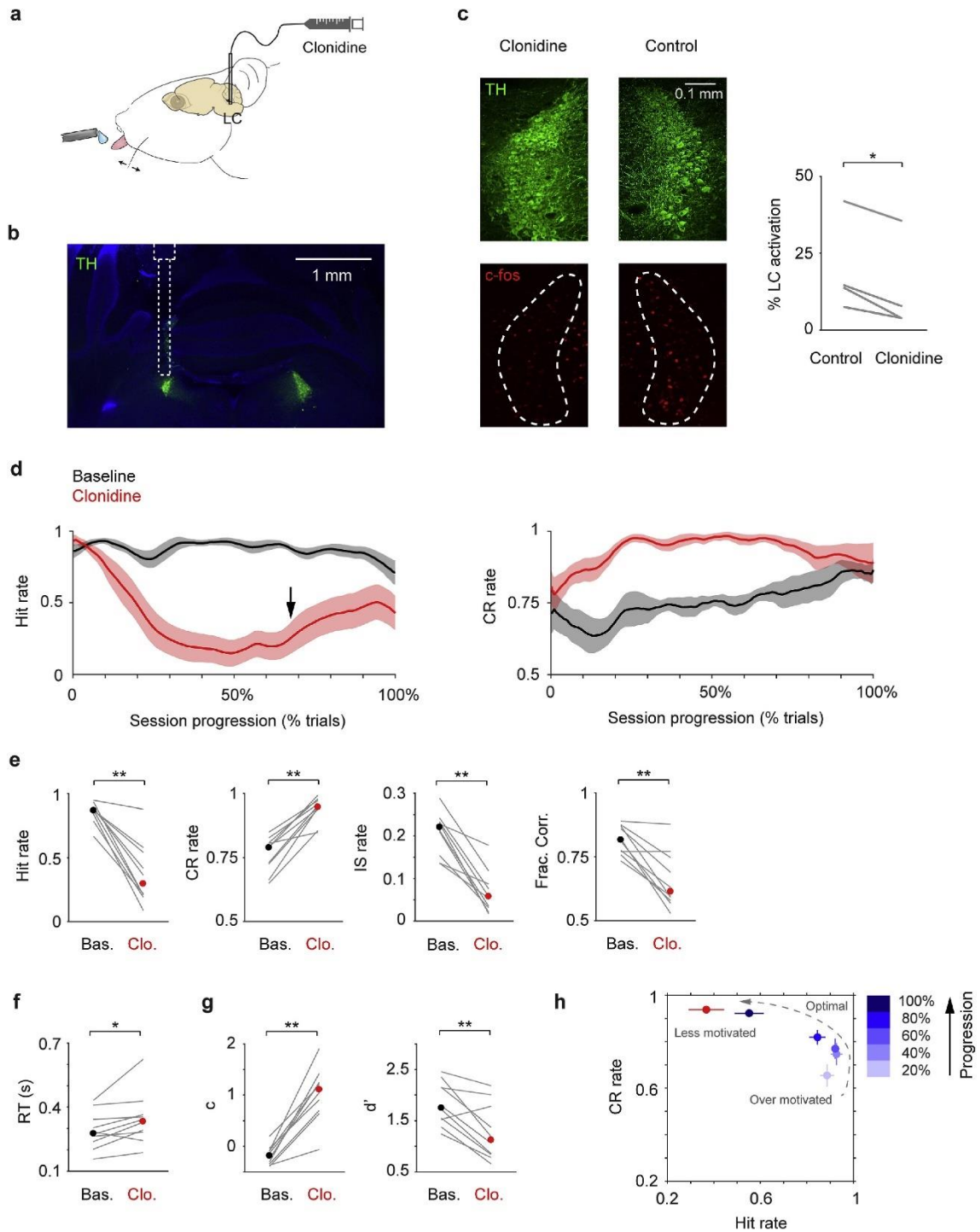
Figure 1.4 Localized clonidine infusion impairs tactile detection.
*(**a**) Schematic of drug infusion setup. (**b**) Histological section showing LC (green) and the tract of the infusion cannula, overlaid with an illustration of cannula placement. (**c**) Left: Example c-fos expression (red) in the LC (green) after localized clonidine infusion. The contralateral LC serves as a basal level control. Right: c-fos expression was reduced upon clonidine infusion in 4 awake mice (p = 0.014, two-tailed paired t-test. Cell counts for individual mice are shown in Table 1.1). % LC activation was defined as the fraction of TH/c-fos double positive cells among TH positive cells. (**d**) Mean single-session trajectories for Hit (left) and CR (right) rates during baseline and clonidine sessions (± s.e.m.). Baseline sessions were recorded one day before infusion. Black arrow indicates the onset of Hit rate recovery. (**e-g**) Hit rate, CR rate, IS rate, Fraction Correct, RT, decision bias (c) and detection sensitivity (d') for baseline (black dot, median) and clonidine (red dot, median) sessions. Gray lines indicate individual consecutive two-day, baseline-clonidine pairs. Hit rate, p = 0.002, Signed rank = 55; CR rate, p = 0.002, Signed rank = 0; IS rate, p = 0.002, Signed rank = 55; Frac. Corr., p = 0.0039, Signed rank = 54; RT, p = 0.019, Signed rank = 5; c, p = 0.002, Signed rank = 0; d', p = 0.0059, Signed rank = 53. n = 10. (**h**) CR rate vs. Hit rate trajectory showing clonidine reduces motivation (low Hit rate and high CR rate), which coincides with mouse behavior toward the end of normal baseline sessions.*
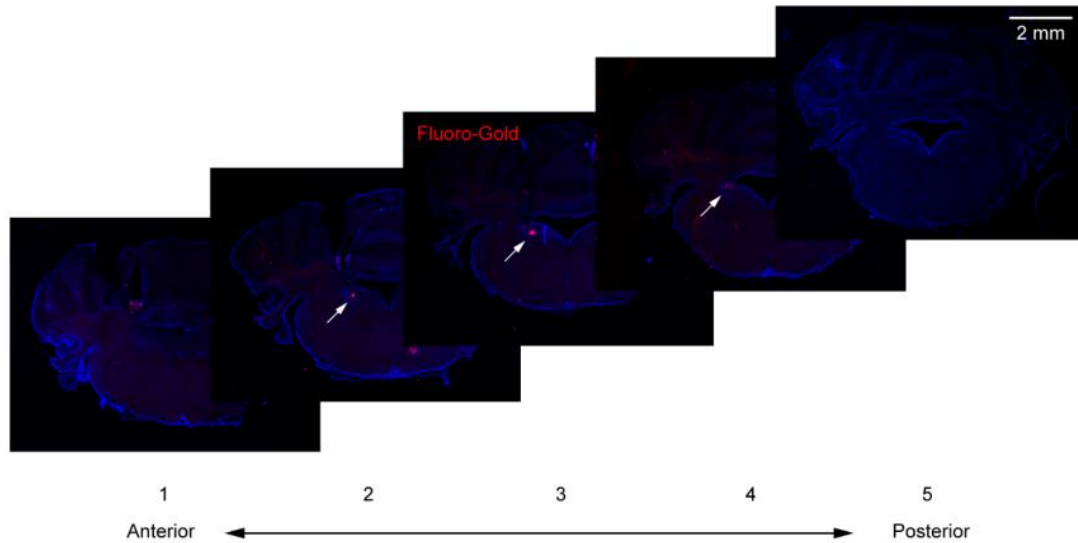
Figure 1.5 Drug spread approximately 400um.
5 consecutive 100 μm coronal sections from a mouse where 300 nL Fluoro-Gold was locally infused. Arrows point to visible Fluoro-Gold (red) in sections 2-4. Fluoro-Gold in the most anterior and posterior sections (1 and 5) is very faint.
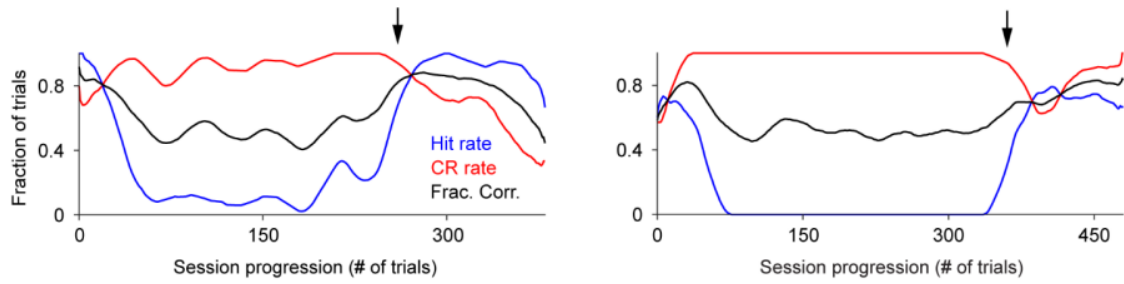
Figure 1.6 Two example behavior sessions of localized clonidine infusion.
Mouse behavior tended to recover later in the session (Hit rate increased and CR rate decreased), indicated by the arrows.
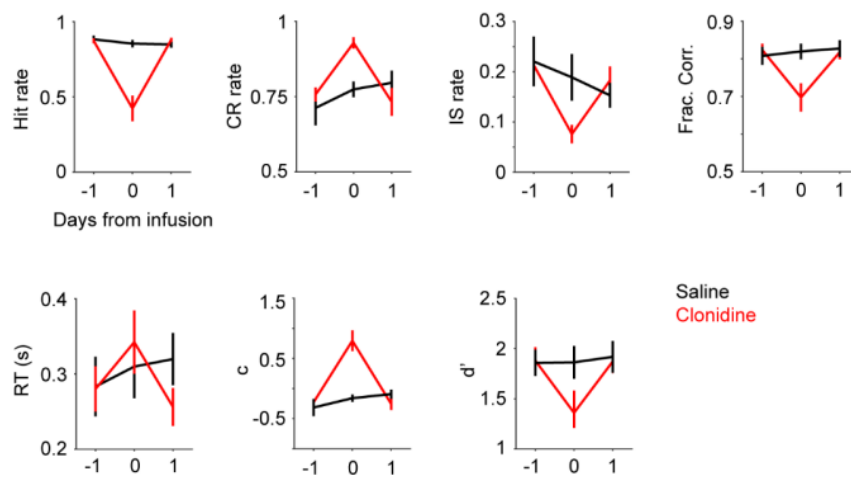
Figure 1.7 Comparing the effects local clonidine and saline infusions.
Mean Hit rate, CR rate, IS rate, Fraction Correct, RT, decision bias (c) and detection sensitivity (d') for 3 consecutive days (± s.e.m.). Black: saline, n = 6; Red: clonidine, n = 8.
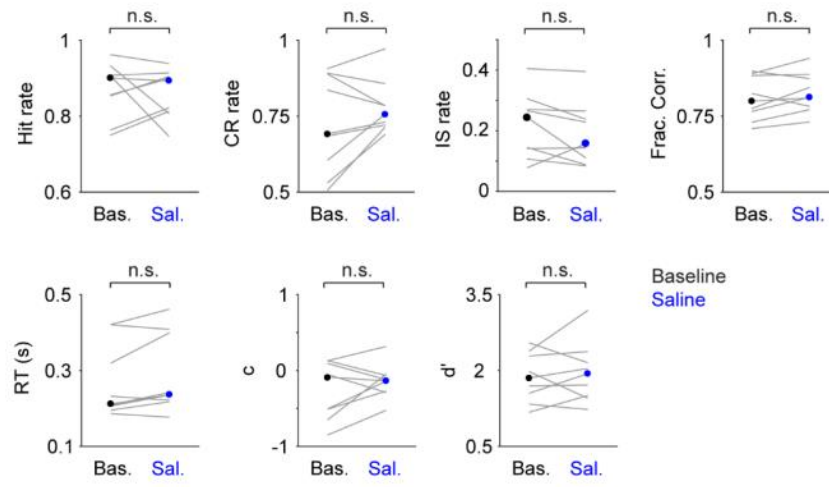
Figure 1.8 Localized saline infusion did not affect behavior.
Hit rate, P = 1, Signed rank = 22; CR rate, P = 0.20, Signed rank = 11; IS rate, P = 0.13, Signed rank = 36; Frac. Corr., P = 0.16, Signed rank = 10; RT, P = 0.055, Signed rank = 6; c, P = 0.30, Signed rank = 13; d', P = 0.65, Signed rank = 18. n = 9.
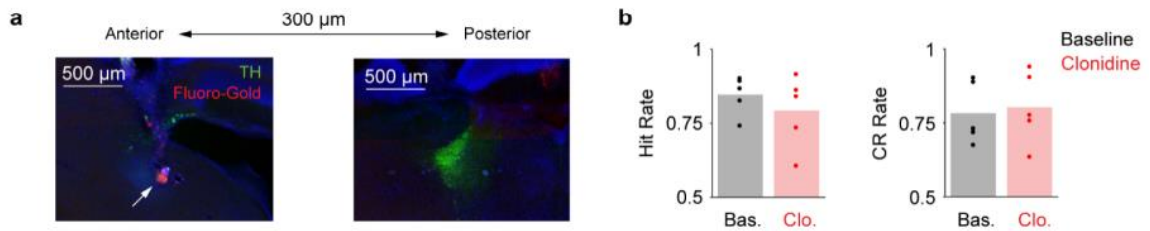
Figure 1.9 Clonidine minimally affected behavior when the infusion was outside of LC.
(a) Example histological sections showing off-target infusion. The location of drug infusion was estimated by Fluoro-Gold (red), which is ~300 μm anterior to the LC (green). (b) Hit and CR rates during baseline and off-target clonidine sessions (Hit rate, 0.85 ± 0.03 vs. 0.79 ± 0.05; CR rate, 0.78 ± 0.05 vs. 0.80 ± 0.05, mean ± s.e.m., n = 5).
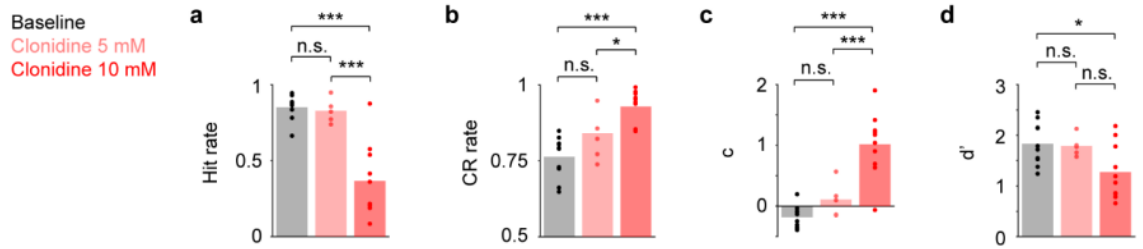
Figure 1.10 Clonidine infusions exhibit a dose dependent trend.
Hit rate, CR rate, decision bias (c) and detection sensitivity (d') for baseline (black, n = 10), 5 mM clonidine (light red, n = 5), and 10 mM clonidine (red, n = 10) sessions.
(a) Hit rate: one-way ANOVA, F(2,22) = 23.97, P = 3.0e-6. Baseline vs. 5 mM, P = 0.70; Baseline vs. 10 mM, P = 3.5e-6; 5 mM vs. 10 mM, P = 4.0e-4. (b) CR rate: one-way ANOVA, F(2,22) = 18.69, P = 1.8e5. Baseline vs. 5 mM, P = 0.18; Baseline vs. 10 mM, P = 1.2e-5; 5 mM vs. 10 mM, P = 0.013. (c) Decision bias: one-way ANOVA, F(2,22) = 26.47, P = 1.4e-6. Baseline vs. 5 mM, P = 0.36; Baseline vs. 10 mM, P = 1.2e-6; 5 mM vs. 10 mM, P = 6.6e-4. (d) Detection sensitivity: one-way ANOVA, F(2,22) = 4.39, P = 0.025. Baseline vs. 5 mM, P = 0.98; Baseline vs. 10 mM, P = 0.029; 5 mM vs. 10 mM, P = 0.12. All post-hoc pairwise tests were Tukey-Kramer.
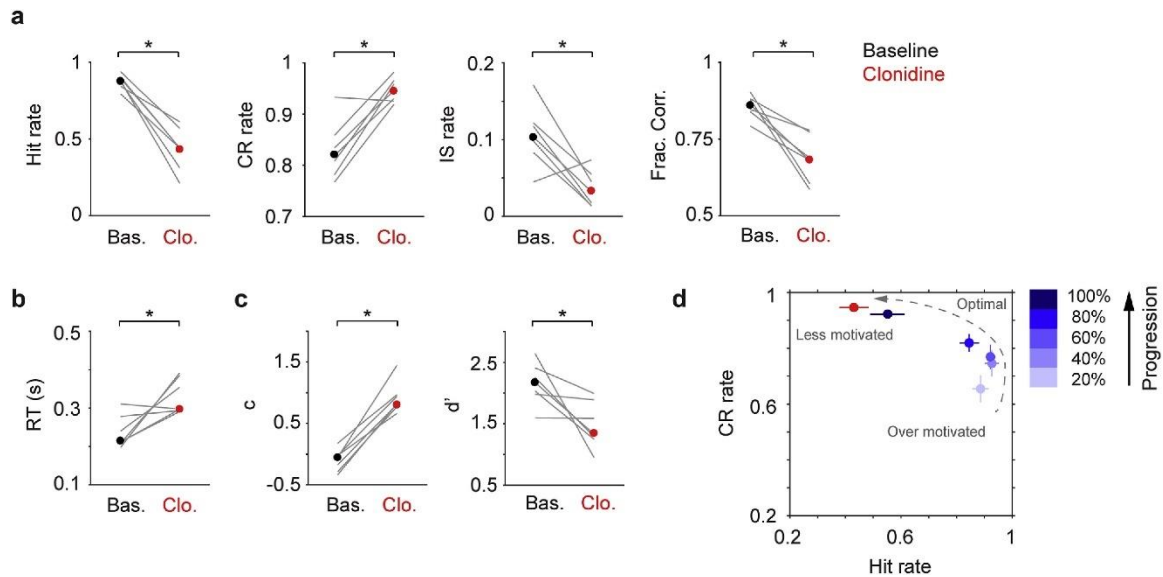
Figure 1.11 Systemic clonidine treatment impairs tactile detection.
*(**a-c**) Hit rate, CR rate, IS rate, Fraction Correct, RT, decision bias (c) and detection sensitivity (d') for baseline (black dot, median) and clonidine (red dot, median) sessions. Gray lines indicate individual consecutive two-day, baseline-clonidine pairs. Hit rate, P = 0.016, Signed rank = 28; CR rate, P = 0.031, Signed rank = 1; IS rate, P = 0.031, Signed rank = 27; Frac. Corr., P = 0.016, Signed rank = 28; RT, P = 0.031, Signed rank = 1; c, P = 0.016, Signed rank = 0; d', P = 0.016, Signed rank = 28. n = 7. (**d**) CR rate vs. Hit rate trajectory showing clonidine reduces motivation (low Hit rate and high CR rate), similar to localized infusion in Fig. 1.4h.*
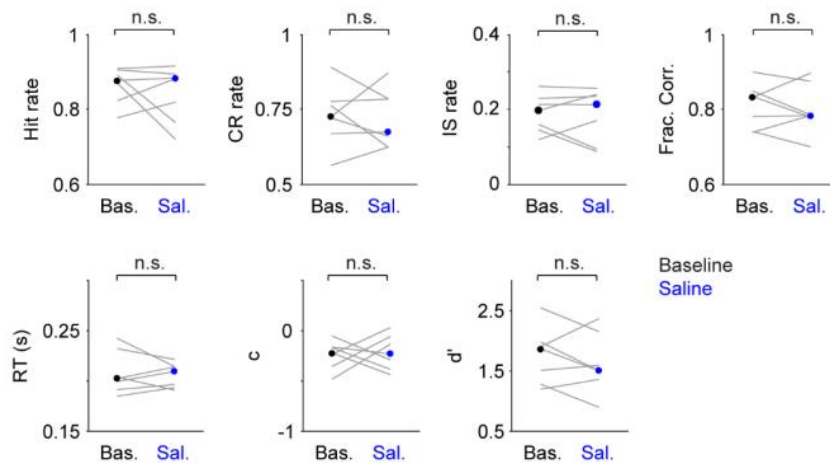
Figure 1.12 Systemic saline administration did not affect behavior.
Hit rate, P = 0.81, Signed rank = 16; CR rate, P = 1, Signed rank = 14; IS rate, P = 0.70, Signed rank = 16.5; Frac. Corr., P = 0.81, Signed rank = 16; RT, P = 0.69, Signed rank = 17; c, P = 0.58, Signed rank = 10; d', P = 0.47, Signed rank = 19. n = 7.

a

Yohimbine   Control

TH

0.1 mm

c-fos

% LC activation

**

60

30

0

Control Yohimbine

b

Baseline
Yohimbine

Hit rate

1

0.9

0.8

0.7

0   50%   100%

CR rate

1

0.8

0.6

0.4

0   50%   100%

Session progression (% trials)

c

Hit rate

1

0.9

0.8

0.7

n.s.

Bas. Yoh.

CR rate

0.9

0.3

**

Bas. Yoh.

IS rate

0.4

0.2

0

**

Bas. Yoh.

Frac. Corr.

1

0.8

0.6

**

Bas. Yoh.

d

RT (s)

0.4

0.3

0.2

0.1

n.s.

Bas. Yoh.

e

c

0.2

-0.4

-1

n.s.

Bas. Yoh.

d'

3

2

1

**

Bas. Yoh.

f

CR rate

1

0.6

0.2

Optimal

Less motivated

Over motivated

0.2   0.6   1

Hit rate

100%
80%
60%
40%
20%

Progression

59

Figure 1.13 Localized yohimbine infusion improves tactile detection.
*(**a**) Left: Example c-fos expression (red) in the LC (green) after localized yohimbine infusion. The contralateral LC serves as a basal level control. Right: c-fos expression was enhanced upon yohimbine infusion in 5 mice (P = 0.0033, two-tailed paired t-test. 2 under anesthesia, black lines; 3 during wakefulness, gray lines. Cell counts for individual mice are shown in Table 1.2). % LC activation was defined as the fraction of TH/c-fos double positive cells among TH positive cells. (**b**) Mean single-session trajectories for Hit (top) and CR (bottom) rates during baseline and yohimbine sessions (± s.e.m.). Baseline sessions were recorded one day before infusion. (**c-e**) Hit rate, CR rate, IS rate, Fraction Correct, RT, decision bias (c) and detection sensitivity (d') for baseline (black dot, median) and yohimbine (magenta dot, median) sessions. Gray lines indicate individual consecutive two-day, baseline-yohimbine pairs. Hit rate, P = 0.20, Signed rank = 11; CR rate, p = 0.0039, Signed rank = 0; IS rate, p = 0.0078, Signed rank = 44; Frac. Corr., p = 0.0039, Signed rank = 0; RT, p = 0.074, Signed rank = 7; c, p = 0.30, Signed rank = 11; d', p = 0.0078, Signed rank = 1. n = 9. (**f**) CR rate vs. Hit rate trajectory showing yohimbine transitioned mouse behavior to a near-optimal regime (high Hit rate and high CR rate), similar to mouse behavior around the middle of normal baseline sessions.*
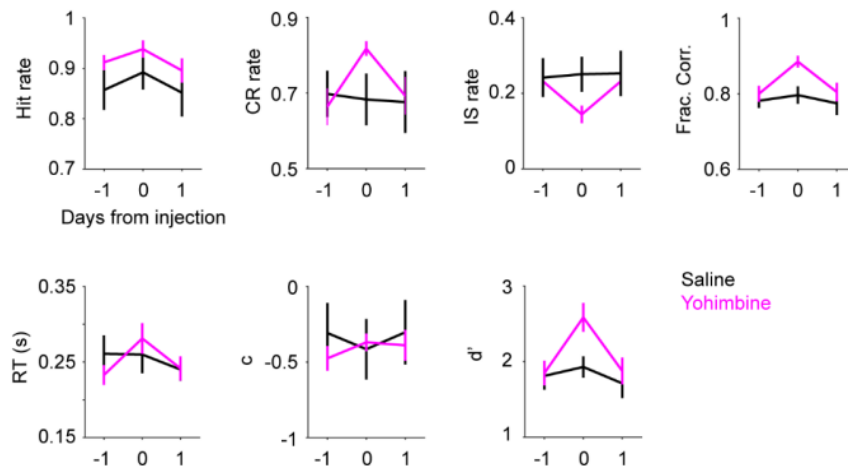
Figure 1.14 Comparing the effects of local yohimbine and saline infusions.
Mean Hit rate, CR rate, IS rate, Fraction Correct, RT, decision bias (c) and detection sensitivity (d') for 3 consecutive days (± s.e.m.). Black: saline, n = 7; Magenta: yohimbine, n = 9.
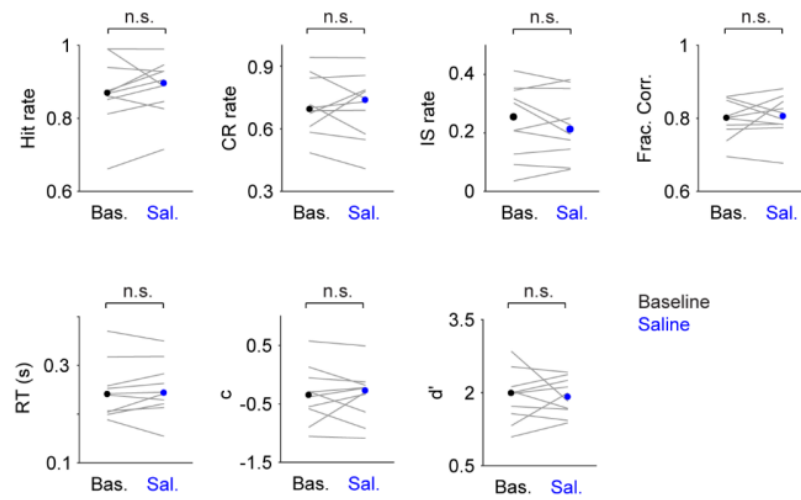
Figure 1.15 Localized saline injection did not affect behavior.
Hit rate, P = 0.32, Signed rank = 17; CR rate, P = 0.92, Signed rank = 29; IS rate, P = 0.70, Signed rank = 32; Frac. Corr., P = 0.63, Signed rank = 22; RT, P = 0.43, Signed rank = 19; c, P = 0.77, Signed rank = 31; d', P = 0.86, Signed rank = 25. n = 10.
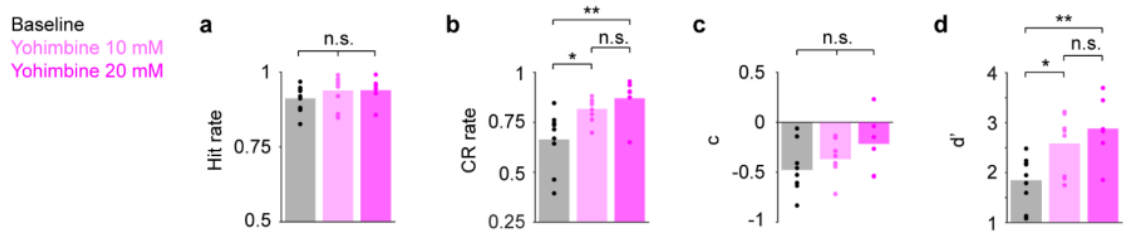
Figure 1.16 Yohimbine infusions exhibit a dose dependent trend.

*Hit rate, CR rate, decision bias (c) and detection sensitivity (d') for baseline (black, n =
9), 10 mM yohimbine (light magenta, n = 9), and 20 mM yohimbine (magenta, n = 6)
sessions. (a) Hit rate: one-way ANOVA, $F(2,21) = 0.89$, $P = 0.42$. Baseline vs. 10 mM, P
= 0.48; Baseline vs. 20 mM, P = 0.53; 10 mM vs. 20 mM, P = 1.0. (**b**) CR rate: one-way
ANOVA, $F(2,21) = 7.36$, $P = 0.0038$. Baseline vs. 10 mM, P = 0.021; Baseline vs. 20
mM, P = 0.0055; 10 mM vs. 20 mM, P = 0.66. (**c**) Decision bias: one-way ANOVA,
$F(2,21) = 2.17$, $P = 0.14$. Baseline vs. 10 mM, P = 0.61; Baseline vs. 20 mM, P = 0.18;
10 mM vs. 20 mM, P = 0.45. (**d**) Detection sensitivity: oneway ANOVA, $F(2,21) = 6.9$, P
= 0.0047. Baseline vs. 10 mM, P = 0.029; Baseline vs. 20 mM, P = 0.0061; 10 mM vs. 20
mM, P = 0.58. All post-hoc pairwise tests were Tukey-Kramer.*
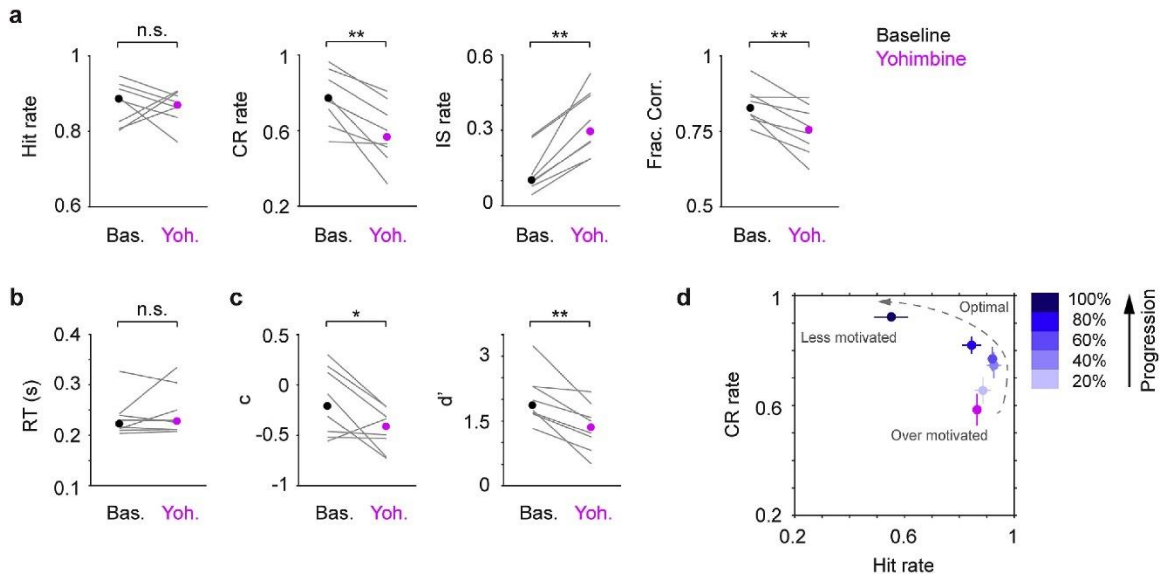
Figure 1.17 Systemic yohimbine treatment impairs tactile detection.
*(**a-c**) Hit rate, CR rate, IS rate, Fraction Correct, RT, decision bias (c) and detection*
sensitivity (d') for baseline (black dot, median) and yohimbine (magenta dot, median)
sessions. Gray lines indicate individual consecutive two-day, baseline-yohimbine pairs.
Hit rate, P = 1, Signed rank = 18; CR rate, P = 0.0078, Signed rank = 36; IS rate,
P = 0.0078, Signed rank = 0; Frac. Corr., P = 0.0078, Signed rank = 36; RT, P = 0.84,
Signed rank = 16; c, P = 0.039, Signed rank = 33; d', P = 0.0078, Signed rank = 36.
*n = 8. (**d**) CR rate vs. Hit rate trajectory showing yohimbine promotes impulsivity (high*
Hit rate and low CR rate), which coincides with mouse behavior at the beginning of
normal baseline sessions.

Clonidine								
Mouse Number	1		2		3		4	
	Left	Right	Left	Right	Left	Right	Left	Right
TH positive cells	424	406	389	252	299	325	169	178
TH/c-fos double positive cells	16	56	15	19	106	130	13	26
c-fos expression level (%)	3.8	13.8	3.9	7.5	35.5	40.0	7.7	14.6
	p < 1e-5		p = 0.0021		p = 0.060		p = 0.0049	

Table 1.1 Quantification of c-fos expression to examine the effect of localized clonidine infusion on LC activity in 4 awake mice.
Clonidine was infused in the left LC. The right LC serves as a basal level control. Permutation test was performed (10^5 iterations) to compare c-fos expression levels between the left and right LC in individual mice.

Yohimbine										
Mouse Number	1		2		3		4		5	
	Left	Right	Left	Right	Left	Right	Left	Right	Left	Right
TH positive cells	531	536	416	402	100	196	355	382	501	458
TH/c-fos double positive cells	209	106	112	12	52	51	191	153	104	48
c-fos expression level (%)	39.4	19.8	26.9	3.0	52.0	26.0	53.8	40.1	20.8	10.5
	p < 1e-5		p < 1e-5		p < 1e-5		p < 1e-5		p < 1e-5	

Table 1.2 Quantification of c-fos expression to examine the effect of localized yohimbine infusion on LC activity in 5 mice.
Yohimbine was infused in the left LC (Mouse 1 and 2: anesthesia; Mouse 3–5: awake). The right LC serves as a basal level control. Permutation test was performed (10^5 iterations) to compare c-fos expression levels between the left and right LC in individual mice.

Saline				
Mouse Number	1		2	
	Left	Right	Left	Right
TH positive cells	453	442	586	577
TH/c-fos double positive cells	40	41	117	132
c-fos expression level (%)	8.8	9.3	20.0	22.9
	p = 0.41		p = 0.051	

Table 1.3 Quantification of c-fos expression to examine the effect of localized saline infusion on LC activity in 2 awake mice.
Saline was infused in the left LC. The right LC serves as a basal level control. Permutation test was performed (105 iterations) to compare c-fos expression levels between the left and right LC in individual mice.

Chapter 2 - The Locus Coeruleus Mediates Behavioral Flexibility

Abstract

Behavioral flexibility refers to the ability to adjust behavioral strategies in response to changing environmental contingencies. A major hypothesis in the field posits that the activity of neurons in the locus coeruleus (LC) plays an important role in mediating behavioral flexibility. To test this hypothesis, we developed a novel context-dependent bilateral tactile detection task where mice responded to left and right whisker deflections in a rule-dependent manner and exhibited varying degrees of flexible switching behavior. Recording from optogenetically-tagged neurons in the LC during task performance revealed a prominent graded correlation between baseline LC activity and behavioral flexibility, where higher baseline activity following a rule change was associated with faster behavioral switching to the new rule. Increasing baseline LC activity with optogenetic activation improved task performance and accelerated task switching. Overall, our study provides strong evidence to demonstrate that LC activity mediates behavioral flexibility.

Introduction

Behavioral flexibility, the ability to adapt goal-directed responses to changing environmental contexts and demands, is critical to the survival of organisms. For example, a pedestrian in New York should first look left to check incoming traffic before crossing a street. The same person in London would suppress this habitual response and

look to the right instead. Inappropriate behavioral adaptations are observed in a broad spectrum of psychiatric disorders and aging (Uddin, 2021). Understanding the neural substrates of behavioral flexibility is a major topic of systems neuroscience research.

Several key brain structures have been implicated in supporting flexible behavioral switching (Devauges and Sara, 1990; Birrell and Brown, 2000; Lapiz and Morilak, 2006; Rich and Shapiro, 2009; Durstewitz et al., 2010; Janitzky et al., 2015; Martins and Froemke, 2015; Glennon et al., 2019; Bartolo and Averbeck, 2020), including the noradrenergic nucleus locus coeruleus (LC). A major hypothesis in the field posits that the activity of LC neurons plays a critical role in mediating behavioral flexibility (Aston-Jones et al., 1999; Aston-Jones and Cohen, 2005; Sara and Bouret, 2012). This hypothesis is primarily built upon electrophysiological evidence from non-human primates and rodents showing that LC responds to salient stimuli and that LC activity reflects behavioral states and task performance (e.g., Aston-Jones and Bloom, 1981; Aston-Jones et al., 1994; Rajkowski et al., 1994, 2004; Usher et al., 1999; Clayton et al., 2004). Other studies have reported that LC activity is associated with rule changes (Aston-Jones et al., 1997; Bouret and Sara, 2004; Janitzky et al., 2015; Martins and Froemke, 2015; Glennon et al., 2019; Xiang et al., 2019). However, to the best of our knowledge, it is currently unknown whether and how LC activity is linked to different degrees of behavioral flexibility. Furthermore, no prior work has directly tested this hypothesis by recording and perturbing genetically-defined noradrenergic neurons in the LC during a rule-shift task to determine causal relationships between LC activity and behavioral flexibility. Answering these questions is a critical step toward unraveling the

molecular, cellular and circuit mechanisms underlying LC modulation of behavioral flexibility and cognitive functions.

To bridge these knowledge gaps and to assess the extent to which the LC contributes to flexible task switching, we developed a novel context-dependent bilateral tactile detection task in head-fixed mice, where mice were trained to respond to left and right single-whisker deflections in a rule-dependent manner and exhibited varying degrees of flexible switching behavior within individual sessions. During task performance, we recorded from optogenetically-tagged noradrenergic neurons in the LC and established a graded relationship between LC spiking activity and flexible task switching. Higher behavioral flexibility (faster switching to the new rule) was characterized by a greater increase in baseline LC activity upon the rule change compared with lower behavioral flexibility (slower switching to the new rule). Increasing baseline LC activity with optogenetic activation led to robust improvements in task switching and task performance. Together, our data provide strong evidence to support that the LC is critical in mediating flexible behavioral switching.

Results

Mice exhibit flexible and inflexible behaviors within single sessions

We developed a novel context-dependent bilateral tactile detection task to probe behavioral flexibility in head-fixed mice. There were two rules (contexts) in the task: Left Go and Right Go, and mice were trained to adapt to repeated rule changes within individual behavioral sessions (Figure 2.1a-c, Methods). On each trial, one of the two

whiskers (left or right C2) was stimulated. For the Left Go rule, the left whisker

deflection was the Go stimulus and the right whisker deflection was the NoGo stimulus,

and vice versa for the Right Go rule. Licking during a response window following

whisker stimulation determined trial outcome (Figure 2.1b-c). Individual sessions

typically consisted of 2-3 blocks, with each block consisting of 100-200 trials. The rule of

the first block (Block 1) was randomly assigned, and each subsequent block had the

alternate rule as the preceding block (e.g., Block 1: Left Go; Block 2: Right Go, Figure

2.1a). The beginning of each block consisted of 5-10 'cueing trials', where the

presentation of the Go stimulus was paired with water delivery (Methods). Since block 1

did not involve a rule change, subsequent analyses were focused on the blocks following

block 1, with switch performance referring to task performance (fraction correct) in these

blocks. The training process took several weeks (Figure 2.1d), and mice were considered

well trained once their switch performance in block 2 was above 65% for two

consecutive days (Chevée et al., 2021) (Methods). Mice were able to perform Left Go

and Right Go blocks at similar levels (i.e., no apparent 'handedness', Figure 2.2a), so

both types of blocks were pooled in subsequent analyses.

We noticed that well-trained mice exhibited varying degrees of switch

performance following a rule change (Figure 2.1e, f). To quantify the degree of flexible

task switching, we defined a behavioral switch point where task performance in a 50-trial

moving window surpassed a threshold of 85% (Methods). Notably, behavioral switch

point exhibited a strong negative correlation with switch performance (Figure 2.1g).

Since behavioral switch point followed a bimodal distribution separated around trial 50,

we referred to blocks with behavioral switch point below trial 50 as 'flexible blocks' and those above as 'inflexible blocks' (Figure 2.1h). As expected, switch performance in flexible blocks was significantly higher than in inflexible blocks (Figure 2.1i). To test whether such changes in switch performance were due to variations in motivational states (Berditchevskaia et al., 2016; Allen et al., 2019; McBurney-Lin et al., 2020), we did further analysis to show that neither flexible nor inflexible blocks were preferentially concentrated toward the beginning or the end of individual sessions (Figure 2.2b). Additionally, reaction time and number of licks were not different between flexible and inflexible blocks (Figure 2.2c). These results strongly suggest that motivational changes during a session cannot account for the differences in task switching between flexible and inflexible blocks. Together, our data demonstrate that mice exhibited varying degrees of flexible switching behavior in the novel context-dependent bilateral tactile detection task.

LC spiking is monotonically linked to task switching

Next, we recorded spiking activity from optogenetically-tagged single units in the LC and pupil diameter during task performance (Figure 2.3a, b). Based on previous work (Aston-Jones et al., 1997; Usher et al., 1999; Yang et al., 2021), we hypothesized that the pre-stimulus baseline LC activity was associated with the degree of behavioral flexibility. To test this, we first analyzed baseline LC activity (quantified in 1-s window preceding whisker stimulation onset) before and after the rule change in a subset of sessions where both a flexible block and an inflexible block occurred (14 blocks from 7 sessions, for paired comparison) and found that LC spiking was elevated following the rule change

only in the flexible blocks (Figure 2.3c-e). That is, in blocks where mice more promptly adapted their responses to the new rule, baseline LC activity was transiently elevated following the rule change (After), compared with the baseline LC activity right before the rule change (i.e., at the end of the previous block - Before, Figure 2.3e, f, Methods). The changes in baseline activity upon the rule shift (ΔFiring rate: After – Before) was also higher in flexible blocks than inflexible blocks (Flexible vs. Inflexible, 0.50 ± 0.16 vs. -0.28 ± 0.16 sp/s, $p = 0.02$, Figure 2.3f). Similar trends held when we included flexible and inflexible blocks that were not necessarily from the same sessions (i.e., unpaired comparison, Figure 2.4a). Importantly, changes in baseline LC activity upon the rule shift exhibited a graded and significant negative correlation with behavioral switch point (Figure 2.3g, Pearson correlation coefficient = -0.42, $p = 0.0026$), substantiating and extending the findings based on the binarized flexible and inflexible blocks. Licking behavior during flexible and inflexible blocks were similar (Figure 2.4b), and the trend of LC activity held when we only included hit trials in the analysis (Figure 2.4c, d). In addition, baseline activity was quantified prior to any possible licking events in a trial. Together, these lines of evidence strongly suggest that the observed changes in LC activity were not a direct effect of licking itself (Zagha et al., 2022).

To further determine whether the observed changes in baseline LC activity reflected true changes in behavioral flexibility, we quantified task performance in trial blocks immediately preceding the identified flexible and inflexible blocks. Performance in blocks immediately preceding the flexible blocks (i.e., blocks with a different rule) was comparable to the performance in those flexible blocks. In contrast, task performance in

blocks immediately preceding the inflexible blocks was higher than the performance in the inflexible blocks (Figure 2.4e). These results strongly suggest that 1) the identified flexible blocks and the associated LC activity reflected true flexible task switching, such that mice were adapting to both rules, instead of simply following one rule; and 2) the identified inflexible blocks and the associated LC activity reflected true inability to switch to the new rule, instead of an overall lack of performance in the task. Although pupil diameter was bigger in the After period in both flexible and inflexible blocks, the changes in pupil diameter upon the rule shift (ΔPupil: After - Before) were slightly bigger in the flexible blocks than the inflexible blocks (Figure 2.4f), consistent with the trend of LC activity. Overall, our data show that baseline LC activity was correlated with the degree of flexible task switching, such that higher baseline activity following the rule change was associated with a faster behavioral adaptation to the new rule.

LC activation improves task switching

Next, to determine the causal role of LC activity in behavioral flexibility, we optogenetically activated LC neurons during behavior. We recruited mice that had been trained for >4 weeks with switch performance consistently below the 65% threshold. Adapted from the paradigm used in a previous study (Glennon et al., 2019), optical stimulation (10 Hz, 10 mW) was delivered in a 0.5-s window prior to whisker stimulation onset in trials following the rule change (Figure 2.5a, Methods). Channelrhodopsin-2 (ChR2) was expressed in the LC of both test and control groups, but test group had the optical fiber implanted in the LC, and the control group with optical fiber implanted away

74

from the LC (Figure 2.6a). The fiber implant was confirmed by pupil responses to optical stimulation (Figure 2.5b, Privitera et al., 2020; Megemont et al., 2022). Switch performance of the test group noticeably improved upon LC stimulation compared with previous sessions without stimulation (Baseline vs. Stimulation: 0.52 ± 0.02 vs. 0.69 ± 0.02 fraction correct, $p = 1.6e-5$), and the improvement was also present in individual mice (Figure 2.5c, d, f. For extended baseline periods refer to Figure 2.6b, c). The behavioral effects appeared to be specific to switching behavior as task performance in the first block (block 1) was not affected (Figure 2.6d). LC stimulation also accelerated task switching in the test group (Behavioral switch point, Baseline vs. Stimulation: 154 ± 8 vs. 116 ± 13 trials, $p = 0.02$, Figure 2.5g). In contrast, optogenetic stimulation had no effect on task switching in the control group (Figure 2.5c, e-g, Figure 2.6b, c). The behavioral improvement in the test group appeared to be due to an increase of correct rejection rate, but not hit rate (Figure 2.5h, i, Figure 2.6e, f), in line with a previous report (Glennon et al., 2019). Licking behavior was not affected by optical stimulation thus cannot account for the increase in correct rejection rate (Figure 2.6g, h). In summary, increasing baseline LC activity with optogenetics facilitated flexible task switching.

Discussion

In this work, we set out to test the hypothesis that the LC is involved in mediating behavioral flexibility. We developed a novel context-dependent bilateral tactile detection task where head-fixed mice exhibited varying degrees of flexible task switching upon a rule change within single sessions. Using this task, we found that the magnitude of

baseline LC activity following the rule change was closely correlated with the degree of flexible task switching. Specifically, higher baseline activity upon the rule shift was associated with faster behavioral switching. Next, we optogenetically enhanced baseline LC activity and observed improved task performance and accelerated task switching. Overall, our study highlights the role of LC in behavioral flexibility and provides strong evidence to support that LC activity mediates flexible task switching.

Pre-stimulus baseline LC activity exhibited a relatively small (<1 spike/s) yet significant increase during flexible switching, in line with prior work showing similar magnitude of firing rate changes (commonly referred to as tonic activity) associated with behavioral states or rule shifts (e.g., Aston-Jones and Bloom, 1981; Aston-Jones et al., 1997; Usher et al., 1999; Xiang et al., 2019). Importantly, we uncovered that such activity exhibited a graded, negative relationship with the degree of behavioral flexibility. We also noted that LC neurons transiently responded to the auditory tone and whisker stimulation (commonly referred to as phasic activity in the literature), and found relatively weak relationships between such responses and task switching (Figure 2.7).

Our perturbation data support recent work showing that activating the LC facilitated auditory reversal learning (Martins and Froemke, 2015; Glennon et al., 2019). One major distinction in our study is that the current task is essentially a continuous reversal task where prior to LC stimulation mice had been trained to adapt to multiple reversal stages (blocks) within single sessions, similar to the task structure of a recent study (Chevée et al., 2021). This task design allows us to assess the relationship between LC activity and rapid, 'real-time' behavioral switching within individual sessions.

Specifically, the association between baseline LC activity and the degree of flexible task switching was transient (~20 trials, equivalent to 2-3 minutes, Figure 2.3e. Also see Aston-Jones et al., 1997). Secondly, LC optical stimulation was delivered in a subset of trials (a total of ~20-30 trials per block, Methods) and the behavioral improvement was present from the first stimulation session (day 1, Figure 2.5c). As a result, long-term plasticity mechanisms, such as structural synaptic changes, are unlikely to underlie such rapid associations between LC activity and behavioral switching. Nevertheless, it is worth noting that in a recent study where LC stimulation was paired with the target tone in a relatively long-term fashion, rats were found to better suppress their responses to non-target tones (Glennon et al., 2019), consistent with an increase of correct rejection rate in our task. Together, these studies suggest that LC activity facilitates behavioral flexibility across different time scales, likely through different mechanisms.

How does LC activity drive behavioral flexibility? This remains a major challenge in the field. Ample prior research has shown that noradrenergic (NA) signaling from the LC modulates neuronal responses to sensory stimuli in various sensory-related brain structures (Berridge and Waterhouse, 2003; McBurney-Lin et al., 2019). Thus, the transient increase of LC activity following the rule change may modulate neuronal responses to the new Go and/or NoGo stimulus (Devilbiss and Waterhouse, 2004; Devilbiss et al., 2006; Martins and Froemke, 2015; Rodenkirch et al., 2019) to better separate signal and noise representations. Another possibility is that LC-NA signaling facilitates the reshaping of the relevant stimulus representation to more effectively influence behavior (Ruff and Cohen, 2016, 2019). On the other hand, decades of work

has established the importance of the prefrontal cortex (PFC) in behavioral flexibility (Miller and Cohen, 2001; Le Merre et al., 2021; Uddin, 2021), and LC-NA signaling heavily influences PFC functions (Arnsten and Li, 2004; Ramos and Arnsten, 2007; Arnsten et al., 2012). Transient changes in LC activity may dynamically modulate synaptic efficacy and recurrent activity in the PFC to affect top-down regulation of the relevant and irrelevant stimuli (Arnsten et al., 2012; Zagha, 2020) and to facilitate reorienting behavior (Sara and Bouret, 2012). Future experiments with simultaneous recordings from LC-NA and sensory/executive areas will elucidate how LC-NA activity modulates bottom-up processing and top-down commands to influence behavioral flexibility.

Methods

Mice

All procedures were performed in accordance with protocols approved by UC Riverside Animal Care and Use Committee (AUP 20190031). Mice were DBH-Cre (B6.FVB(Cg)-Tg(Dbh-cre) KH212Gsat/Mmucd, 036778-UCD, MMRRC); Ai32 (RCL-ChR2(H134R)/EYFP, 012569, JAX), singly housed in a vivarium with a reversed light-dark cycle (12 hr/12 hr).

Surgery

Procedures for headpost and custom optrode microdrive implants have been described in detail previously (Yang et al., 2016, 2021). Briefly, 8-12 week old male and

female mice were implanted with titanium headposts, leaving a window open above the left cerebellum for subsequent tetrode implants. Custom tetrode microdrives were made with eight tetrode wires surrounding an optic fiber (0.39 NA, 200 um core) to make extracellular recordings from opto-tagged LC neurons. The microdrive was implanted targeting the left LC. Mice were then allowed to recover for at least 72 hours before beginning water restriction and behavior training.

Behavior task

Mice were water restricted to 1mL/day for at least seven days prior to behavior training. Behavior tasks were controlled via a custom-based Arduino hardware and software and acquired in WaveSurfer (https://www.janelia.org/open-science/wavesurfer), and one behavior session was performed per day. Mice were first trained to a modified version of the Go/NoGo single-whisker detection task described previously (Yang et al., 2016; McBurney-Lin et al., 2020). In brief, mice reported whether they perceived a brief deflection (0.2-s, 25-Hz sinusoidal deflection) to either the right or the left C2 whisker by licking a water port during a 1-s response window. On Go trials, stimulation of the right or the left whisker was delivered in alternating blocks (e.g., first 100 trials, stimuli are presented to the right whisker, following 100 trials to the left, etc.). On NoGo trials, no whisker stimulation was delivered and mice were trained to withhold licking. Mice readily learned this stage within 7 days (>75% overall performance). Mice were then introduced to the second stage of training, in which an identical whisker deflection was presented in NoGo trials on the contralateral side to the Go stimulus (e.g., left stimulus:

Go; right stimulus: NoGo). Similar to the first stage of training, the stimuli were presented in block structures, with the Go stimulus alternating from left to right whiskers. Early during this stage of training, a single rule switch was implemented and each block consisted of 200 trials. The first block rule was randomly assigned as either left Go/right NoGo or right Go/left NoGo. As the mouse became more proficient in switching, the blocks were shortened in increments of 50 trials and additional 1-2 rule changes added. Therefore, as mice learned the task, more rule changes were introduced into single sessions. The mice in this study could execute between one and three rule changes in a session.

The beginning of each block consisted of a 'cueing window', which was a period of 5-10 consecutive Go trials where whisker stimulation was paired with water delivery, designed to facilitate adaptation to the new rule. A 0.1-s auditory cue (8 kHz, ~80 dB SPL) signaled the start of each trial, followed by a 1.5-s delay before whisker stimulation. If mice licked in this delay window, the trial was aborted and the next trial began after a 5-10 second timeout. Ambient white noise (cut off at 40 kHz, ~80 dB SPL) was played continuously to mask any potential cues that can be associated with the task. Go and NoGo trials represented 90% of all trials. Catch trials represented the remaining 10%, in which no whisker stimulation was presented, and mice were trained to withhold licking. In Go trials, the Go stimulus for the current block was delivered, and mice were expected to report its presence by licking the water port within a 1-s window immediately following stimulus cessation. Correct responses to the Go stimulus presentation were qualified as 'hit' trials and rewarded with a water drop (~5uL). Withholding licking to the

Go stimulus were qualified as 'miss' trials. Withholding licking to the NoGo stimulus and in catch trials were unrewarded and qualified as 'correct rejection'. Licking to the NoGo stimulus and in catch trials were qualified as 'false alarm' and punished with a 5-s timeout. If the mouse licked again within the timeout period but at least 1-s after the initial response, there was a subsequent 5-s punishment, with up to three consecutive timeouts allowed per trial. To further assist mice suppress licking to the NoGo stimulus, a NoGo trial was designed to follow a 'false alarm' trial (Aruljothi et al., 2020), and up to 4 consecutive NoGo trials were allowed to occur. As a result, behavioral sessions typically consisted of more NoGo trials than Go trials (~55% vs. 45%).

Electrophysiology

Once mice reached the trained performance threshold (65%, block 2), the microdrive was advanced at regular intervals (75 um/day) towards LC. LC neurons were identified by optogenetic tagging, tail pinch response, and post-hoc lesions. Thirty-four single-unit recordings (cluster quality measure Lratio: 0.01 ± 0.005; firing rate: 2.44 ± 0.30 spikes/s; percent ISI < 10 ms: $1.21\% \pm 0.42\%$) from six mice performing the context-dependent bilateral tactile detection task (see below) were extracted using MClust (Redish, 2014), along with synchronous recording of the left pupil. Optogenetic activation experiments were acquired from 7 mice (4 test, 3 control) that had been trained for >4 weeks on the bilateral task with performance consistently below the 65% threshold. Prior to optogenetic experiments, placement of optic fibers was assessed by pupil responses to optical stimulation under anesthesia (10 ms pulses, 10 Hz, 10 mW).

Optogenetics

Optogenetic stimulation (10 ms pulses, 10 Hz, 10 mW) was delivered using a 450 nm blue diode laser (UltraLasers, MDL-III-450-200mW) and controlled by WaveSurfer. The mating between sleeve and ferrule was covered with polymer clay to prevent light leakage. Stimulation of LC neurons was delivered on Go trials during a 0.5-s window prior to whisker stimulation onset. Video of the left pupil was acquired at 20 Hz using a Basler acA1300-200um camera and Pylon software. Pupil diameter was measured offline using DeepLabCut (Mathis et al., 2018). Electrophysiology recording, pupil tracking, and optogenetic stimulation were synchronized via a common TTL pulse train.

Histology

At the conclusion of all experiments, electrolytic lesions were made and brains perfused with PBS, followed by 4% PFA. The brains were post-fixed in 4% PFA overnight, then cut into 100 um coronal sections and stained with anti-Tyrosine Hydroxylase (TH) antibody (Thermo-fisher OPA1-04050) and anti-EGFP antibody (Thermo-fisher A-11039).

Data analysis

Switch performance (fraction correct) was quantified in blocks other than the first block (block 1) in a session. To compute the behavioral switch point in a block, task performance was first quantified using a 50-trial moving window. Behavioral switch point was defined as the beginning of the moving window within which the average task

performance surpassed 85% threshold (Figure 2.3 results held when using other thresholds between 75% and 85%, data not shown). If this criterion was never met, i.e., task performance in the 50-trial moving window never reached 85% threshold within the block, switch point was set as the total number of trials in that block. For Figure 2.1d, switch performance was quantified in block 2 as early training sessions only had 2 blocks. For Figure 2.1g-i, 84 blocks from 11 mice were included.

For Figure 2.3, baseline LC activity was quantified in a 1-s window prior to whisker stimulation onset. 20 trials before the rule change (i.e., last 20 trials in the previous block) were considered as the Before period, and 20 trials after the rule change were considered as the After period. For Figure 2.3d, the average firing rate in the Before and After periods was smoothed using a 150-ms window. Figure 2.3e quantified the 10-trial averaged baseline firing rate for ±50 trials from the rule change. The change (Δ) in baseline firing rate was calculated as baseline LC activity in the Before period subtracted from the After period (After - Before; Figure 2.3f, g). For Figure 2.3g, 49 blocks from 6 mice were presented, a subset of the sessions as in Figure 2.1g-i.

In Figure 2.5, optogenetic stimulation began at the beginning of each block and ended 50 trials after the cueing trials. Stimulation (10-ms pulse train at 10 Hz and 10 mW) was delivered on Go trials only, starting at 0.5 s before whisker stimulation onset and ending at the onset. Switch performance and switch point were quantified in block 2 as majority of the sessions had 2 blocks. 5 consecutive baseline sessions (no stimulation) and 5 consecutive stimulation sessions from each mouse were included for analysis (1 session per day). For Figure 2.5d, e, analyses were performed for individual mice

separately. For Figure 2.5 f-i, sessions were pooled from all mice in each condition (i.e., 20 sessions from the test group (4 mice) and 15 sessions from the control group (3 mice) in each condition).

Data were reported as mean ± s.e.m. unless otherwise noted. We did not use statistical methods to predetermine sample sizes. Sample sizes are similar to those reported in the field. We assigned mice to experimental groups arbitrarily, without randomization or blinding. Statistical tests were two-tailed Wilcoxon signed rank (paired) or rank sum (unpaired) unless otherwise noted.

References

Allen WE, Chen MZ, Pichamoorthy N, Tien RH, Pachitariu M, Luo L, Deisseroth K (2019) Thirst regulates motivated behavior through modulation of brainwide neural population dynamics. Science (80-) 364:0–10.

Arnsten AFT, Wang MJ, Paspalas CD (2012) Neuromodulation of Thought: Flexibilities and Vulnerabilities in Prefrontal Cortical Network Synapses. Neuron 76:223–239 Available at: http://dx.doi.org/10.1016/j.neuron.2012.08.038.

Arnsten AFTT, Li B (2004) Neurobiology of executive functions: Catecholamine influences on prefrontal cortical functions. Biol Psychiatry Available at: https://linkinghub.elsevier.com/retrieve/pii/S0006322304009333.

Aruljothi K, Marrero K, Zhang Z, Zareian B, Zagha E (2020) Functional Localization of an Attenuating Filter within Cortex for a Selective Detection Task in Mice. J Neurosci 40:JN-RM-2993-19.

Aston-Jones G, Bloom FE (1981) Activity of norepinephrine-containing locus coeruleus neurons in behaving rats anticipates fluctuations in the sleep-waking cycle. J Neurosci 1:876–886.

Aston-Jones G, Cohen JD (2005) An integrative theory of locus coeruleus-norepinephrine function: Adaptive gain and optimal performance. Annu Rev Neurosci 28:403–450.

Aston-Jones G, Rajkowski J, Cohen J (1999) Role of locus coeruleus in attention and behavioral flexibility. Biol Psychiatry 46:1309–1320.

Aston-Jones G, Rajkowski J, Kubiak P (1997) Conditioned responses of monkey locus coeruleus neurons anticipate acquisition of discriminative behavior in a vigilance task. Neuroscience 80:697–715 Available at: http://linkinghub.elsevier.com/retrieve/pii/S0306452297000602.

Aston-Jones G, Rajkowski J, Kubiak P, Alexinsky T (1994) Locus coeruleus neurons in monkey are selectively activated by attended cues in a vigilance task. J Neurosci 14:4467–4480.

Bartolo R, Averbeck BB (2020) Prefrontal Cortex Predicts State Switches during Reversal Learning. Neuron 106:1044-1054.e4.

Berditchevskaia A, Cazé RD, Schultz SR (2016) Performance in a GO/NOGO perceptual task reflects a balance between impulsive and instrumental components of behaviour. Sci Rep 6:1–15 Available at: http://dx.doi.org/10.1038/srep27389.

Berridge CW, Waterhouse BD (2003) The locus coeruleus-noradrenergic system: Modulation of behavioral state and state-dependent cognitive processes. Brain Res Rev 42:33–84 Available at: http://www.ncbi.nlm.nih.gov/pubmed/12668290.

Birrell JM, Brown VJ (2000) Medial frontal cortex mediates perceptual attentional set shifting in the rat. J Neurosci 20:4320–4324 Available at: http://www.ncbi.nlm.nih.gov/pubmed/10818167.

Bouret S, Sara SJ (2004) Reward expectation, orientation of attention and locus coeruleus-medial frontal cortex interplay during learning. Eur J Neurosci 20:791–802 Available at: http://www.ncbi.nlm.nih.gov/pubmed/15255989 [Accessed July 10, 2014].

Chevée M, Finkel EA, Kim S-J, O'Connor DH, Brown SP (2021) Neural activity in the mouse claustrum in a cross-modal sensory selection task. Neuron:1–16 Available at: https://linkinghub.elsevier.com/retrieve/pii/S089662732100951X.

Clayton EC, Rajkowski J, Cohen JD, Aston-Jones G (2004) Phasic activation of monkey locus ceruleus neurons by simple decisions in a forced-choice task. J Neurosci 24:9914–9920 Available at: http://www.jneurosci.org/cgi/doi/10.1523/JNEUROSCI.2446-04.2004.

Devauges V, Sara SJ (1990) Activation of the noradrenergic system facilitates an attentional shift in the rat. Behav Brain Res 39:19–28.

Devilbiss DM, Page ME, Waterhouse BD (2006) Locus Ceruleus Regulates Sensory Encoding by Neurons and Networks in Waking Animals. J Neurosci 26:9860–9872.

Devilbiss DM, Waterhouse BD (2004) The effects of tonic locus ceruleus output on sensory-evoked responses of ventral posterior medial thalamic and barrel field cortical neurons in the awake rat. J Neurosci 24:10773–10785 Available at: http://www.ncbi.nlm.nih.gov/pubmed/15574728 [Accessed July 11, 2014].

Durstewitz D, Vittoz NM, Floresco SB, Seamans JK (2010) Abrupt transitions between prefrontal neural ensemble states accompany behavioral transitions during rule learning. Neuron 66:438–448

Glennon E, Carcea I, Martins ARO, Multani J, Shehu I, Svirsky MA, Froemke RC (2019) Locus coeruleus activation accelerates perceptual learning. Brain Res 1709:39–49

Janitzky K, Lippert MT, Engelhorn A, Tegtmeier J, Goldschmidt J, Heinze H-J, Ohl FW (2015) Optogenetic silencing of locus coeruleus activity in mice impairs cognitive flexibility in an attentional set-shifting task. Front Behav Neurosci 9:1–8

Lapiz MDS, Morilak DA (2006) Noradrenergic modulation of cognitive function in rat medial prefrontal cortex as measured by attentional set shifting capability. Neuroscience 137:1039–1049.

Le Merre P, Ährlund-Richter S, Carlén M (2021) The mouse prefrontal cortex: Unity in diversity. Neuron:1–20 Available at: https://linkinghub.elsevier.com/retrieve/pii/S0896627321002051.

Martins ARO, Froemke RC (2015) Coordinated forms of noradrenergic plasticity in the locus coeruleus and primary auditory cortex. Nat Neurosci 18:1483–1492 Available at: http://www.nature.com/doifinder/10.1038/nn.4090.

McBurney-Lin J, Lu J, Zuo Y, Yang H (2019) Locus coeruleus-norepinephrine modulation of sensory processing and perception: A focused review. Neurosci Biobehav Rev 105:190–199 Available at: https://linkinghub.elsevier.com/retrieve/pii/S0149763418309771.

McBurney-Lin J, Sun Y, Tortorelli LS, Nguyen QAT, Haga-Yamanaka S, Yang H (2020) Bidirectional pharmacological perturbations of the noradrenergic system differentially affect tactile detection. Neuropharmacology 174.

Megemont M, McBurney-Lin J, Yang H (2022) Pupil diameter is not an accurate real-time readout of locus coeruleus activity. Elife 11:1–17 Available at: https://elifesciences.org/articles/70510.

Miller EK, Cohen JD (2001) An Integrative Theory of Prefrontal Cortex Function. Annu Rev Neurosci 24:167–202 Available at: http://www.annualreviews.org/doi/10.1146/annurev.neuro.24.1.167.

Privitera M, Ferrari KD, von Ziegler LM, Sturman O, Duss SN, Floriou-Servou A, Germain P, Vermeiren Y, Wyss MT, De Deyn PP, Weber B, Bohacek J (2020) A complete pupillometry toolbox for real-time monitoring of locus coeruleus activity in rodents. Nat Protoc Available at: http://dx.doi.org/10.1038/s41596-020-0324-6.

Rajkowski J, Kubiak P, Aston-Jones G (1994) Locus coeruleus activity in monkey: Phasic and tonic changes are associated with altered vigilance. Brain Res Bull 35:607–616.

Rajkowski J, Majczynski H, Clayton E, Aston-Jones G (2004) Activation of monkey locus coeruleus neurons varies with difficulty and performance in a target detection task. J Neurophysiol 92:361–371.

Ramos BP, Arnsten AFT (2007) Adrenergic pharmacology and cognition: Focus on the prefrontal cortex. Pharmacol Ther 113:523–536.

Rich EL, Shapiro M (2009) Rat prefrontal cortical neurons selectively code strategy switches. J Neurosci 29:7208–7219.

Rodenkirch C, Liu Y, Schriver BJ, Wang Q (2019) Locus coeruleus activation enhances thalamic feature selectivity via norepinephrine regulation of intrathalamic circuit dynamics. Nat Neurosci 22:120–133 Available at: http://www.nature.com/articles/s41593-018-0283-1.

Ruff DA, Cohen MR (2016) Attention Increases Spike Count Correlations between Visual Cortical Areas. J Neurosci 36:7523–7534 Available at: http://www.jneurosci.org/cgi/doi/10.1523/JNEUROSCI.0610-16.2016.

Ruff DA, Cohen MR (2019) Simultaneous multi-area recordings suggest that attention improves performance by reshaping stimulus representations. Nat Neurosci Available at: http://dx.doi.org/10.1038/s41593-019-0477-1.

Sara SJ, Bouret S (2012) Orienting and Reorienting: The Locus Coeruleus Mediates Cognition through Arousal. Neuron 76:130–141 Available at: http://dx.doi.org/10.1016/j.neuron.2012.09.011.

Uddin LQ (2021) Cognitive and behavioural flexibility: neural mechanisms and clinical considerations. Nat Rev Neurosci

Usher M, Cohen JD, Servan-Schreiber D, Rajkowski J, Aston-Jones G (1999) The Role of Locus Coeruleus in the Regulation of Cognitive Performance. Science (80-) 283:549–554

Xiang L, Harel A, Gao HY, Pickering AE, Sara SJ, Wiener SI (2019) Behavioral correlates of activity of optogenetically identified locus coeruleus noradrenergic neurons in rats performing T-maze tasks. Sci Rep 9:1–13.

Yang H, Bari BA, Cohen JY, O'Connor DH (2021) Locus coeruleus spiking differently correlates with S1 cortex activity and pupil diameter in a tactile detection task. Elife 10:1–14 Available at: https://elifesciences.org/articles/64327.

Zagha E (2020) Shaping the Cortical Landscape: Functions and Mechanisms of Top-Down Cortical Feedback Pathways. Front Syst Neurosci 14:1–17.

Zagha E, Erlich JC, Lee S, Lur G, O'Connor DH, Steinmetz NA, Stringer C, Yang H (2022) The importance of accounting for movement when relating neuronal activity to sensory and cognitive processes. J Neurosci:JN-TS-1919-21

Figures
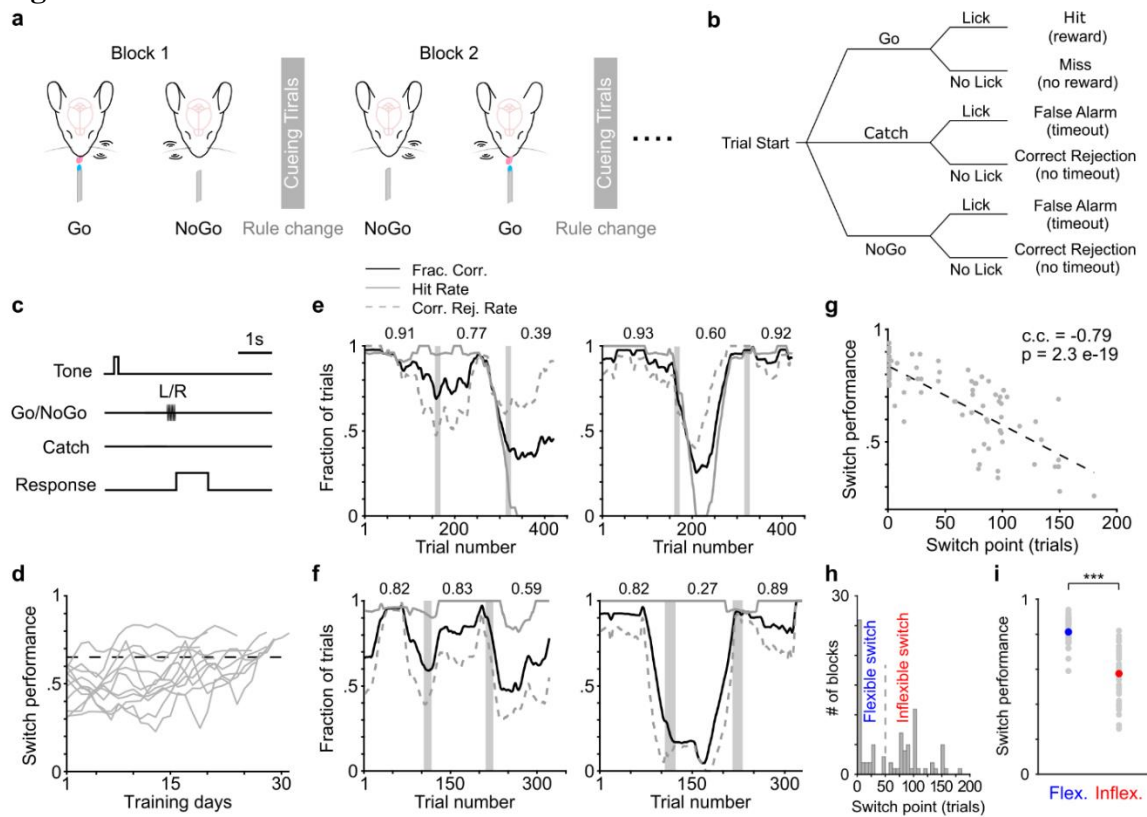
Figure 2.1 A novel context-dependent tactile detection task to probe flexible task switching

(*a-c*) *Schematic of the novel context-dependent bilateral tactile detection task in head-fixed mice (a), with illustrations of trial types (b) and trial structure (c). (d) Switch performance (fraction correct in block 2) during training (n = 11 mice). Dotted line indicates 65% threshold. (e, f) Example behavioral sessions for two mice, respectively, with performance in each block indicated. Left panels illustrate higher switch performance in block 2, and right panels illustrate higher switch performance in block 3. Vertical gray bars indicate rule switch and subsequent cueing trials. (g) The relationship between behavioral switch point and switch performance. c.c., Pearson correlation coefficient. (h) Histogram of behavioral switch point (84 blocks from 11 mice). We used 50 trials (dashed line) to separate flexible and inflexible blocks. (i) Switch performance for flexible and inflexible blocks shown in (h). Flexible (40 blocks) vs. Inflexible (44 blocks): 0.81 ± 0.011 vs 0.58 ± 0.022, p = 2.9e-12, rank sum = 2480. Gray dots represent individual blocks, blue and red dots represent mean.*

Figure 2.2 Behavioral variables within the novel context-dependent switching task
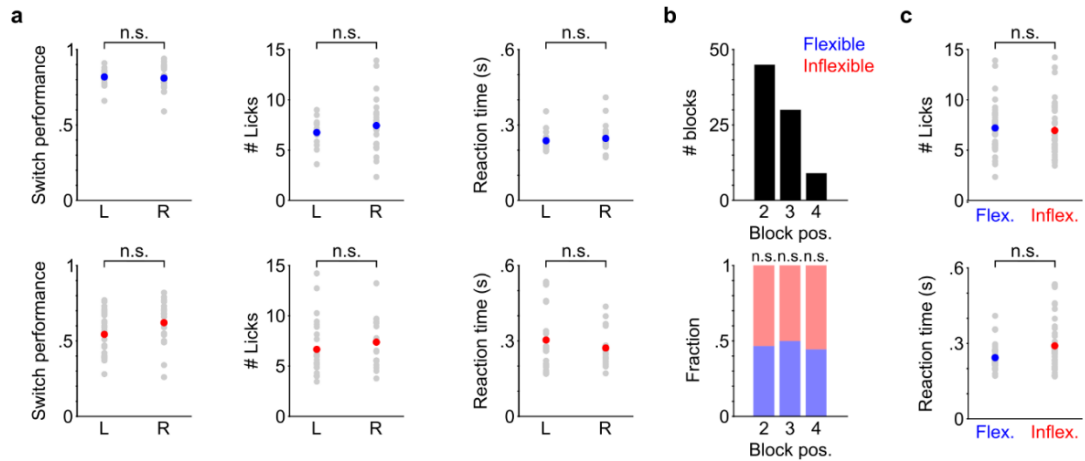*(**a**) Behavioral variables quantified for Left Go blocks (L) and Right Go blocks (R) in flexible (Blue, Top: L, n = 14; R, n = 26) and inflexible (Red, Bottom: L, n = 26; R, n = 18) switches. Flexible: switch performance, L vs. R: 0.82 ± 0.02 vs. 0.81± 0.01, p = 0.71, rank sum = 301; Number of licks, L vs. R: 6.76 ± 0.38 vs. 7.44 ± 0.53, p = 0.42, rank sum = 258; Reaction time, L vs. R: 0.24 ± 0.01 vs. 0.25 ± 0.01 s, p = 0.41, rank sum = 257. Inflexible switches: switch performance, L vs. R: 0.54 ± 0.03 vs. 0.62 ± 0.04, p = 0.095, rank sum = 515; Number of licks, L vs. R: 6.66 ± 0.53 vs. 7.38 ± 0.58, p = 0.25, rank sum = 536; Reaction time, L vs. R: 0.30 ± 0.02 vs. 0.27 ± 0.02 s, p = 0.59, rank sum = 608. Gray dots represent individual blocks, red and blue dots represent mean. Number of licks and reaction time were quantified in hit trials. Reaction time was calculated as the latency from whisker stimulation onset to the time of the first lick. (**b**) The distribution of block positions within a session for the blocks shown in Fig. 2.1g-i (Top, n = 84), and the proportion of flexible (blue) and inflexible (red) blocks in each position within a session (Bottom). Block 2: Flexible vs. Inflexible: 0.47 vs. 0.53, p = 0.53, t-stat = 0.40; block 3: Flexible vs. Inflexible: 0.50 vs. 0.50, p = 1, t-stat = 0; block 4: Flexible vs. Inflexible: 0.44 vs. 0.56, p = 0.64, t-stat = 0.22, Chi-squared test. (**c**) Comparison of lick responses (top) and reaction time (bottom) between flexible and inflexible blocks (40 vs. 44 blocks). Number of licks, Flexible vs. Inflexible: 7.20 ± 0.37 vs. 6.96 ± 0.39, p = 0.38, rank sum = 1800; Reaction time, Flexible vs. Inflexible: 0.24 ± 0.01 vs. 0.29 ± 0.02 s, p = 0.056, rank sum = 1486. Gray dots represent individual blocks, blue and red dots represent mean.*

a LC recording

Pupil tracking

TH
ChR2
100 μm

b
1 s
Energy - Ch1
.1
.05
0   .05   .1
Energy - Ch2
1 ms

c
↓ Tone   ↓ Stimulus
Trials
Flexible switch

Trials
Inflexible switch
0.5 s
Rule shift

d
Flexible switch
Before
After
0 spike/s

Inflexible switch
Before
After
0 spike/s   1 spike/s
Tone   Stimulus   1 s

e
0 spike/s
Before   After
Rule change
0.5 spikes/s
20 trials

f
*
Firing Rate (sp/s)
4
2
0
Before   After

n.s.
4
2
0
Before   After

*
Δ Firing Rate (sp/s)
2
0
-2
Flex.   Inflex.

g
c.c. = -0.42
p = 0.0026
2
Δ Firing Rate (sp/s)
0
-2
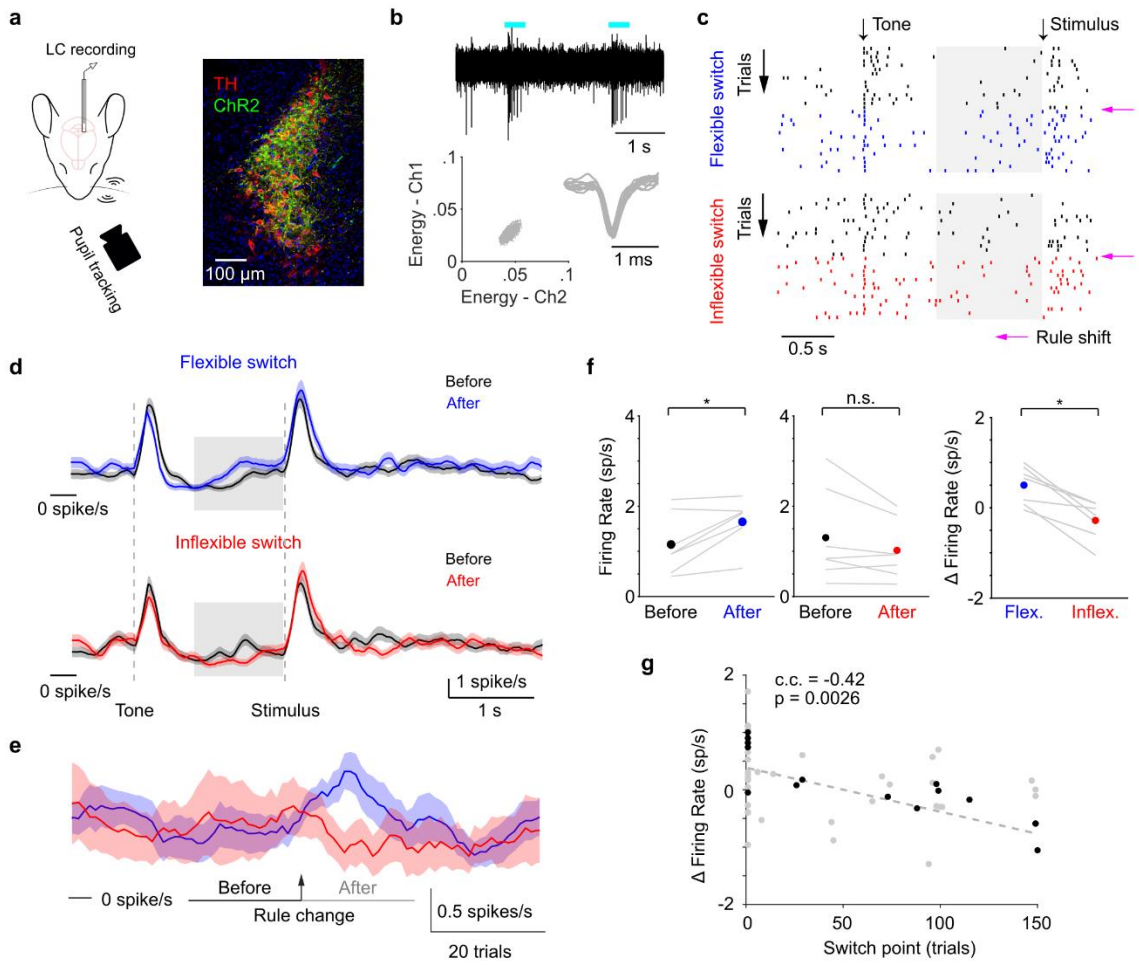0   50   100   150
Switch point (trials)

91

Figure 2.3 Correlating LC activity with flexible task switching
*(**a**) Schematic of experimental setup during behavior (Left) and ChR2 expression in a DBH;Ai32 mouse (Right. TH: tyrosine hydroxylase). (**b**) Top: Responses of an example ChR2-expressing LC neuron to optical stimulation (cyan bars). Bottom: spike-sorting diagram and waveforms of this unit. (**c**) Example spike raster from an example LC unit in a behavior session with both a flexible (Top) and an inflexible (Bottom) block. Rows represent individual trials. Magenta arrows indicate the rule shift. Trials in the previous block are in black, and trials in the current block are in blue (flexible) or red (inflexible). Shaded gray areas represent the 1-s time window to quantify baseline activity. (**d**) Average PSTH of LC activity from flexible (Top, n = 7) and inflexible (Bottom, n = 7) switches, quantified before (last 20 trials in the previous block, Before) and after the rule change (first 20 trials in the new block, After). Shaded gray areas represent the 1-s time window to quantify baseline activity. (**e**) Average baseline LC activity in a 100-trial window centered at the rule change (arrow) for flexible (blue) and inflexible (red) switches (same blocks as in d). Horizontal bars indicate Before and After trial periods to compare baseline LC activity in d, f, g. (**f**) Baseline LC activity during the Before and After periods for flexible (Left, Before vs. After: 1.15 ± 0.25 vs. 1.65 ± 0.19 spikes/s, p = 0.03, signed rank = 1, n = 7) and inflexible switches (Middle, Before vs. After: 1.30 ± 0.39 vs. 1.02 ± 0.24 spikes/s, p = 0.16, signed rank = 23, n = 7). Changes in baseline activity (Δ Firing rate: After - Before) were higher during flexible switches than inflexible switches (Right, Flexible vs. Inflexible: 0.50 ± 0.16 vs. -0.28 ± 0.16 spikes/s, p = 0.02, signed rank = 28, n = 7). Lines represent individual paired flexible-inflexible blocks from the same session. Dots represent mean. (**g**) The relationship between behavioral switch point and the changes in baseline LC activity. Gray dots represent individual blocks (n = 49). Black dots represent the paired blocks shown in (d-f). c.c., Pearson correlation coefficient.*
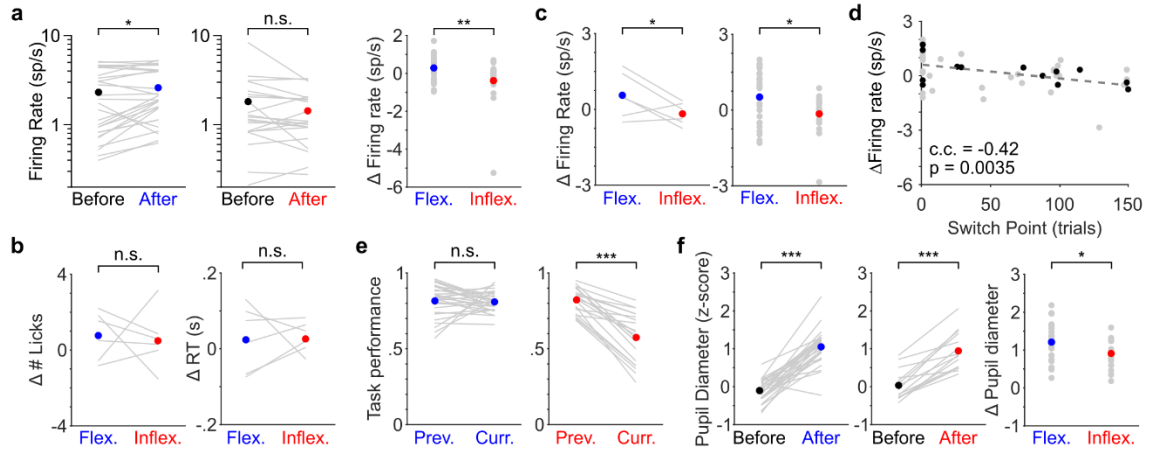
Figure 2.4 Baseline LC spike rate is associated with behavioral flexibility across all sessions and across all hit trials
*(**a**) Baseline LC activity during the Before and After periods for flexible (Left: Before vs. After: 2.31 ± 0.31 vs. 2.60 ± 0.30 spikes/s, p = 0.03, signed rank = 109.5, n = 28) and inflexible (Middle: Before vs. After: 1.81 ± 0.38 vs. 1.43 ± 0.20 spikes/s, p = 0.10, signed rank = 163, n = 21) switches. Changes in baseline activity (ΔFiring rate: After - Before) were higher during flexible switches than inflexible switches (Right: Flexible vs. Inflexible: 0.29 ± 0.12 vs. -0.38 ± 0.26 spikes/s, p = 0.0074, rank sum = 833).*
*(**b**) Changes in number of licks (Left: Δ# licks, After – Before, Flexible vs. Inflexible: 0.79 ± 0.52 vs. 0.56 ± 0.62, p = 0.96, t-stat = -0.05, n = 6) and reaction time (Right: ΔRT, Flexible vs. Inflexible: 0.03 ± 0.04 vs. 0.03 ± 0.02 s, p = 0.83, t-stat = 0.22, n = 6) for the paired flexible-inflexible blocks shown in Fig. 2.3d-f. (**c**) Changes in baseline LC activity for the paired flexible-inflexible blocks (n = 6) as in Fig. 2.3d-f (Left, Flexible vs. Inflexible: 0.56 ± 0.36 vs. -0.18 ± 0.18 spikes/s, p = 0.041, t-stat = 2.16, two-tailed t-test) and all blocks (n = 47) as in Fig. 2.4a (Right, Flexible vs. Inflexible: 0.51 ± 0.20 vs. -0.15 ± 0.17 spikes/s, p = 0.037, rank sum = 722) quantified in hit trials only. For b and c, there were no hit trials during the Before period of 2 blocks from the original full dataset (n = 49), and they were removed from analyses. 1 block was included in the original paired analysis (n = 7), so the associated flexible-inflexible pair was removed from analyses. (**d**) The relationship between behavioral switch point and the changes in baseline LC activity quantified in hit trials only as shown in (c). Conventions are as in Fig. 2.3g. (**e**) Left: Comparison of task performance quantified in blocks immediately preceding the flexible blocks (Previous) and quantified in the flexible blocks (Current). Previous vs. Current: 0.82 ± 0.02 vs. 0.81 ± 0.01, p = 0.29, signed rank = 157, n = 28. Right: Comparison of task performance quantified in blocks immediately preceding the inflexible blocks (Previous) and quantified in the inflexible blocks (Current). Previous vs. Current: 0.82 ± 0.02 vs. 0.57 ± 0.03, p = 5.9e-5, signed rank = 0, n = 21. (**f**) Pupil diameter during the Before and After periods for flexible (Left, Before vs. After: -0.10 ± 0.06 vs. 1.05 ± 0.09 s.d., p = 4.7e-6, signed rank = 404, n = 28) and inflexible (Middle, Before vs. After: 0.045 ± 0.08 vs. 0.93 ± 0.13 s.d., p = 1.8e-4, signed rank = 188, n = 19) switches. Changes in pupil diameter (ΔPupil diameter: After - Before) was higher during flexible switches than inflexible switches (Right, Flexible vs. Inflexible: 1.15 ± 0.10 vs. 0.88 ± 0.11 s.d., p = 0.044, rank sum = 751). 2 inflexible blocks with poor pupil tracking were excluded from this analysis. Pupil diameter was calculated as the average pupil diameter during a baseline pupil window. The baseline pupil window was defined as a 1-s window starting 1.5 s after the start of the baseline LC window, based on the time lag between LC activity and pupil response (Yang et al., 2021).*

a LC activation

Tone
Go
NoGo
Response
1s

Block1   Block 2   Block 3

b
Pupil diameter (s.d.)
Test
Control
Time from light onset (s)

c
Switch performance
Test
Control
Days from stimulation

d
Switch performance
Baseline (Test)
Stimulation
** ** * *
#1 #2 #3 #4

e
Switch performance
Baseline (Control)
Stimulation
n.s. n.s. n.s.
#5 #6 #7

f
Switch performance
Test ***
Control n.s.
Base. Stim.   Base. Stim.

g
Switch Point (trials)
*
n.s.
Base. Stim.   Base. Stim.

h
Hit Rate
Test n.s.
Control n.s.
Base. Stim.   Base. Stim.

i
CR Rate
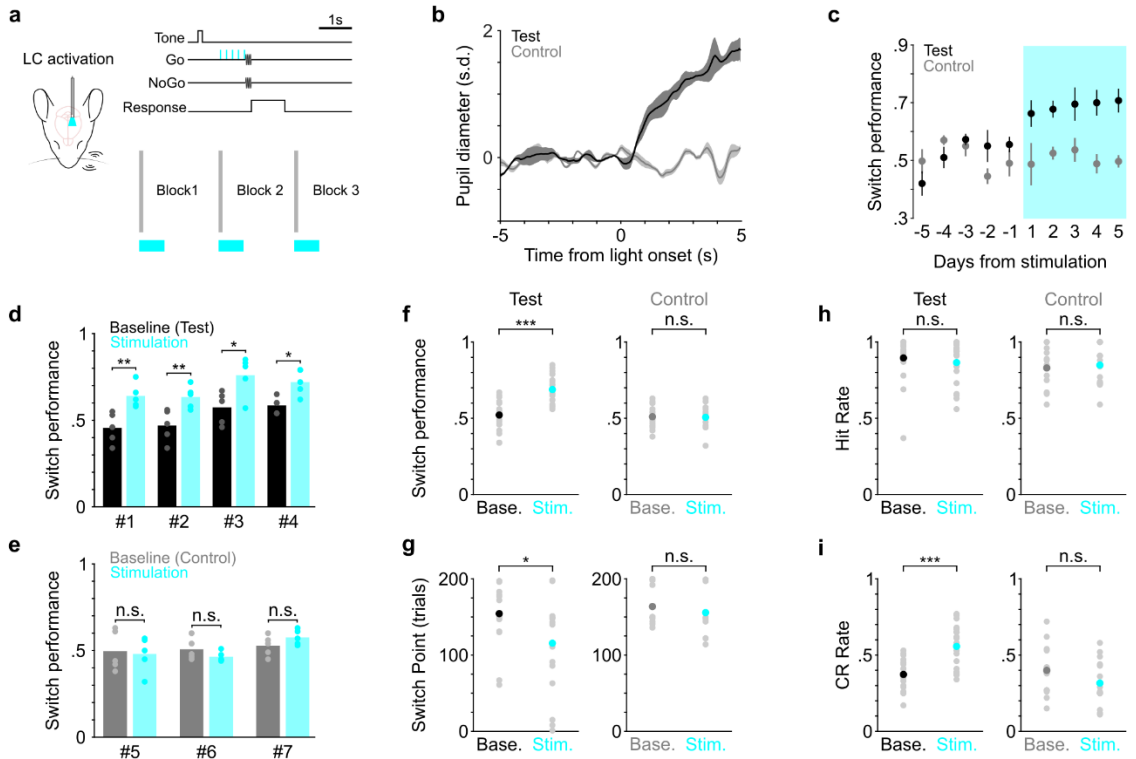***
n.s.
Base. Stim.   Base. Stim.

95

Figure 2.5 Determining the causal link between LC activity and flexible task switching
(a) Schematic of optogenetic LC stimulation during task performance. (b) Example pupil responses to optical stimulation for a test (black) and control (gray) mouse. (c) Group average switch performance for the test (black) and control (gray) groups during baseline (5 consecutive days prior to stimulation) and optical stimulation (5 consecutive days with stimulation, cyan) sessions. Day -1 represents the last day without stimulation. Day 1 represents the first day with stimulation. (d) Switch performance for individual mice in the test group (n = 4), compared between baseline (black) and stimulation sessions (cyan). Baseline vs. Stimulation, Mouse #1: 0.46 ± 0.04 vs. 0.64 ± 0.03, p = 0.008; Mouse #2: 0.47 ± 0.04 vs. 0.63 ± 0.03, p = 0.004; Mouse #3: 0.57 ± 0.04 vs. 0.76 ± 0.05, p = 0.012; Mouse #4: 0.59 ± 0.02 vs. 0.72 ± 0.03, p = 0.024. Permutation test.
(e) Switch performance for individual mice in the control group (n = 3), compared between baseline (gray) and stimulation sessions (cyan). Baseline vs. Stimulation, Mouse #5: 0.50 ± 0.05 vs. 0.48 ± 0.05, p = 0.80; Mouse #6: 0.51 ± 0.03 vs. 0.46 ± 0.02, p = 0.24; Mouse #7: 0.53 ± 0.03 vs. 0.58 ± 0.01, p = 0.18. Permutation test. (f) Comparison of switch performance for test (Left) and control (Right) groups between baseline and stimulation sessions. Baseline vs. Stimulation, Test group: 0.52 ± 0.02 vs. 0.69 ± 0.02, p = 1.6e-5, rank sum = 250, n = 20; Control group: 0.51 ± 0.02 vs. 0.51 ± 0.02, p = 1.0, rank sum = 232, n = 15. Black, dark gray and cyan dots represent mean. (g) Comparison of behavioral switch point for test (Left) and control (Right) groups between baseline and stimulation sessions. Baseline vs. Stimulation, Test group: 154 ± 8 vs. 116 ± 13 trials, p = 0.02, rank sum = 495, n = 20; Control group: 164 ± 7 vs. 156 ± 8 trials, p = 0.23, rank sum = 262, n = 15. Black, dark gray and cyan dots represent mean. (h) Comparison of hit rate for test (Left) and control (Right) groups between baseline and stimulation sessions. Baseline vs. Stimulation, Test group: 0.90 ± 0.03 vs. 0.87 ± 0.03, p = 0.56, rank sum = 432, n = 20; Control group: 0.83 ± 0.03 vs. 0.85 ± 0.04, p = 0.79, rank sum = 162, n = 15. Black, dark gray and cyan dots represent mean. (i) Comparison of correct rejection rate for test (Left) and control (Right) groups between baseline and stimulation sessions. Baseline vs. Stimulation, Test group: 0.37 ± 0.02 vs. 0.56 ± 0.03, p = 2.4e-4, rank sum = 274, n = 20; Control group: 0.40 ± 0.04 vs. 0.32 ± 0.04, p = 0.15, rank sum = 268, n = 15. Black, dark gray and cyan dots represent mean.
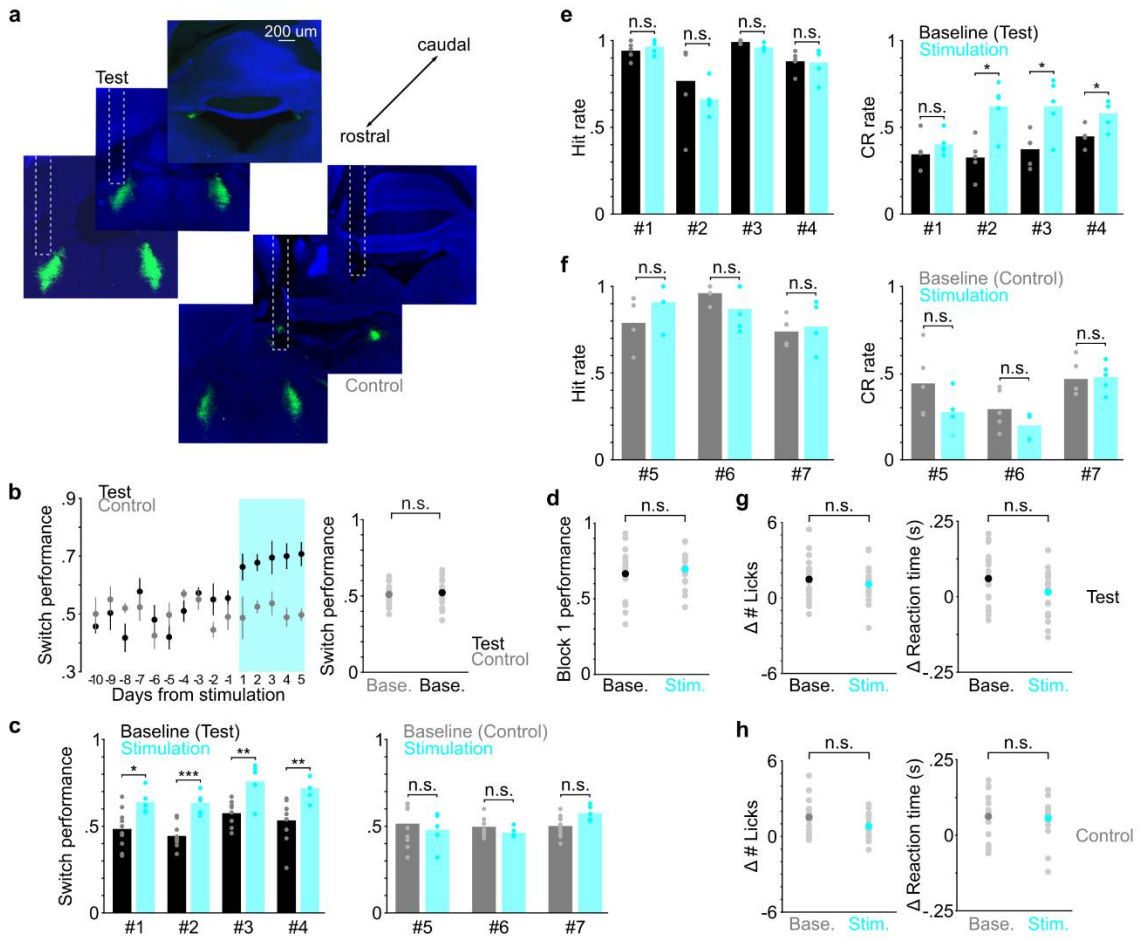
97 of 163

Figure 2.6 Optogenetic activation of LC drives robust increase in performance without affecting licking behaviors
*(**a**) Three histological sections showing the LC (green) and the optical fiber tract from a test (Top, LC stimulation) and a control (Bottom, off-LC stimulation) mouse, respectively.*
*(**b**) Left: Group average switch performance for the test and control groups during an extended baseline period (10 consecutive days prior to stimulation) and optical stimulation period (5 consecutive days, cyan). Day -1 represents the last day without stimulation. Day 1 represents the first day with stimulation. Right: Switch performance during the 10-day baseline period for the test (n = 40 blocks) and control (n = 30 blocks) groups (Test vs. Control: 0.52 ± 0.02 vs. 0.51 ± 0.02, p = 0.62, rank sum = 255).*
*(**c**) Switch performance for individual mice (as in Fig. 2.5d, e), but compared between a 10-day baseline period and 5-day stimulation period (cyan) for the test (Left, n = 4; Baseline vs. Stimulation, Mouse #1: 0.48 vs. 0.64, p = 0.013; Mouse #2: 0.44 vs. 0.63, p = 0.001; Mouse #3: 0.58 vs. 0.76, p = 0.008; Mouse #4: 0.53 vs. 0.72, p = 0.0060, Permutation test) and control (Right, n = 3; Mouse #5: 0.52 vs. 0.48, p = 0.57; Mouse #6: 0.50 vs. 0.46, p = 0.31; Mouse #7: 0.50 vs. 0.58, p = 0.060, Permutation test) groups.*
*(**d**) Comparison of task performance in block 1 between Baseline (n = 20) and Stimulation (n = 20) sessions for the test group (Baseline vs. Stimulation: 0.67 ± 0.03 vs. 0.70 ± 0.02, p = 0.54, rank sum = 387). (**e**) Hit rate (Left) and correct rejection rate (Right) for individual mice in the test group (n = 4). Hit rate, Baseline vs. Stimulation, Mouse #1: 0.94 vs. 0.97, p = 0.45; Mouse #2: 0.77 vs. 0.66, p = 0.44; Mouse #3: 0.99 vs. 0.96, p = 0.49; Mouse #4: 0.88 vs. 0.87, p = 0.90, Permutation test; Correct rejection rate, Baseline vs. Stimulation, Mouse #1: 0.34 vs. 0.40, p = 0.32; Mouse #2: 0.32 vs. 0.62, p = 0.023; Mouse #3: 0.37 vs. 0.62, p = 0.036; Mouse #4: 0.45 vs. 0.58, p = 0.024, Permutation test. (**f**) Same as in (e) but for the control group (n = 3). Hit rate, Baseline vs. Stimulation, Mouse #5: 0.79 vs. 0.81, p = 0.21; Mouse #6: 0.96 vs. 0.87, p = 0.18; Mouse #7: 0.74 vs. 0.77, p = 0.71, Permutation test; Correct rejection rate, Baseline vs. Stimulation, Mouse #5: 0.44 vs. 0.27, p = 0.10; Mouse #6: 0.29 vs. 0.20, p = 0.13; Mouse #7: 0.47 vs. 0.48, p = 0.88, Permutation test. (**g**) Comparison of changes in number of licks (Left, Δ# Licks, Before - After) and reaction time (Right, ΔRT) between baseline (n = 20) and stimulation (n = 20) sessions for the test group. Δ# Licks, Baseline vs. Stimulation: 1.48 ± 0.37 vs. 1.10 ± 0.33, p = 0.49, rank sum = 425; ΔRT, Baseline vs. Stimulation: 0.06 ± 0.02 vs. 0.01 ± 0.02 s, p = 0.13, rank sum = 455. For stimulation sessions, the change (Δ) was calculated by subtracting the variable (# licks or RT) quantified in hit trials during optical stimulation trials from the variable quantified in hit trials during the last 50 trials of the previous block (i.e., no optical stimulation). For baseline sessions, no optical stimulation was delivered, and the change (Δ) was calculated by subtracting the variable quantified in hit trials during the first 50 trials following the rule change from the variable quantified in hit trials during the last 50 trials of the previous block. (**h**) Same as in (g) but for the control group. Left: Changes in number of licks, Baseline vs. Stimulation: 1.53 ± 0.37 vs. 0.81 ± 0.28, p = 0.17, rank sum = 266. Right: Changes in reaction time, Baseline vs. Stimulation: 0.06 ± 0.02 vs. 0.06 ± 0.02 s, p = 0.80, rank sum = 239.*
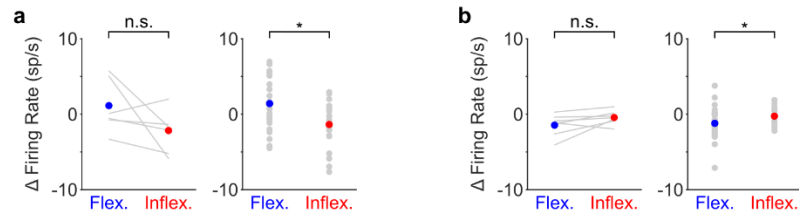
Figure 2.7 Phasic LC responses exhibit a weak correlation to task switching
*(**a**) Changes in LC responses to whisker stimulation (Before - After) in hit trials during flexible and inflexible blocks (Left: paired Flexible vs. Inflexible: 1.14 ± 1.24 vs. -2.16 ± 1.01 spikes/s, p = 0.14, t-stat = 1.75, n = 6, two-tailed t-test; Right: unpaired Flexible vs. Inflexible: 1.41 ± 0.63 vs. -1.37 ± 0.66 spikes/s, p = 0.012, rank sum = 783, n = 47). LC responses to whisker stimulation were quantified in a 100-ms window beginning at stimulus onset, subtracted from LC activity quantified in a 0.5-s baseline window ending at stimulus onset. There were no hit trials during the Before period for 2 blocks from the original full dataset (n = 49), and they were removed from this analysis. 1 block was included in the original paired analysis (n = 7), so the associated flexible-inflexible pair was removed from this analysis. (**b**) The same as in (a) but for LC responses to the auditory tone (Left: paired Flexible vs. Inflexible: -1.45 ± 0.55 vs. -0.44 ± 0.34, p = 0.11 spikes/s, signed rank = 4, n = 7; Right: unpaired Flexible (n = 28) vs. Inflexible (n = 21): -1.21 ± 0.38 vs. -0.26 ± 0.27 spikes/s, p = 0.042, rank sum = 599, n = 49). Tone responses were quantified in a 300-ms window beginning at tone onset, subtracted from LC activity quantified in a 0.5-s baseline window ending at tone onset.*

Chapter 3 - Pupil Diameter is not an Accurate Real-time Readout of Locus Coeruleus Activity

Marine Megemont [b*], Jim McBurney-Lin [a,b*], and Hongdian Yang[a,b]

[a] Neuroscience Graduate Program,

[b] Department of Molecular, Cell and Systems Biology,

University of California, Riverside, CA 92521, USA

* Equal contributions

Abstract

Pupil diameter is often treated as a non-invasive readout of activity in the locus coeruleus (LC). However, how accurately it can be used to index LC activity is not known. To address this question, we established a graded relationship between pupil size changes and LC spiking activity in mice, where pupil dilation increased monotonically with the number of LC spikes. However, this relationship exists with substantial variability such that pupil diameter can only be used to accurately predict a small fraction of LC activity on a moment- by- moment basis. In addition, pupil exhibited large session-to- session fluctuations in response to identical optical stimulation in the LC. The variations in the pupil–LC relationship were strongly correlated with decision bias-related behavioral variables. Together, our data show that substantial variability exists in an overall graded relationship between pupil diameter and LC activity, and further suggest that the pupil–LC relationship is dynamically modulated by brain states, supporting and extending our previous findings (Yang et al., 2021).

Introduction

Fluctuations of brain states, such as arousal and attention, strongly impact sensory processing, decision- making, and animal behavior (Harris and Thiele, 2011; Lee and Dan, 2012; Thiele and Bellgrove, 2018; Petersen, 2019; McCormick et al., 2020). It is thus critical to understand the neural substrates of brain states and how state changes can account for the variability embedded in neuronal and behavioral data (Cano et al., 2006; Poulet and Petersen, 2008; Polack et al., 2013; Fu et al., 2014; Zagha and McCormick, 2014; Lee et al., 2020). Changes in pupil diameter under constant luminance are tightly linked to states of arousal and attention (McGinley et al., 2015a; Joshi and Gold, 2020). Dynamic pupil responses are associated with membrane potential fluctuations, sensory evoked responses, salience detection, error estimation, decision- making, and task performance (Kahneman and Beatty, 1966; Bijleveld et al., 2009; Nassar et al., 2012; de Gee et al., 2014; de Gee et al., 2020; Reimer et al., 2014; Vinck et al., 2015; McGinley et al., 2015b; Lee and Margolis, 2016; Schriver et al., 2018; Schriver et al., 2020; Kucewicz et al., 2018; Ebitz and Moore, 2019). As a result, pupil diameter has been widely used to monitor brain states and their neural substrates.

A multitude of neural circuits have been implicated in mediating brain state and pupil size changes, most notably the neuromodulatory systems (Yu and Dayan, 2005; Lee and Dan, 2012; Thiele and Bellgrove, 2018; Joshi and Gold, 2020). The locus coeruleus (LC)–noradrenergic system has long been thought to play a critical role in controlling arousal and attention (Aston- Jones et al., 1999; Berridge and Waterhouse, 2003; Aston-Jones and Cohen, 2005; Sara, 2009; Sara and Bouret, 2012), and LC activity closely

tracks brain states and cognitive processes (Foote et al., 1980; Aston- Jones and Bloom, 1981; Berridge and Foote, 1991; Aston- Jones et al., 1994; Rajkowski et al., 1994; Usher et al., 1999; Takahashi et al., 2010; Carter et al., 2010; Eschenko et al., 2012; Vazey and Aston- Jones, 2014; Kalwani et al., 2014; Varazzani et al., 2015; Bouret and Richmond, 2015; Fazlali et al., 2016; Swift et al., 2018). Importantly, work mainly in the past decade has provided correlative and causal evidence linking pupil size changes to LC activity (Rajkowski et al., 1994; Murphy et al., 2014; Varazzani et al., 2015; Joshi et al., 2016; Reimer et al., 2016; de Gee et al., 2017; Liu et al., 2017; Breton- Provencher and Sur, 2019; Hayat et al., 2020; Privitera et al., 2020), leading to the increased utilization of pupil diameter as a non-invasive readout of LC (Aston- Jones and Cohen, 2005; Gilzenrat et al., 2010; Preuschoff et al., 2011; Konishi et al., 2017; Gelbard- Sagiv et al., 2018; Zhao et al., 2019; Aminihajibashi et al., 2020; Clewett et al., 2020). However, a few recent studies demonstrated that the correlation between pupil and LC could be neuron- and task epoch- specific (Joshi et al., 2016; Breton- Provencher and Sur, 2019; Yang et al., 2021), raising the possibility that pupil diameter can be dissociated from LC activity. To the best of our knowledge, we do not know to what extent pupil diameter is linked to LC activity. More importantly, we do not know whether and how pupil diameter can be used to make accurate inferences of LC activity on a moment- by- moment basis.

To address these questions, we recorded spiking activity from optogenetically tagged LC neurons simultaneously with pupil diameter in head- fixed mice trained to perform a tactile detection task (McBurney- Lin et al., 2020; Yang et al., 2021). We established a graded relationship between pupil and LC, where pupil dilation increased

monotonically with LC spiking activity. However, this relationship exists with substantial

variability such that pupil size changes can only accurately predict a small fraction of LC

spiking on a moment- by- moment basis. Using optogenetics to activate LC neurons, we

showed that pupil responses exhibited large session- to- session fluctuations to identical

optical stimulation, despite stable LC responses. Notably, decision bias- related

behavioral variables explained the variations in the pupil–LC relationship. Together, our

data show that substantial variability exists in an overall positive relationship between

pupil diameter and LC activity, and that only under limited conditions can pupil be used

as an accurate real- time readout of LC. Our work further suggests that brain states

dynamically modulate the coupling between pupil and LC.

Results

The magnitude of the pupil-LC relationship varies considerably

We recorded spiking activity from optogenetically tagged single units in the LC

together with pupil diameter in head- fixed mice during behavior (Figure 3.1a). To

quantify a graded relationship between pupil size changes and LC spiking, we first

grouped adjacent spikes into individual clusters (Hahn et al., 2010; Yu et al., 2017) based

on each unit's median interspike interval (Figure 3.1b, Figure 3.2, Methods). The

magnitude of pupil responses following a spike cluster (quantified in a 6- s window from

cluster onset) progressively increased with cluster size (the number of spikes in a cluster,

Figure 3.1c, d). The latency of peak pupil diameter did not systematically vary with

cluster size and ranged between 2.5 and 4 s (Figure 3.3). This latency is consistent with

our previous report (Yang et al., 2021). Overall, we found a positive, monotonic

relationship between peak pupil diameter and LC cluster size in the majority of paired

recordings (linear regression R2>0.6 in 13 out of 19 paired recordings, Figure 3.1e), in

line with previous findings in non-human primates (Varazzani et al., 2015; Joshi et al.,

2016). Similar relationships held when pupil responses were quantified as % changes

from baseline (Cazettes et al., 2021) or the time derivatives of pupil (Reimer et al., 2016;

Yang et al., 2021; Figure 3.4). However, substantial variations existed in the relationship

(linear slopes ranging from 0.12 to 0.51. 0.24 ± 0.11, mean ± standard deviation [SD], n

= 13), indicating variable couplings between pupil and LC neurons.

Pupil diameter accurately represents a small proportion of LC activity

Although pupil diameter exhibited an overall monotonic relationship with LC

spiking, it did not necessarily warrant pupil diameter being an accurate readout of LC

activity. We tested the extent to which pupil size changes can be used as a proxy for LC

activity, that is, can we use pupil diameter to make accurate inferences of LC spiking on a

moment- by- moment basis? We asked how well an ideal observer (Green and Swets,

1966) can predict LC cluster size given the associated peak pupil responses (Methods).

Receiver- operating- characteristic (ROC) analysis showed that as cluster size increased,

peak pupil diameter can better predict LC activity (Figure 3.1f, g, Figure 3.5). However,

only peak pupil diameter associated with large clusters (≥5–6 spikes) can achieve a

performance threshold of d' = 1 (translates to ~0.75 area under the curve Simpson and

Fitter, 1973, Figure 3.1g). Since larger clusters occurred less frequently (Figure 3.1d, h,

Figure 3.6), our data suggest that pupil dilation cannot accurately represent the majority of LC spiking activity but can serve as a good proxy for the infrequent (<10%) and strong LC activity in real time (Figure 3.1h).

Only large pupil events accurately predict LC spiking in real-time

Perhaps what is more interesting (and useful) is to assess whether we can directly use pupil diameter to infer the 'ground truth' – LC activity, without recording from LC. To do so, we first detected pupil dilation events based on zero- crossings of pupil derivatives (Joshi et al., 2016; Figure 3.7a) and quantified LC spike counts immediately preceding each dilation event (Methods). Compared with the analyses in Figure 3.1, this method did not require prior knowledge of LC activity for identifying pupil responses and yielded a similar pupil–LC relationship (Figure 3.8). Overall, LC spike counts were monotonically associated with pupil dilation amplitudes (Figure 3.7b–d). However, a wide range of spike counts preceded pupil events of similar sizes (Figure 3.7b, c). We asked how well an ideal observer can predict pupil dilation events given the associated LC activity and found that as pupil dilations became larger, LC spike counts could make better predictions on a moment- by- moment basis. However, only LC activity preceding the infrequent (<10%), large dilation events (>1.5–2 SD, Figure 3.9) performed beyond 75% threshold (Figure 3.7e). Finally, we tested how well we can use the detected pupil dilation events to predict LC activity. Similar to the previous results (Figure 3.1g), we found that only large pupil events can achieve good predictions (Figure 3.7f). Taken together, our data show that pupil diameter and LC spiking are well correlated in a graded

manner and that the infrequent (<10%) but strong (>1.5–2 SD) pupil dilation events can be used to accurately and reliably predict LC activity in real time.

Pupil responses to optogenetic stimulation exhibit substantial variability

Our data presented so far were based on paired pupil–LC recordings, each consisting of a single opto- tagged LC unit. Next, we sought to test whether pupil size changes better reflect population- level LC activity instead of single neurons. To this end, we optogenetically activated groups of LC neurons and quantified the evoked pupil responses. Based on the stimulation parameters, we estimated an excitable volume on the order of 0.05–0.1 mm^3, containing hundreds of LC neurons (Figure 3.10a, b, Figure 3.11, Methods). In a subset of experiments, the putatively same LC units were tracked (typically 1–5 days), based on opto- tagging, spike clustering, and waveform comparison (Figure 3.10c, d). Waveforms from the putatively same units were more similar than the waveforms from the putatively different units (Figure 3.10e–g). These putatively same units responded similarly to optical stimulation in different sessions (Figure 3.10h), suggesting a consistent transduction of optical stimulation to LC spiking activity. In contrast to stable LC responses, the same pupil exhibited variable dilations to optical stimulation under awake, non-task performing conditions (Figure 3.12a, b). Importantly, baseline pupil diameters were similar (0.71 vs. 0.75 mm, Figure 3.13) and thus cannot explain the differences in evoked pupil responses. Group data from multiple mice further demonstrated that significant session- to- session fluctuations of pupil responses were prevalent but not directional (solid lines in Figure 3.12c, d), that is, pupil responses in an

106

earlier session (session 1) were not consistently higher or lower than in a later session (session 2). Therefore, such session- to- session fluctuations were not observable from group comparisons (Figure 3.14, Privitera et al., 2020). To further test whether the variable pupil responses were due to (1) weak LC stimulation with 10 ms pulses, or (2) strong spontaneous pupil fluctuations during wakefulness, we performed the following experiments. First, we evoked pupil responses with stronger stimulation (50 ms pulses instead of 10 ms) in the awake condition. While baseline pupil diameters were similar between sessions, evoked pupil responses still fluctuated significantly (Figure 3.12e, f). In a subset of experiments, pupil exhibited substantial fluctuations in two sessions just several hours apart (4–6 hr, magenta arrows in Figure 3.12c–f). Further analysis showed that across- session variability of pupil responses was comparable to within- session variability (Figure 3.16, Methods). In addition, for the paired sessions that exhibited significantly different responses to optical stimulation (solid lines in Figure 3.12c–f), only a small subset exhibited larger across- session variability than within- session variability (2 pairs out of 12 under 10 ms condition, and 3 pairs out of 11 under 50 ms condition, Methods). Next, we stimulated LC with 10 ms pulses under anesthesia (2% isoflurane) to minimize spontaneous pupil fluctuations (Figure 3.16). Evoked pupil responses were noticeably larger compared with the awake condition in the example recordings, possibly due to a more constricted baseline pupil size under anesthesia (Figure 3.12g, h, left vs. Figure 3.12a, b, 0.3 vs. 0.7 mm). Nevertheless, pupil responses to optical stimulation exhibited substantial session- to- session fluctuations (Figure 3.12g, h). Additional examples of a simultaneously recorded LC unit and pupil diameter in

107

responses to optical stimulation are in Figure 3.17. In summary, pupil responses showed large session- to- session fluctuations to identical LC stimulation.

State-dependent variables may explain dynamic LC-pupil coupling

What may underlie the variable pupil responses? We found that the variations in the relationship between peak pupil diameter and LC cluster size (as in Figure 3.1e) were strongly correlated with hit rate and decision bias during task performance (Figure 3.18a). This effect was not likely due to linear fitting of non-linear relationships (all linear fits are of $R2 > 0.85$. 0.92 ± 0.05, mean $\pm$ SD, $n = 9$), and the results held when the analysis of pupil–LC relationship was restricted to non-licking periods only (Figure 3.18b, Methods). Therefore, although mice licked more during sessions of higher hit rate and lower decision bias, the results cannot be fully explained by a potentially stronger pupil–LC coupling during licking periods. Based on these findings, we conclude that decision bias- related behavioral variables could explain, at least in part, the variations in the pupil–LC relationship. Since fluctuations of these behavioral variables reflect state changes such as impulsivity, motivation, and task engagement (Dickinson and Balleine, 1994; Mayrhofer et al., 2013; Berditchevskaia et al., 2016; Allen et al., 2019; McBurney-Lin et al., 2020), our results suggest that the coupling between pupil and LC is state dependent.

Discussion

In the current study, we have shown that pupil diameter has an overall positive and monotonic relationship with LC spiking activity. However, substantial variability exists in this relationship that only the infrequent and large pupil dilation events (>1.5–2 SD amplitude, <10% occurrence) can accurately predict LC spiking on a moment- by- moment basis. In addition, pupil responses exhibit large session- to- session fluctuations to identical optical stimulation in the LC. Decision bias- related behavioral variables could explain the variations in the pupil–LC relationship. Together, our results strongly caution treating pupil dilation as a real- time readout of LC activity. Averaging multiple repeats/trials of similar pupil responses would yield a much more accurate prediction of LC activity.

We used two methods to establish the pupil–LC relationship: detecting LC activity then linking to the following pupil responses (Figure 3.1); and detecting pupil dilation then linking to the preceding LC activity (Figure 3.4). Both methods yielded similar pupil–LC relationships with the conclusion that only the infrequent, large pupil responses can accurately predict LC spiking on a moment- by- moment basis. Large pupil or LC responses have been reported to correlate with a variety of task- related processes, including sensory cue, decision formation, positive feedback, choice bias, and action (Rajkowski et al., 1994; Usher et al., 1999; Kalwani et al., 2014; Bouret and Richmond, 2015; de Gee et al., 2017; de Gee et al., 2020; Schriver et al., 2020; Yang et al., 2021). In light of this, our work suggests that the infrequent but strong pupil dilation events can be used as an accurate inference of LC activation in response to sensory stimuli and

decision- making processes. However, as discussed below, in general pupil and LC likely respond to task- related processes differently, leading to variations in their relationship.

Recent evidence has uncovered considerable heterogeneity within the LC nucleus, including molecular compositions, physiological properties, released transmitters, and projection targets (Robertson et al., 2013; Chandler et al., 2014; Chandler et al., 2019; Schwarz and Luo, 2015; Schwarz et al., 2015; Kempadoo et al., 2016; Hirschberg et al., 2017; Uematsu et al., 2017; Totah et al., 2018; Borodovitsyna et al., 2020). Our data support these findings (Figure 3.19). Therefore, it is possible that pupil diameter is dynamically coupled with different LC subgroups that are differentially engaged during cognitive processes. However, this is insufficient to explain the session- to- session fluctuations of pupil responses to LC stimulation, since we likely activated a heterogenous group of LC neurons that exhibited similar session- to- session responses to optical stimulation.

The fact that the putatively same neurons tracked across days exhibited similar responses to optical stimulation cannot fully establish the long- term stability of population LC response because slow changes in the tissue due to tetrode/optical fiber implant (gliosis, inflammation, etc.) could alter light transmission to the neurons that were not recorded. However, several lines of evidence in our study did not favor this possibility: (1) Pupil responses in a later session did not systematically or progressively differ from an earlier session (e.g., consistently larger or smaller, Figure 3.14); (2) Significant pupil response variability can be observed in sessions that were a few hours apart (Figure 3.12); (3) Across- session variability of pupil responses was largely

comparable to within- session variability (Figure 3.16). However, optogenetic stimulation tends to synchronize neuronal activity, which may not reflect the physiological condition (Totah et al., 2018). Future experiments with the ability to record from multiple opto-tagged LC neurons simultaneously will further investigate the relationship between pupil diameter and population- level LC activity.

During wakefulness, the state of the brain is constantly fluctuating, both in the presence and absence of external stimuli (Kenet et al., 2003; Fox et al., 2006; Fox and Raichle, 2007; Sakata and Harris, 2009; Luczak et al., 2009; Berkes et al., 2011; Harris and Thiele, 2011; Mohajerani et al., 2013; Romano et al., 2015; Petersen, 2019; McCormick et al., 2020). Pupil response profiles can reflect different behavioral processes (Schriver et al., 2020), and pupil responses also can be dissociated from cognitive processes (Podvalny et al., 2019). Our data extend these observations, supporting that LC and pupil respond to behavioral and cognitive variables differently (Yang et al., 2021).

Fluctuations of hit rate and decision bias reflect state changes such as impulsivity, motivation, and task engagement (Dickinson and Balleine, 1994; Mayrhofer et al., 2013; Berditchevskaia et al., 2016). Although mice licked more during high motivation or high engagement trials (Berditchevskaia et al., 2016; Allen et al., 2019; McBurney- Lin et al., 2020), our data show that licking alone cannot account for the tight correlation between the variations of the behavioral variables and the variations in the pupil–LC relationship (Figure 3.18), suggesting that pupil–LC coupling is brain state dependent.

How may brain states modulate pupil–LC coupling? Pupil size changes have been linked to activity in other brain areas and neuromodulatory systems, including the medial prefrontal cortex, the inferior colliculus, and cholinergic signaling (Joshi et al., 2016; Reimer et al., 2016; Okun et al., 2019; Kucyi and Parvizi, 2020; Pais- Roldán et al., 2020; Sobczak et al., 2021). A recent study found that pupil responses to dorsal raphe stimulation exhibited task uncertainty- dependent variations (Cazettes et al., 2021). Therefore, it is possible that in high motivation/engagement states, multiple circuits including the LC synergistically influence pupil size changes, resulting in the apparently stronger pupil–LC coupling. Future experiments are needed to elucidate how pupil and LC interact with these brain circuits during different behavioral contexts and cognitive processes. Another possibility is that higher engagement states may be intimately associated with more 'uninstructed' movements as revealed by recent work (Musall et al., 2019), which can drive robust neuronal activity throughout the brain (Musall et al., 2019; Steinmetz et al., 2019; Stringer et al., 2019; Salkoff et al., 2020). Future studies with comprehensive movement monitoring will determine whether more frequent movements, both task- related and task- unrelated, during periods of high motivation/engagement underlie the stronger pupil–LC coupling.

Methods

Mice

All procedures were performed in accordance with protocols approved by UC Riverside Animal Care and Use Committee. Mice were DBH- Cre (B6.FVB(Cg)-

Tg(Dbh- cre) KH212Gsat/Mmucd, 036778- UCD, MMRRC); Ai32 (RCL-

ChR2(H134R)/EYFP, 012569, JAX), or DBH- Cre injected with AAV5- EF1α- DIO-

hChR2(H134R)- EYFP (UNC Vector Core), singly housed in a vivarium with reverse

light–dark cycle (12 hr each phase).

Surgery

Male and female mice of 8–12 weeks were implanted with titanium head posts as

described previously (Yang et al., 2016). Procedures for microdrive construction and LC

recording have been described previously (Yang et al., 2021). Briefly, custom

microdrives with eight tetrodes and an optic fiber (0.39 NA, 200 µm core) were built to

make extracellular recordings from LC neurons. Microdrive was implanted in the left LC.

Electrophysiology

LC neurons were identified by optogenetic tagging of DBH+ neurons expressing

ChR2, tail pinch response, and post hoc electrolytic lesions (Yang et al., 2021). For

Figures 3.1 and 3.7, 19 single unit recordings (cluster quality measure Lratio: $0.01 \pm$

0.005; firing rate: 1.65 ± 0.25 spikes/s; percent ISI <10 ms: $0.11\% \pm 0.1\%$) from 7 mice

performing the single- whisker detection task (see below) were extracted using MClust

(Redish, 2014), among which six recordings were from our previous dataset (Yang et al.,

2021). For Figure 3.10, 5 units from 5 mice were tracked over time (between 1 and 5

days). For Figure 3.12, 68 pupil sessions (34 baseline pupil- matched session pairs) to LC

stimulation were acquired from 8 mice, 4 of which were implanted with an optical fiber

only (0.39 NA, 200 µm core), and the time between sessions 1 and 2 was 4.4 ± 0.9 days.

Optogenetics

Electrophysiology, pupil tracking, and optogenetic stimulation were synchronized

via a common TTL pulse train. The mating sleeve connecting two ferrules was covered

with black tape to prevent light leak. An ambient blue LED was used to constrict the

pupil and to mask any potential light leak. <15 mW (RMS) of blue light was measured at

the tip of optical fiber. We estimated an excitable volume on the order of 0.05–0.1 mm^3

for a 30° cylindrical cone based on 10- mW light power, 2.5 mW/mm^2 excitation

threshold and 1.4 refractive index of brain tissue (Boyden et al., 2005; Sun et al., 2012)

(brain tissue light transmission calculator: https://web.stanford.edu/group/dlab/cgi-

bin/graph/chart.php), containing hundreds of neurons in the LC. Stimulation patterns

were delivered every 10–30 s and randomized.

Behavior task

Behavior task was controlled by BControl (C. Brody, Princeton University) or

custom- based Arduino hardware and software as described previously (Yang et al.,

2016; Yang et al., 2021; McBurney- Lin et al., 2020). In brief, mice were trained to

perform a head- fixed, Go/NoGo single- whisker detection task, in which mice reported

whether they perceived a brief deflection (0.5 s, 40 Hz or 0.2 s, 25 Hz sinusoidal

deflection) to the right C2 whisker by licking toward a water port. A 0.1- s auditory cue

(8 kHz tone, ~80 dB SPL) was introduced starting 1–1.5 s before stimulus onset. During

all sessions, ambient white noise (cutoff at 40 kHz, ~80 dB SPL) was played through a

separate speaker to mask any other potential auditory cues associated with movement of

the piezo stimulator. Video of the left pupil (ipsilateral to LC recording and stimulation)

was acquired at 50 Hz using a PhotonFocus camera and StreamPix 5 software, or at 20

Hz using a Basler acA1300- 200 µm camera and Pylon software. 450 nM blue diode

lasers (UltraLasers, MDL- III- 450–200 mW) controlled by WaveSurfer (https://www.

janelia.org/open-science/wavesurfer) were used for optogenetic stimulation.

Histology

At the conclusion of the experiments, brains were perfused with PBS followed by

4% paraformaldehyde, postfixed overnight, then cut into 100-µm coronal sections and

stained with anti- tyrosine hydroxylase antibody (Thermo Fisher OPA1- 04050).

Data analysis

For Figure 3.1, in each recording if the interval between two adjacent spikes was

shorter than median inter- spike interval of that unit, the spikes were grouped into a single

cluster. Using other time windows (0.1–0.5 s) to group spikes did not affect this analysis

for the majority of recordings (data not shown). Peak pupil dilation was defined as the

absolute maximum value in a 6- s window following the onset of each cluster (time of the

first spike). ROC analysis in Figure 3.1f–h was performed between peak pupil diameter

associated with clusters of a given size and number- matched, randomly selected pupil diameter.

For Figure 3.4, pupil traces were first smoothed with a 500 ms window to avoid false- positive slope detections. Pupil slopes were then estimated every 200 ms, and a pupil dilation event was defined as the maximum pupil size between sequential positive zero- crossings of the slopes (Joshi et al., 2016). For each dilation event, LC spikes were quantified in a −2 to −4 s window from the event. Using a −1 to −3 s window did not affect this analysis (data not shown). Pupil dilation events falling in a bin of 0.3 SD were considered of similar sizes. ROC analysis in Figure 3.4e was performed between LC spike counts associated with pupil dilation events of a similar size and LC spike counts associated with number- matched, randomly selected pupil sizes. ROC analysis in Figure 3.4f was performed the same way as in Figure 3.1.

For Figure 3.12, pupil responses in each session were first bootstrapped 100 times with replacement to estimate the mean and confidence interval. Pupil responses to the same optical stimulation were pooled from the two different sessions, and then randomly assigned to session 1 or 2 with replacement. The reported p value represented the proportion of iterations where mean peak pupil responses from the two permutated sessions exceeded the observed difference from 1000 iterations.

For Figure 3.16, across- session variability (standard deviation of peak pupil responses) was estimated by resampling trials pooled from all sessions in each condition. The iteration of resampling matched the total number of sessions in that condition. To test whether within- session variability was similar to across- session variability for

116

individual session pairs which exhibited significantly different pupil responses, we first estimated the distribution of across- session variability by resampling trials pooled from both sessions for 1000 iterations and examined whether the variability of individual sessions fell outside 5% of the distribution.

For Figure 3.18, 9 recordings (out of 13 shown in Figure 3.1e) from 4 mice during behavior were included with >100 trials and $R2 > 0.6$. For Figure 3.18b, LC clusters occurring within ± 0.5 s from each licking event were excluded from analyzing the pupil–LC relationship as in Figure 3.1e. This window was chosen based on previous results that LC spiking peaked within a few hundred milliseconds of licking onset (Yang et al., 2021).

Data were reported as mean $\pm$ standard error of the mean unless otherwise noted. We did not use statistical methods to predetermine sample sizes. Sample sizes are similar to those reported in the field. We assigned mice to experimental groups arbitrarily, without randomization or blinding.

References

Allen WE, Chen MZ, Pichamoorthy N, Tien RH, Pachitariu M, Luo L, Deisseroth K (2019) Thirst regulates motivated behavior through modulation of brainwide neural population dynamics. Science (80-) 364:0–10.

Aminihajibashi S, Hagen T, Laeng B, Espeseth T (2020) Pupillary and behavioral markers of alerting and orienting: An individual difference approach. Brain Cogn 143:105597 Available at: https://doi.org/10.1016/j.bandc.2020.105597.

Aston-Jones G, Bloom FE (1981) Activity of norepinephrine-containing locus coeruleus neurons in behaving rats anticipates fluctuations in the sleep-waking cycle. J Neurosci 1:876–886 Available at: http://www.ncbi.nlm.nih.gov/pubmed/7346592.

Aston-Jones G, Cohen JD (2005) An integrative theory of locus coeruleus-norepinephrine function: adaptive gain and optimal performance. Annu Rev Neurosci 28:403–450

Aston-Jones G, Rajkowski J, Cohen J (1999) Role of locus coeruleus in attention and behavioral flexibility. Biol Psychiatry 46:1309–1320.

Aston-Jones G, Rajkowski J, Kubiak P, Alexinsky T (1994) Locus Coeruleus Neurons in Monkey Are Selectively Activated by Attended Cues in a Vigilance Task. J Neurosci 14:4467–4480.

Becket Ebitz R, Moore T (2019) Both a gauge and a filter: Cognitive modulations of pupil size. Front Neurol 10:1–14.

Berditchevskaia A, Cazé RD, Schultz SR (2016) Performance in a GO/NOGO perceptual task reflects a balance between impulsive and instrumental components of behaviour. Sci Rep 6:1–15 Available at: http://dx.doi.org/10.1038/srep27389.

Berkes P, Orbán G, Lengyel M, Fiser J (2011) Spontaneous cortical activity reveals hallmarks of an optimal internal model of the environment. Science 331:83–87

Berridge CW, Foote SL (1991) Effects of locus coeruleus activation on electroencephalographic activity in neocortex and hippocampus. J Neurosci 11:3135–3145 Available at: http://www.ncbi.nlm.nih.gov/pubmed/1682425.

Berridge CW, Waterhouse BD (2003) The locus coeruleus-noradrenergic system: Modulation of behavioral state and state-dependent cognitive processes. Brain Res Rev 42:33–84.

Bijleveld E, Custers R, Aarts H (2009) The Unconscious Eye Opener. Psychol Sci 20:1313–1315.

Borodovitsyna O, Duffy BC, Pickering AE, Chandler DJ (2020) Anatomically and functionally distinct locus coeruleus efferents mediate opposing effects on anxiety-like behavior. Neurobiol Stress 13:100284

Bouret S, Richmond BJ (2015) Sensitivity of Locus Ceruleus Neurons to Reward Value for Goal-Directed Actions. J Neurosci 35:4005–4014 Available at: http://www.jneurosci.org/cgi/doi/10.1523/JNEUROSCI.4553-14.2015.

Boyden ES, Zhang F, Bamberg E, Nagel G, Deisseroth K (2005) Millisecond-timescale, genetically targeted optical control of neural activity. Nat Neurosci 8:1263–1268 Available at: http://www.ncbi.nlm.nih.gov/pubmed/16116447 [Accessed July 9, 2014].

Breton-Provencher V, Sur M (2019) Active control of arousal by a locus coeruleus GABAergic circuit. Nat Neurosci 22:218–228 Available at: https://www.biorxiv.org/content/early/2018/09/09/412338.

Cano M, Bezdudnaya T, Swadlow HA, Alonso JM (2006) Brain state and contrast sensitivity in the awake visual thalamus. Nat Neurosci 9:1240–1242.

Carter ME, Yizhar O, Chikahisa S, Nguyen H, Adamantidis A, Nishino S, Deisseroth K, de Lecea L (2010) Tuning arousal with optogenetic modulation of locus coeruleus neurons. Nat Neurosci 13:1526–1533

Cazettes F, Reato D, Morais JP, Renart A, Mainen ZF (2020) Phasic Activation of Dorsal Raphe Serotonergic Neurons Increases Pupil Size. Curr Biol:1–6.

Chandler DJ, Gao W-J, Waterhouse BD (2014) Heterogeneous organization of the locus coeruleus projections to prefrontal and motor cortices. Proc Natl Acad Sci U S A 111:6816–6821.

Chandler DJ, Jensen P, McCall JG, Pickering AE, Schwarz LA, Totah NK (2019) Redefining Noradrenergic Neuromodulation of Behavior: Impacts of a Modular Locus Coeruleus Architecture. J Neurosci 39:8239–8249.

Clewett D, Gasser C, Davachi L (2020) Pupil-linked arousal signals track the temporal organization of events in memory. Nat Commun 11:1–14 Available at: http://dx.doi.org/10.1038/s41467-020-17851-9.

Clewett D, Huang R, Velasco R, Lee T-H, Mather M (2018) Locus coeruleus activity strengthens prioritized memories under arousal. J Neurosci 38:2097–17

de Gee JW, Colizoli O, Kloosterman NA, Knapen T, Nieuwenhuis S, Donner TH (2017) Dynamic modulation of decision biases by brainstem arousal systems. Elife 6:1–36.

de Gee JW, Knapen T, Donner TH (2014) Decision-related pupil dilation reflects upcoming choice and individual bias. Proc Natl Acad Sci 111:E618–E625 Available at: http://www.pnas.org/lookup/doi/10.1073/pnas.1317557111.

de Gee JW, Tsetsos K, Schwabe L, Urai AE, McCormick D, McGinley MJ, Donner TH (2020) Pupil-linked phasic arousal predicts a reduction of choice bias across species and decision domains. Elife 9:1–25.

Dickinson A, Balleine B (1994) Motivational control of goal-directed action. Anim Learn Behav 22:1–18 Available at: http://journals.sagepub.com/doi/10.1111/1467-8721.ep11512272.

Eschenko O, Magri C, Panzeri S, Sara SJ (2012) Noradrenergic neurons of the locus coeruleus are phase locked to cortical up-down states during sleep. Cereb Cortex 22:426–435 Available at: http://www.ncbi.nlm.nih.gov/pubmed/21670101 [Accessed July 17, 2014].

Fazlali Z, Ranjbar-Slamloo Y, Adibi M, Arabzadeh E (2016) Correlation between cortical state and locus coeruleus activity: Implications for sensory coding in rat barrel cortex. Front Neural Circuits 10:1–16.

Foote SL, Aston-Jones G, Bloom FE (1980) Impulse activity of locus coeruleus neurons in awake rats and monkeys is a function of sensory stimulation and arousal. Proc Natl Acad Sci U S A 77:3033–3037.

Fox MD, Raichle ME (2007) Spontaneous fluctuations in brain activity observed with functional magnetic resonance imaging. Nat Rev Neurosci 8:700–711 Available at: http://www.ncbi.nlm.nih.gov/pubmed/17704812.

Fox MD, Snyder AZ, Zacks JM, Raichle ME (2006) Coherent spontaneous activity accounts for trial-to-trial variability in human evoked brain responses. Nat Neurosci 9:23–25

Fu Y, Tucciarone JM, Espinosa JS, Sheng N, Darcy DP, Nicoll R a, Huang ZJ, Stryker MP (2014) A cortical circuit for gain control by behavioral state. Cell 156:1139–1152

Gelbard-Sagiv H, Magidov E, Sharon H, Hendler T, Nir Y (2018) Noradrenaline Modulates Visual Perception and Late Visually Evoked Activity. Curr Biol 28:2239-2249.e6 Available at: https://doi.org/10.1016/j.cub.2018.05.051.

Gilzenrat MS, Nieuwenhuis S, Jepma M, Cohen JD (2010) Pupil diameter tracks changes in control state predicted by the adaptive gain theory of locus coeruleus function. Cogn Affect Behav Neurosci 10:252–269

Green DM, Swets JA (1966) Signal detection theory and psychophysics. John Wiley and Sons Inc.

Hahn G, Petermann T, Havenith MN, Yu S, Singer W, Plenz D, Nikolić D, Nikolic D (2010) Neuronal avalanches in spontaneous activity in vivo. J Neurophysiol 104:3312–3322

Harris KD, Thiele A (2011) Cortical state and attention. Nat Rev Neurosci 12:509–523

Hayat H, Regev N, Matosevich N, Sales A, Paredes-Rodriguez E, Krom AJ, Bergman L, Li Y, Lavigne M, Kremer EJ, Yizhar O, Pickering AE, Nir Y (2020) Locus coeruleus norepinephrine activity mediates sensory-evoked awakenings from sleep. Sci Adv 6.

Hirschberg S, Li Y, Randall A, Kremer EJ, Pickering AE (2017) Functional dichotomy in spinal-vs prefrontal-projecting locus coeruleus modules splits descending noradrenergic analgesia from ascending aversion and anxiety in rats. Elife 6:1–26.

Joshi S, Gold JI (2020) Pupil Size as a Window on Neural Substrates of Cognition. Trends Cogn Sci 24:466–480

Joshi S, Li Y, Kalwani RM, Gold JI (2016) Relationships between Pupil Diameter and Neuronal Activity in the Locus Coeruleus, Colliculi, and Cingulate Cortex. Neuron 89:221–234 Available at: http://dx.doi.org/10.1016/j.neuron.2015.11.028.

Kahneman D, Beatty J (1966) Pupil Diameter and Load on Memory. Science (80-) 154:1583–1585

Kalwani RM, Joshi S, Gold JI (2014a) Phasic Activation of Individual Neurons in the Locus Ceruleus/Subceruleus Complex of Monkeys Reflects Rewarded Decisions to Go But Not Stop. J Neurosci 34:13656–13669

Kalwani RM, Joshi S, Gold JI (2014b) Phasic Activation of Individual Neurons in the Locus Ceruleus/Subceruleus Complex of Monkeys Reflects Rewarded Decisions to Go But Not Stop. J Neurosci 34:13656–13669

Kempadoo KA, Mosharov E V., Choi SJ, Sulzer D, Kandel ER (2016) Dopamine release from the locus coeruleus to the dorsal hippocampus promotes spatial learning and memory. Proc Natl Acad Sci 113:14835–14840 Available at: http://www.pnas.org/lookup/doi/10.1073/pnas.1616515114

Kenet T, Bibitchkov D, Tsodyks M, Grinvald A, Arieli A (2003) Spontaneously emerging cortical representations of visual attributes. Nature 425:954–956 Available at: http://www.ncbi.nlm.nih.gov/pubmed/14586468.

Konishi M, Brown K, Battaglini L, Smallwood J (2017) When attention wanders: Pupillometric signatures of fluctuations in external attention. Cognition 168:16–26 Available at: http://dx.doi.org/10.1016/j.cognition.2017.06.006.

Kucewicz MT, Dolezal J, Kremen V, Berry BM, Miller LR, Magee AL, Fabian V, Worrell GA (2018) Pupil size reflects successful encoding and recall of memory in humans. Sci Rep 8:1–7 Available at: http://dx.doi.org/10.1038/s41598-018-23197-6.

Kucyi A, Parvizi J (2020) Pupillary dynamics link spontaneous and task-evoked activations recorded directly from human insula. J Neurosci 40:JN-RM-0435-20.

Lee CCY, Kheradpezhouh E, Diamond ME, Arabzadeh E (2020) State-Dependent Changes in Perception and Coding in the Mouse Somatosensory Cortex. Cell Rep 32:108197 Available at: https://doi.org/10.1016/j.celrep.2020.108197.

Lee CR, Margolis DJ (2016) Pupil Dynamics Reflect Behavioral Choice and Learning in a Go/NoGo Tactile Decision-Making Task in Mice. Front Behav Neurosci 10:1–14

Lee SH, Dan Y (2012) Neuromodulation of Brain States. Neuron 76:109–222

Liu Y, Rodenkirch C, Moskowitz N, Schriver B, Wang Q (2017) Dynamic Lateralization of Pupil Dilation Evoked by Locus Coeruleus Activation Results from Sympathetic, Not Parasympathetic, Contributions. Cell Rep 20:3099–3112.

Luczak A, Barthó P, Harris KD (2009) Spontaneous events outline the realm of possible sensory responses in neocortical populations. Neuron 62:413–425

Mayrhofer JM, Skreb V, Von der Behrens W, Musall S, Weber B, Haiss F (2013) Novel two-alternative forced choice paradigm for bilateral vibrotactile whisker frequency discrimination in head-fixed mice and rats. J Neurophysiol 109:273–284.

McBurney-Lin J, Sun Y, Tortorelli LS, Nguyen QAT, Haga-Yamanaka S, Yang H (2020) Bidirectional pharmacological perturbations of the noradrenergic system differentially affect tactile detection. Neuropharmacology 174.

McCormick DA, Nestvogel DB, He BJ (2020) Neuromodulation of Brain State and Behavior. Annu Rev Neurosci 43:391–415

McGinley MJ, David S V., McCormick DA (2015a) Cortical Membrane Potential Signature of Optimal States for Sensory Signal Detection. Neuron 87:179–192

McGinley MJ, Vinck M, Reimer J, Batista-Brito R, Zagha E, Cadwell CR, Tolias AS, Cardin JA, McCormick DA (2015b) Waking State: Rapid Variations Modulate Neural and Behavioral Responses. Neuron 87:1143–1161

Mohajerani MH, Chan AW, Mohsenvand M, Ledue J, Liu R, McVea D a, Boyd JD, Wang YT, Reimers M, Murphy TH (2013) Spontaneous cortical activity alternates between motifs defined by regional axonal projections. Nat Neurosci 16:1426–1435

Murphy PR, O'Connell RG, O'Sullivan M, Robertson IH, Balsters JH (2014) Pupil diameter covaries with BOLD activity in human locus coeruleus. Hum Brain Mapp 35:4140–4154.

Musall S, Kaufman MT, Juavinett AL, Gluf S, Churchland AK (2019) Single-trial neural dynamics are dominated by richly varied movements. Nat Neurosci 22:1677–1686

Nassar MR, Rumsey KM, Wilson RC, Parikh K, Heasly B, Gold JI (2012) Rational regulation of learning dynamics by pupil-linked arousal systems. Nat Neurosci 15:1040–1046.

Okun M, Steinmetz NA, Lak A, Dervinis M, Harris KD (2019) Distinct structure of cortical population activity on fast and infraslow timescales. Cereb Cortex 29:2196–2210.

Pais-Roldán P, Takahashi K, Sobczak F, Chen Y, Zhao X, Zeng H, Jiang Y, Yu X (2020) Indexing brain state-dependent pupil dynamics with simultaneous fMRI and optical fiber calcium recording. Proc Natl Acad Sci U S A 117:6875–6882.

Petersen CCH (2019) Sensorimotor processing in the rodent barrel cortex. Nat Rev Neurosci Available at: http://www.nature.com/articles/s41583-019-0200-y.

Podvalny E, Flounders MW, King LE, Holroyd T, He BJ (2019) A dual role of prestimulus spontaneous neural activity in visual object recognition. Nat Commun 10:1–13 Available at: http://dx.doi.org/10.1038/s41467-019-11877-4.

Polack P-O, Friedman J, Golshani P (2013) Cellular mechanisms of brain state–dependent gain modulation in visual cortex. Nat Neurosci 16:1331–1339

Poulet J FA, Petersen CCH (2008) Internal brain state regulates membrane potential synchrony in barrel cortex of behaving mice. Nature 454:881–885

Preuschoff K, 't Hart BM, Einhäuser W (2011) Pupil dilation signals surprise: Evidence for noradrenaline's role in decision making. Front Neurosci 5:1–12.

Privitera M, Ferrari KD, von Ziegler LM, Sturman O, Duss SN, Floriou-Servou A, Germain P, Vermeiren Y, Wyss MT, De Deyn PP, Weber B, Bohacek J (2020) A complete pupillometry toolbox for real-time monitoring of locus coeruleus activity in rodents. Nat Protoc

Rajkowski J, Kubiak P, Aston-Jones G (1994) Locus coeruleus activity in monkey: Phasic and tonic changes are associated with altered vigilance. Brain Res Bull 35:607–616.

Redish AD (2014) MClust Spike sorting toolbox Documentation for version 4.4.

Reimer J, Froudarakis E, Cadwell CR, Yatsenko D, Denfield GH, Tolias AS (2014) Pupil Fluctuations Track Fast Switching of Cortical States during Quiet Wakefulness. Neuron 84:355–362

Reimer J, McGinley MJ, Liu Y, Rodenkirch C, Wang Q, McCormick DA, Tolias AS (2016) Pupil fluctuations track rapid changes in adrenergic and cholinergic activity in cortex. Nat Commun 7:13289

Robertson SD, Plummer NW, de Marchena J, Jensen P (2013) Developmental origins of central norepinephrine neuron diversity. Nat Neurosci 16:1016–1023

Romano SAA, Pietri T, Pérez-Schuster V, Jouary A, Haudrechy M, Sumbre G (2015) Spontaneous neuronal network dynamics reveal circuit's functional adaptations for behavior. Neuron 85:1070–1085

Sakata S, Harris KD (2009) Laminar Structure of Spontaneous and Sensory-Evoked Population Activity in Auditory Cortex. Neuron 64:404–418

Salkoff DB, Zagha E, McCarthy E, McCormick DA (2020) Movement and Performance Explain Widespread Cortical Activity in a Visual Detection Task. Cereb Cortex 30:421–437.

Sara SJ (2009) The locus coeruleus and noradrenergic modulation of cognition. Nat Rev Neurosci 10:211–223 Available at: http://www.ncbi.nlm.nih.gov/pubmed/19190638

Sara SJ, Bouret S (2012) Orienting and Reorienting: The Locus Coeruleus Mediates Cognition through Arousal. Neuron 76:130–141

Schriver BJ, Bagdasarov S, Wang Q (2018) Pupil-linked arousal modulates behavior in rats performing a whisker deflection direction discrimination task. J Neurophysiol 120:1655–1670.

Schriver BJ, Perkins SM, Sajda P, Wang Q (2020) Interplay between components of pupil-linked phasic arousal and its role in driving behavioral choice in Go/No-Go perceptual decision-making. Psychophysiology 57:1–20.

Schwarz LA, Luo L (2015) Organization of the locus coeruleus-norepinephrine system. Curr Biol 25:R1051–R1056

Schwarz LA, Miyamichi K, Gao XJ, Beier KT, Weissbourd B, DeLoach KE, Ren J, Ibanes S, Malenka RC, Kremer EJ, Luo L (2015) Viral-genetic tracing of the input–output organization of a central noradrenaline circuit. Nature 524:88–92

Simpson AJ, Fitter MJ (1973) What is the best index of detectability? Psychol Bull 80:481–488 Available at: http://content.apa.org/journals/bul/80/6/481.

Sobczak F, Pais-Roldán P, Takahashi K, Yu X (2021) Decoding the brain state-dependent relationship between pupil dynamics and resting state fMRI signal fluctuation. Elife 10:2021.02.24.432768

Steinmetz NA, Zatka-Haas P, Carandini M, Harris KD (2019) Distributed coding of choice, action, and engagement across the mouse brain. Nature in press

Stringer C, Pachitariu M, Steinmetz N, Reddy CB, Carandini M, Harris KD (2019) Spontaneous behaviors drive multidimensional, brainwide activity. Science (80-) 364.

Sun J, Lee SJ, Wu L, Sarntinoranont M, Xie H (2012) Refractive index measurement of acute rat brain tissue slices using optical coherence tomography. Opt Express 20:1084.

Swift KM, Gross BA, Frazer MA, Bauer DS, Clark KJD, Vazey EM, Aston-Jones G, Li Y, Pickering AE, Sara SJ, Poe GR (2018) Abnormal Locus Coeruleus Sleep Activity Alters Sleep Signatures of Memory Consolidation and Impairs Place Cell Stability and Spatial Memory. Curr Biol 28:3599-3609.e4

Takahashi K, Kayama Y, Lin JS, Sakai K (2010) Locus coeruleus neuronal activity during the sleep-waking cycle in mice. Neuroscience 169:1115–1126

Thiele A, Bellgrove MA (2018) Neuromodulation of Attention. Neuron 97:769–785

Totah NK, Neves RM, Panzeri S, Logothetis NK, Eschenko O (2018) The Locus Coeruleus Is a Complex and Differentiated Neuromodulatory System. Neuron 99:1055-1068.e6

Uematsu A, Tan BZ, Ycu EA, Cuevas JS, Koivumaa J, Junyent F, Kremer EJ, Witten IB, Deisseroth K, Johansen JP (2017) Modular organization of the brainstem noradrenaline system coordinates opposing learning states. Nat Neurosci 20:1602–1611.

Usher M, Cohen JD, Servan-Schreiber D, Rajkowski J, Aston-Jones G (1999) The role of locus coeruleus in the regulation of cognitive performance. Science (80-) 283:549–554

Varazzani C, San-Galli a., Gilardeau S, Bouret S (2015) Noradrenaline and Dopamine Neurons in the Reward/Effort Trade-Off: A Direct Electrophysiological Comparison in Behaving Monkeys. J Neurosci 35:7866–7877

Vazey EM, Aston-Jones G (2014) Designer receptor manipulations reveal a role of the locus coeruleus noradrenergic system in isoflurane general anesthesia. Proc Natl Acad Sci U S A 111:3859–3864

Vinck M, Batista-Brito R, Knoblich U, Cardin JAA (2015) Arousal and Locomotion Make Distinct Contributions to Cortical Activity Patterns and Visual Encoding. Neuron 86:740–754.

Yang H, Bari BA, Cohen JY, O'Connor DH (2021) Locus coeruleus spiking differently correlates with S1 cortex activity and pupil diameter in a tactile detection task. Elife 10:1–14 Available at: https://elifesciences.org/articles/64327.

Yang H, Kwon SE, Severson KS, O'Connor DH (2016) Origins of choice-related activity in mouse somatosensory cortex. Nat Neurosci 19:127–134

Yu AJ, Dayan P (2005) Uncertainty, neuromodulation, and attention. Neuron 46:681–692.

Yu S, Ribeiro TL, Meisel C, Chou S, Mitz A, Saunders R, Plenz D (2017) Maintained avalanche dynamics during task-induced changes of neuronal activity in nonhuman primates. Elife 6:1–22 Available at: https://elifesciences.org/articles/27119.

Zagha E, McCormick DA (2014) Neural control of brain state. Curr Opin Neurobiol 29:178–186 Available at: http://dx.doi.org/10.1016/j.conb.2014.09.010.

Zhao S, Chait M, Dick F, Dayan P, Furukawa S, Liao HI (2019) Pupil-linked phasic arousal evoked by violation but not emergence of regularity within rapid sound sequences. Nat Commun 10:1–16

Figures
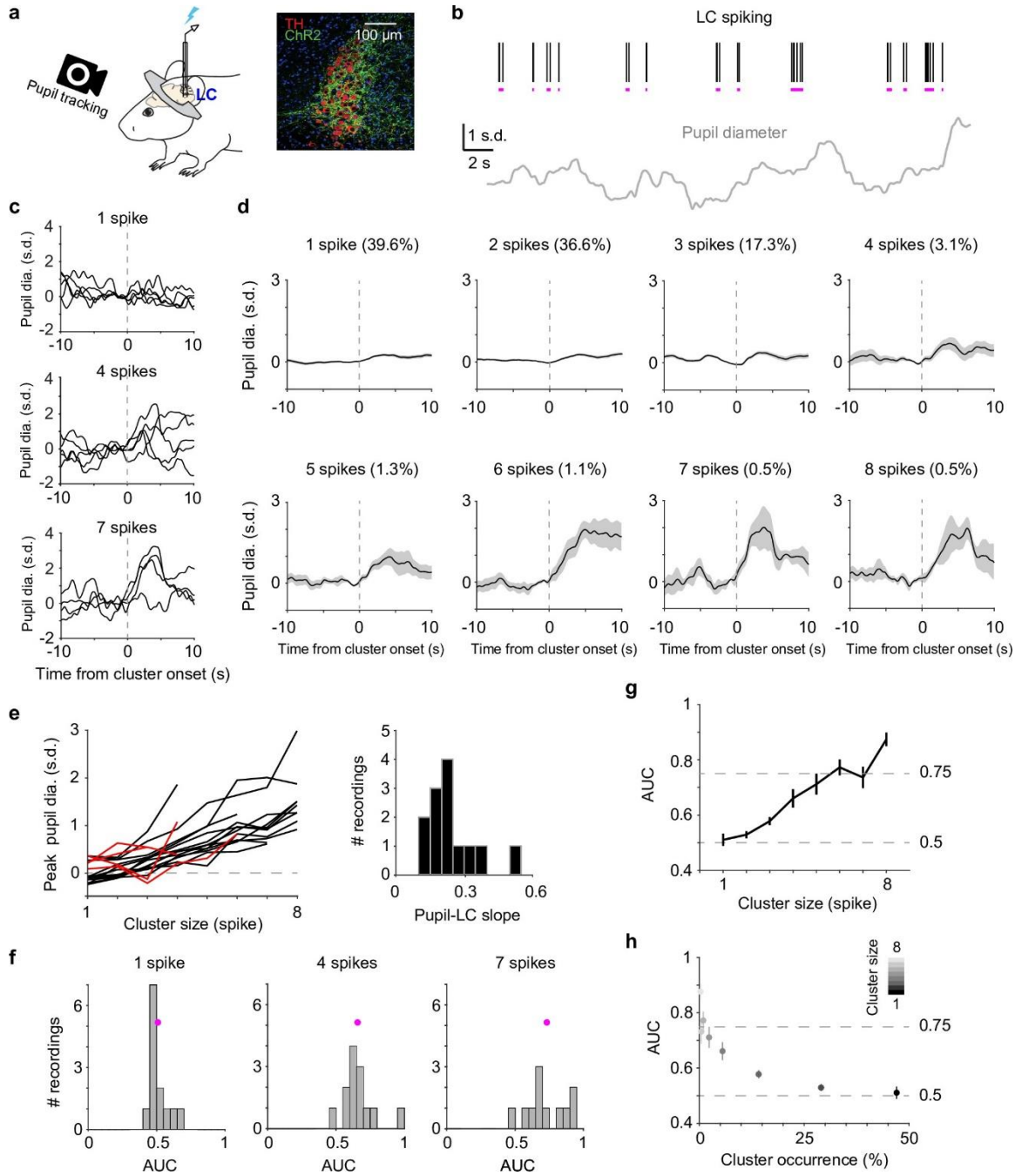
Figure 3.1 Correlating LC activity to pupil responses.
*(**a**) Left: schematic of experimental setup for simultaneous pupil and LC recording/optical stimulation in head-fixed mice. Lightning bolt: light pulse. Right: expression of ChR2 in a DBH;Ai32 mouse (dopamine beta hydroxylase, DBH; ChR2-EYFP: green; tyrosine hydroxylase, TH: red). (**b**) Example simultaneously recorded LC spike raster and z-scored pupil diameter. Vertical black lines represent individual spikes. Horizontal magenta lines indicate spike clusters. (**c**) Example LC spike cluster-triggered pupil responses for cluster sizes 1, 4, and 7. (**d**) Mean LC cluster-triggered pupil responses (±standard error of the mean [SEM]) for cluster sizes 1 through 8 with occurrence (%) indicated in an example recording. (**e**) Left: the relationship between peak pupil diameter and LC cluster size for each paired recording. Curves with linear regression $R^2 > 0.6$ are in black (n = 13), <0.6 in red (n = 4). Two recordings with limited cluster sizes (<3) were not suitable for linear regression and not included here. Right: histogram of the linear slopes for curves with $R^2 > 0.6$. For f–h, the 13 recordings with $R^2 > 0.6$ were included. (**f**) Histograms of area under the curve (AUC) values when using peak pupil diameter to predict the associated cluster sizes 1, 4, and 7. Magenta dot: mean. (**g**) Group mean AUC values when using peak pupil diameter to predict the associated cluster sizes 1 through 8. (**h**) Replot of (**g**) by showing the occurrence (abscissa) associated with each cluster size (gray scale).*
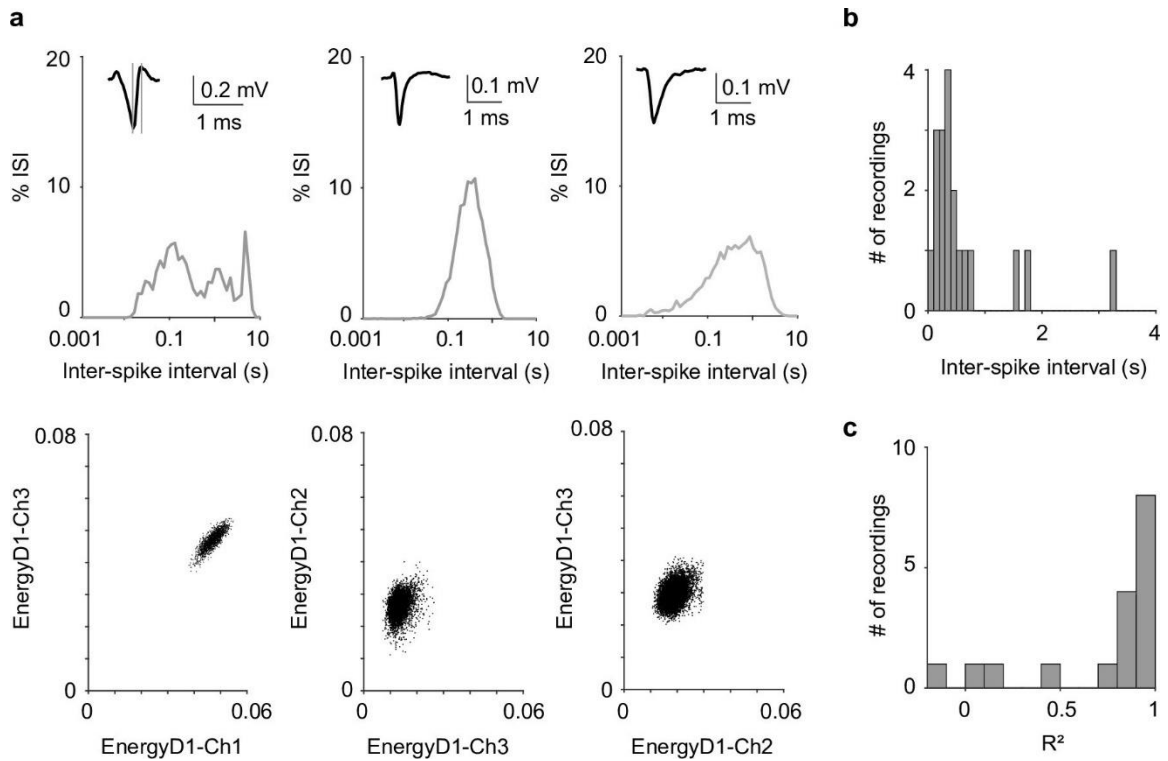
Figure 3.2 Example LC neuron spike characteristics.
(a) Distribution of inter-spike interval, average waveform (top) and spike sorting diagram (bottom) of 3 example recordings with median ISI (left to right: 0.20 s, 0.29 s, 0.36 s) and spike duration (left to right: 0.23 ms, 0.84 ms, 1.25 ms). Spike duration was quantified from trough to peak after-hyperpolarization (AHP). (b) Distribution of median inter-spike interval for 19 recordings. (c) Distribution of R^2 values from linear regressing pupil-LC relationship in Fig. 3.1e (n = 17. 2 recordings with limited cluster sizes (< 3) were not suitable for linear regression and not included).
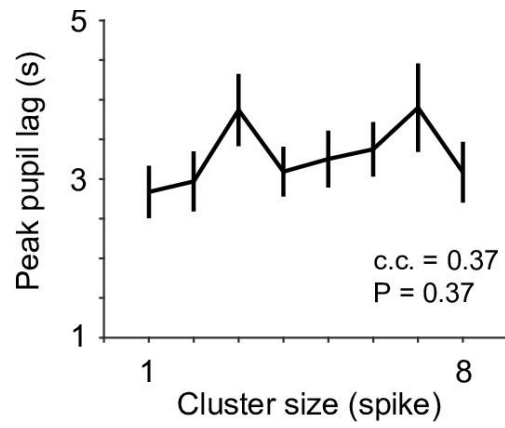
Figure 3.3 The relationship between the latency of peak pupil diameter and LC cluster size.
c.c., Pearson correlation coefficient.
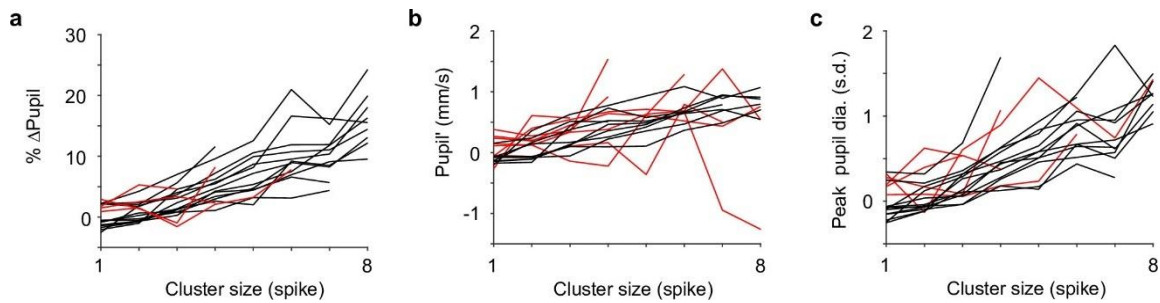
Figure 3.4 The pupil-LC relationships hold when using different methods for quantifying pupil responses.

The relationship between pupil size changes and LC spike cluster when pupil responses were quantified as % changes from baseline (a), time derivative (b) or using a shorter time window (3-s, c). Curves with linear regression $R^2 > 0.6$ are in black, < 0.6 are in red. Specifically, 13 recordings were identified with $R^2 > 0.6$ in (a), and all were the same as the 13 recordings with $R^2 > 0.6$ in Fig. 3.1e. 9 recordings were identified with $R^2 > 0.6$ in (b), and 8 out of 9 were from the 13 recordings in Fig. 3.1e. 12 recordings were identified with $R^2 > 0.6$ in (c), and all were from the 13 recordings in Fig. 3.1e. In addition, only in 1 out of the 13 recordings (with $R^2 > 0.6$ in Fig. 3.1e) did the number of spikes occurring after a given cluster (in-between spikes) significantly correlate with LC cluster size or peak pupil diameter, and overall, the in-between spikes did not strongly correlate with LC cluster size (correlation coefficient = 0.35, P = 0.39) or peak pupil diameter (correlation coefficient = 0.29, P = 0.48). Together, these results strongly suggest that the in-between spikes did not significantly contribute to the variability of the pupil-LC relationship.
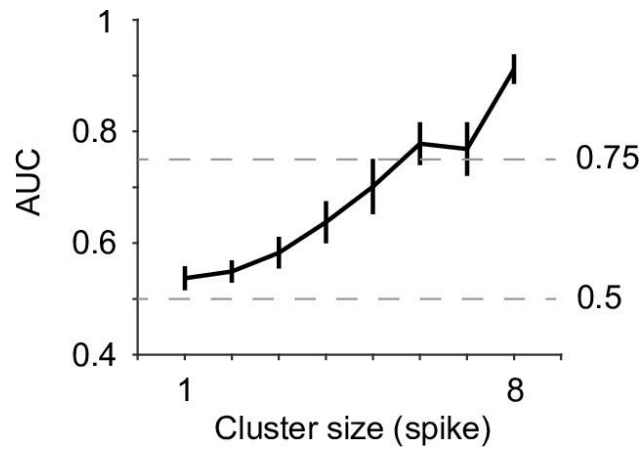
Figure 3.5 Group mean AUC values when using peak pupil diameter to predict the associated cluster size 1 through 8 from all recordings *(n = 19).*
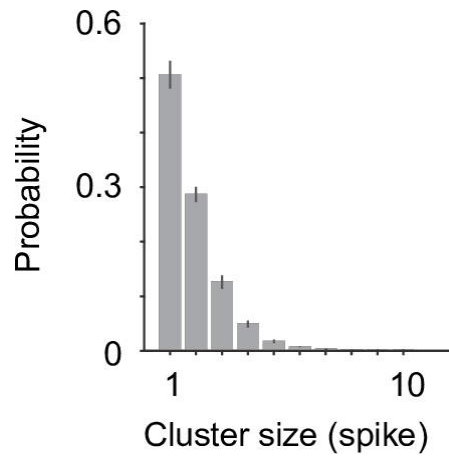
***Figure 3.6 Group mean probability distribution of LC spike clusters** (n = 19).*
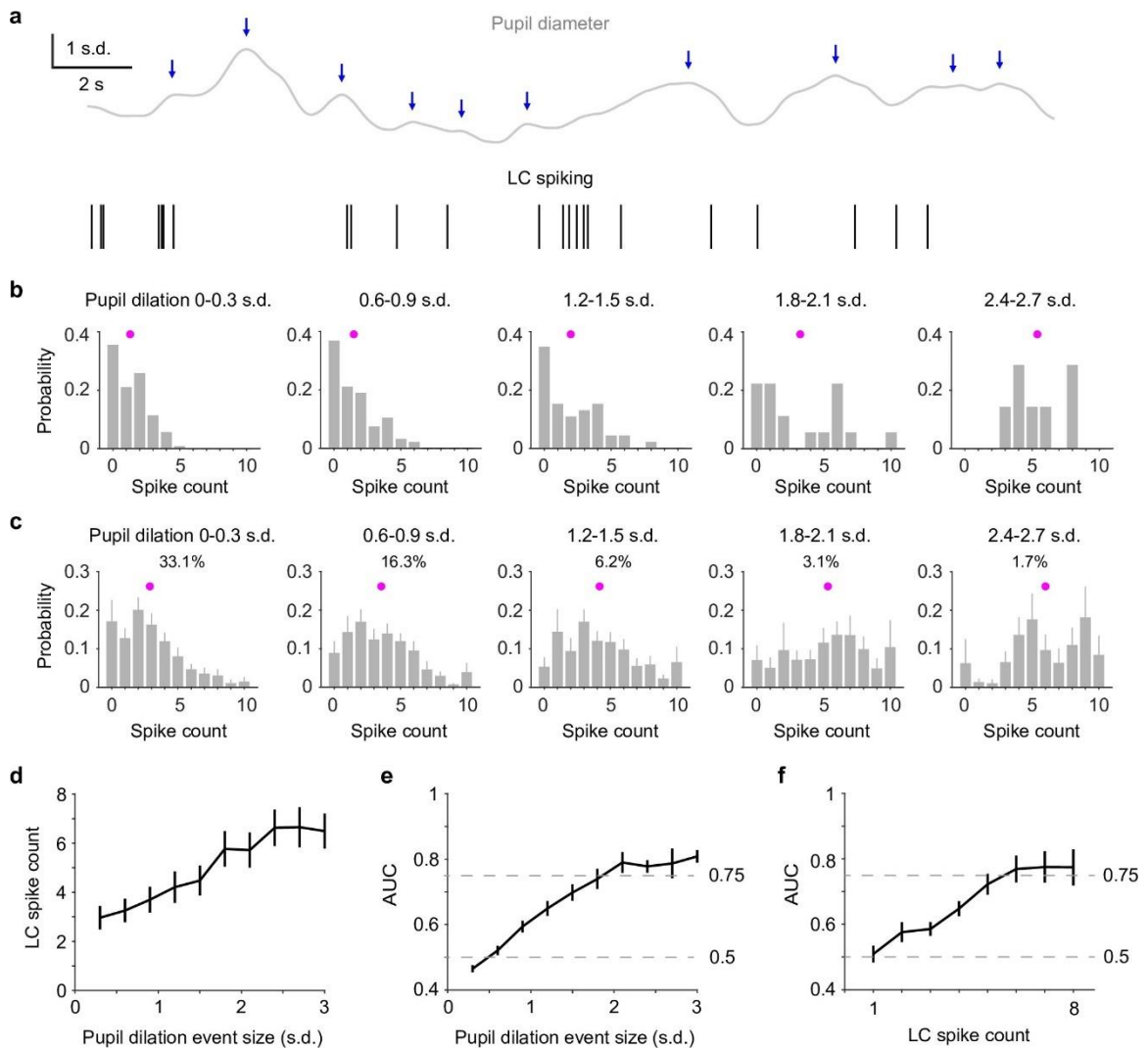
Figure 3.7 Reverse correlating pupil responses to LC activity.
*(**a**) Example pupil–LC traces showing the detected pupil dilation events (blue arrows) based on zero-crossing of pupil derivatives. (**b**) Probability distributions of LC spike counts associated with pupil dilation events of similar sizes in an example recording. Magenta dot: mean. Pupil dilation events were binned every 0.3 standard deviation (SD). (**c**) Group mean probability distributions of LC spikes associated with pupil dilation events of similar sizes. Mean occurrences (%) of pupil dilation events were indicated. (**d**) Group mean relationship between LC spike counts and pupil dilation events binned every 0.3 SD from 0 to 3 SD. (**e**) Group mean area under the curve (AUC) values when using LC spike counts to predict the associated pupil dilation events binned every 0.3 SD from 0 to 3 SD. (**f**) Group mean AUC values when using the detected pupil dilation events to predict the associated LC spike counts 1 through 8, similar to Fig. 3.1g.*
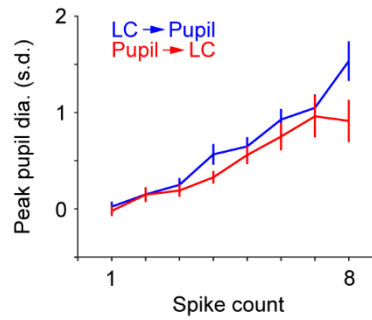
134

Figure 3.8 Group mean relationship between peak pupil diameter and LC spike counts.
*Relationships based on 1) clustering LC spikes then identifying the associated peak pupil responses (blue, Fig. 3.1), and 2) detecting pupil dilation events then identifying the preceding LC spike counts (red, Fig. 3.7**Figure 3.7***).*
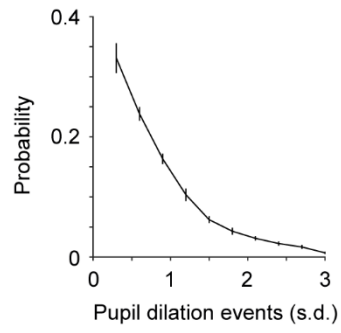
Figure 3.9 Group mean probability distribution of the detected pupil dilation events (n = 19*). Pupil dilation events were binned every 0.3 s.d.*
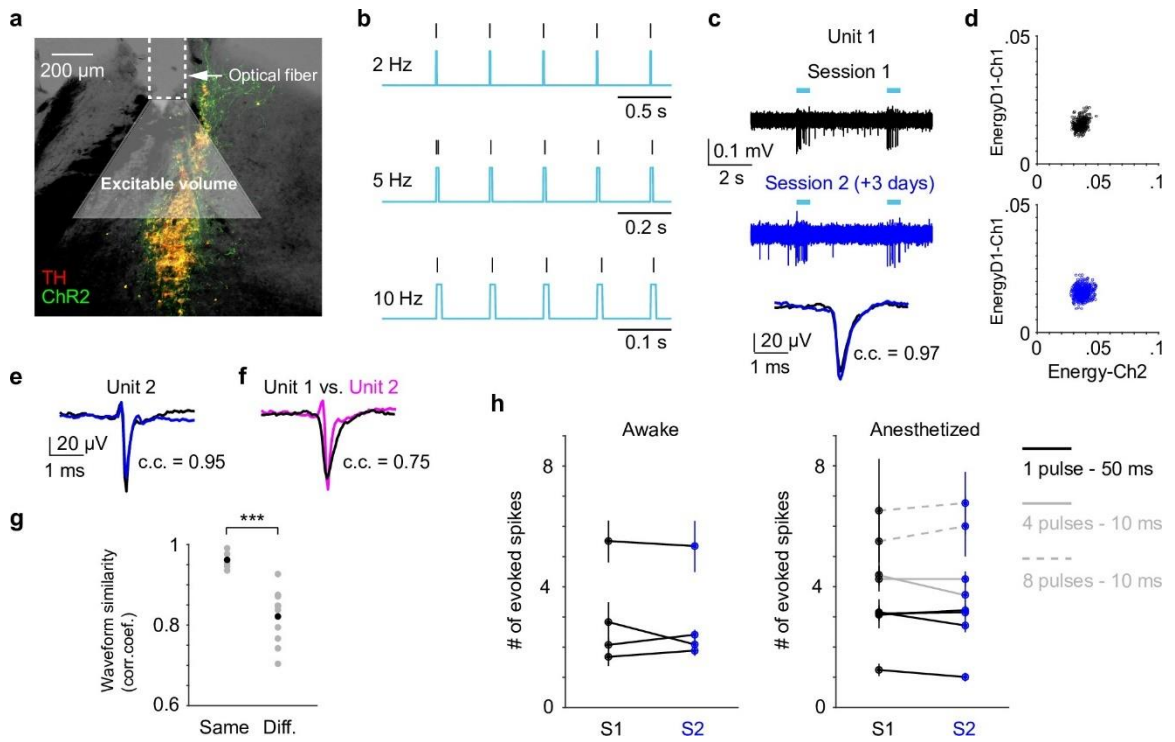
a 200 μm, Optical fiber, Excitable volume, TH, ChR2

b 2 Hz 0.5 s; 5 Hz 0.2 s; 10 Hz 0.1 s

c Unit 1, Session 1, Session 2 (+3 days), 0.1 mV, 2 s, 20 μV, 1 ms, c.c. = 0.97

d EnergyD1-Ch1, .05, 0, .05, .1, Energy-Ch2

e Unit 2, 20 μV, 1 ms, c.c. = 0.95

f Unit 1 vs. Unit 2, c.c. = 0.75

g Waveform similarity (corr.coef.), ***, Same, Diff.

h Awake, Anesthetized, # of evoked spikes, S1, S2, 1 pulse - 50 ms, 4 pulses - 10 ms, 8 pulses - 10 ms

137

Figure 3.10 LC responses to optogenetic stimulation.
*(**a**) Example LC histological section illustrating optical fiber implant and the estimated excitable volume (light gray cone). Estimates were based on 10-mW laser power, 2.5 mW/mm^2 excitation threshold, 1.4 refractive index, and a 30° cylindrical cone. (**b**) Example spiking activity (vertical lines) from an opto-tagged LC unit in response to 10-ms blue pulse trains at different frequencies. (**c**) Example traces (top, middle) and waveforms (bottom) from a putatively same LC unit in response to optical stimulation (cyan bars) in two different sessions (3 days apart). Black and blue indicate an earlier and a later session (sessions 1 and 2), respectively. Waveforms from the two sessions were highly similar with Pearson correlation coefficient (c.c.) = 0.97. (**d**) Spike sorting diagrams corresponding to the two sessions shown in (**c**). The unit was identified in Ch1. (**e**) Waveforms from another putatively same unit in two sessions (1 day apart, waveform c.c. = 0.95). (**f**) Waveforms from the 2 units shown in (**c**) and (**e**) were less similar (session 1 unit 1 vs. session 1 unit 2, c.c. = 0.75). (**g**) Among the tracked 5 units, waveforms from the putatively same units in sessions 1 and 2 (Same) were more similar than waveforms from the putatively different units in session 1 (Different. Same vs. Different, Pearson correlation coefficient (c.c.), 0.96 ± 0.02 vs. 0.82 ± 0.07, mean ± standard deviation (SD), p = 6.6e−4, two-tailed rank sum test). Gray dots: individual pair. Black dots: group mean. (**h**) Responses from the putatively same units to optical stimulation (S1 vs. S2) during awake, non-task performing (4 units, left) and anesthetized (5 units, right) conditions. p > 0.05 for each S1 vs. S2 comparison, permutation test. Evoked spike counts were quantified in response to (1) single 50 ms pulse (solid black line, 4 units); or (2) four 10 ms pulses at 10 Hz (solid gray line, 2 units); or (3) eight 10 ms pulses at 5 Hz (dashed gray line, 2 units).*
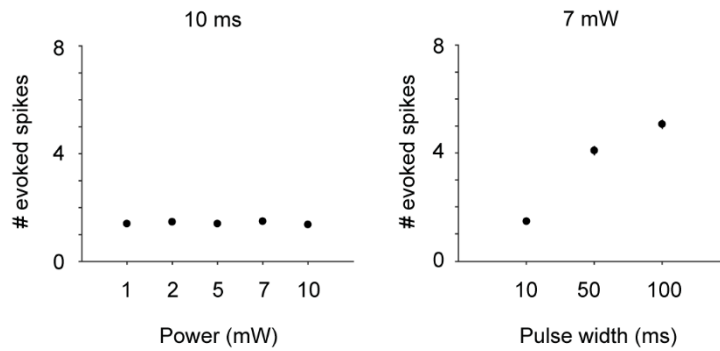
Figure 3.11 The evoked LC neuron responses to varying stimulation parameters.
Number of evoked spikes from an opto-tagged LC unit in response to optical stimulation using different laser power (single 10-ms pulse; Left), or different pulse width (single pulse; Right). Error bars may be too small to be visible.
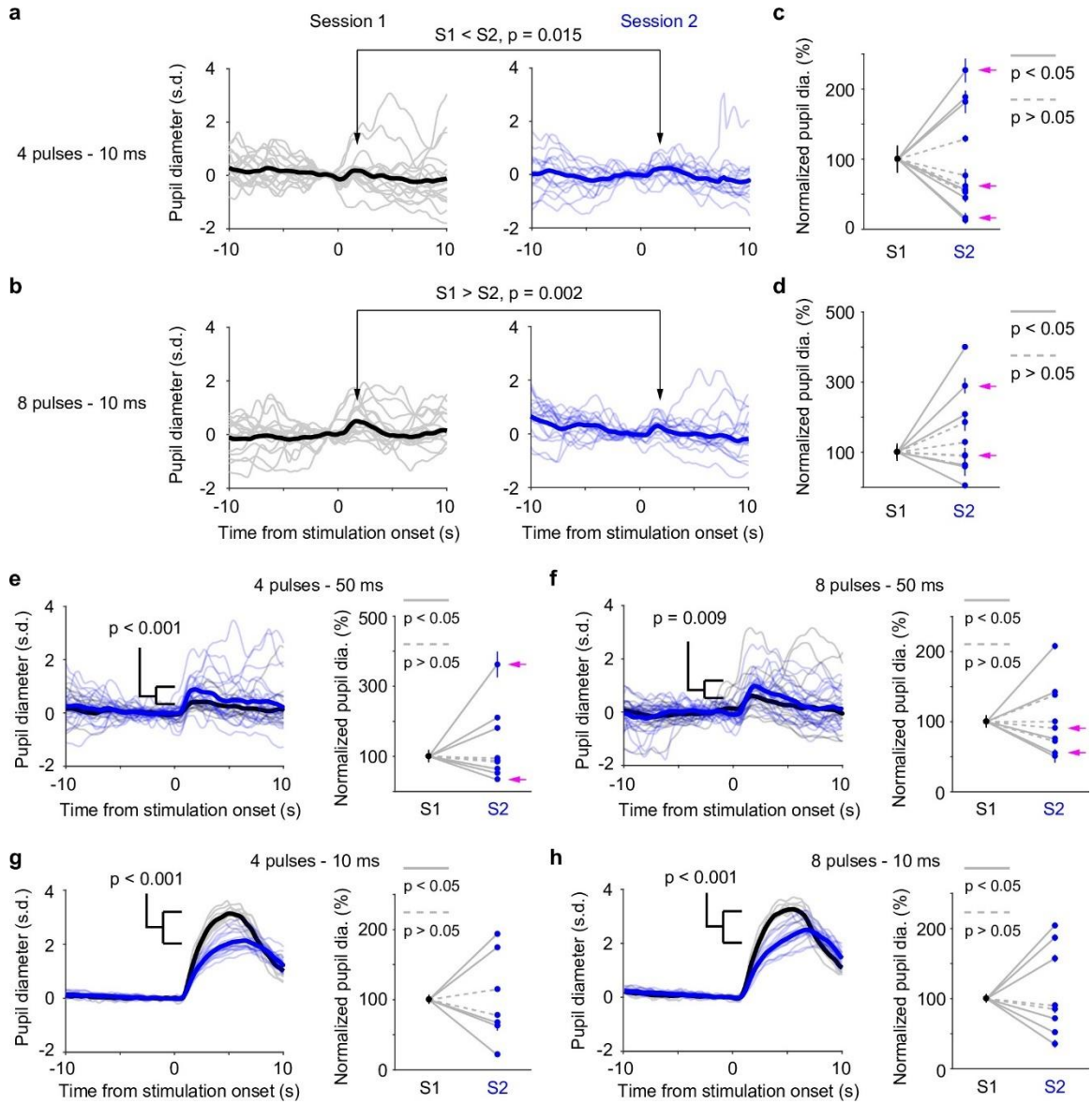
Figure 3.12 Pupil responses to LC optogenetic stimulation.
*(**a**) Example responses from the same pupil to LC stimulation in two awake, baseline pupil-matched sessions (left and right) aligned to the onset of optical stimulation of four 10 ms pulses at 10 Hz. Thin curves: individual responses; thick curves: mean. Baseline pupil diameter S1 vs. S2, 0.71 vs. 0.75 mm. p values were based on permutation test. (**b**) Same as in (**a**), except that optical stimulation was eight 10 ms pulses at 10 Hz. (**a, b**) were from the same recording. (**c**) Group data showing pupil responses to optical stimulation of four 10 ms pulses at 10 Hz in awake, baseline pupil-matched sessions (12 paired sessions from 6 mice). To aid visualization, pupil responses in session 2 were normalized to session 1. Unnormalized data in Fig. 3.14. Dots: mean peak pupil responses. Vertical lines: 95% confidence interval. Solid lines indicate significant difference (p < 0.05, permutation test). Session 1 always preceded session 2. Magenta arrows indicate same-day comparison. (**d**) Group data showing pupil responses to optical stimulation of eight 10 ms pulses at 10 Hz in awake, baseline pupil-matched sessions (11 paired sessions from 7 mice). Unnormalized data in Fig. 3.14. Conventions are as in (**c**). (**e, f**) Left: example pupil responses from one recording. Conventions are as in (**a, b**), except that optical stimulations consisted of 50 ms pulses instead of 10 ms, and that pupil responses from the two sessions were overlaid. Baseline pupil diameter S1 vs. S2, 0.83 vs. 0.80 mm. Right: group pupil responses as in (**c, d**), except that optical stimulations consisted of 50 ms pulses instead of 10 ms. 9 paired sessions from 7 mice in (**e**), and 9 paired sessions from 7 mice in (**f**). Magenta arrows indicate same-day comparison. (**g, h**) Left: example pupil responses from one recording. Conventions are as in (**a, b**), except that the mouse was under anesthesia (2% isoflurane), and that pupil responses from the two sessions were overlaid. Baseline pupil diameter S1 vs. S2, 0.31 vs. 0.35 mm. Right: group pupil responses as in (**c, d**), except that mice were under anesthesia. 7 paired sessions from 3 mice in (**g**), and 8 paired sessions from 3 mice in (**f**).*
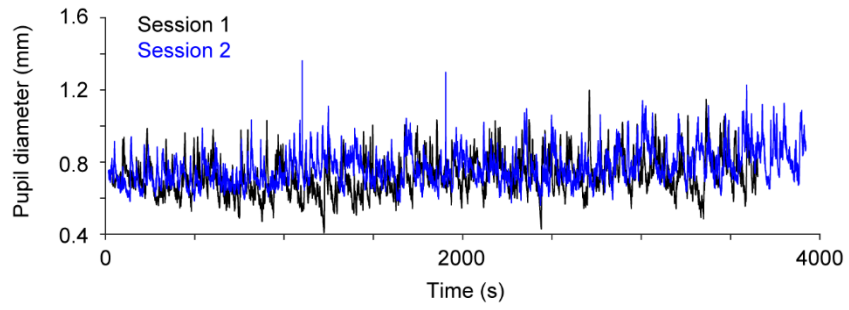
Figure 3.13 Raw pupil traces for the 2 sessions used in Figure 3.12a, b.
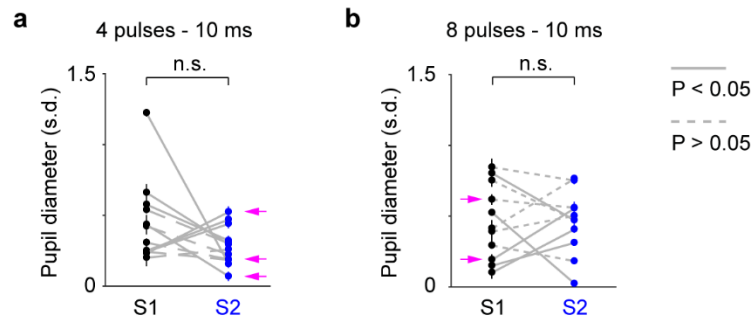
Figure 3.14 Unnormalized group pupil responses as shown in Figure 3.12c, d.
Session-to-session fluctuations were not observable from group comparisons. P = 0.38, n = 12 for (a) and P = 0.63, n = 11 for (b). Magenta arrows indicate same-day comparison.
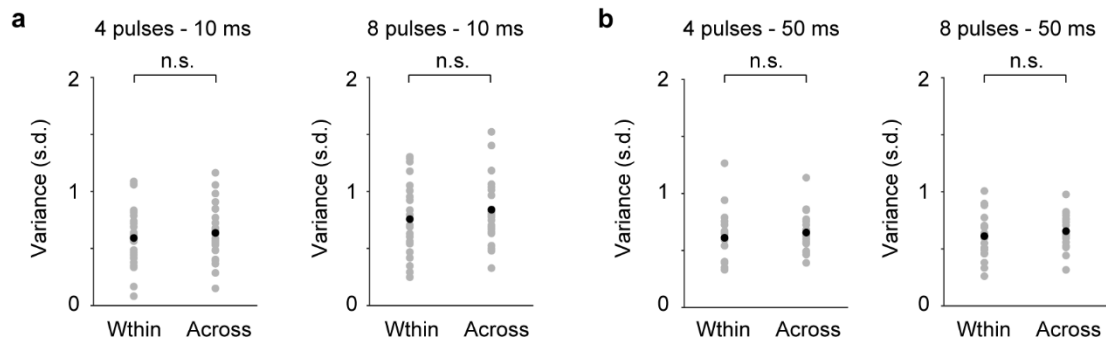
Figure 3.15 The variability of pupil responses to LC optical stimulation within individual sessions (Within) was comparable to that of across sessions (Across) in awake mice.
Across-session variability was estimated by resampling from pooled trials from all sessions in each condition. The repeats of resampling matched the number of sessions in that condition.
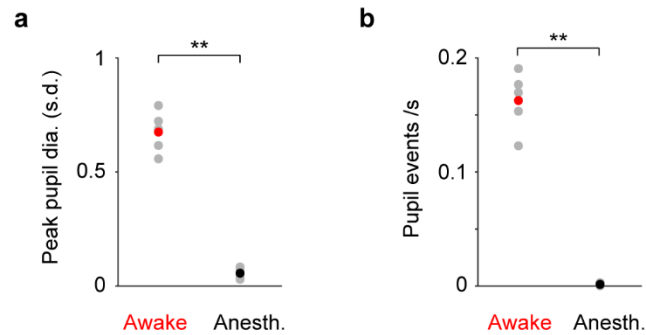
Figure 3.16 Spontaneous pupil diameter in awake and anesthetized mice.
(a) The amplitude of spontaneous pupil dilation events in awake, non-task performing condition was larger than in anesthetized condition (5 sessions from 3 mice in each condition, P = 0.0079, two-tailed rank sum test). Gre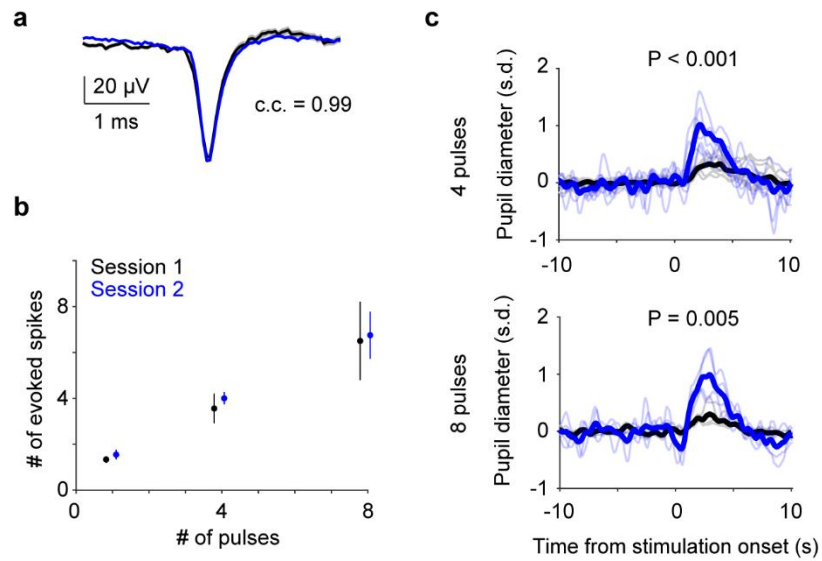y dots: individual sessions. Red and black dots: group mean. (b) The frequency of significant spontaneous pupil dilation events (> 0.3 s.d.) was higher in awake, non-task performing condition than in anesthetized condition (5 sessions from 3 mice in each condition, P = 0.0079, two-tailed rank sum test). Grey dots: individual sessions. Red and black dots: group mean.

Figure 3.17 Example electrophysiology and pupil recordings in two sessions from the same mouse.
Simultaneous recording of an LC unit waveform (a), spike responses (b) and pupil diameter (c) during optogenetic stimulation (10-ms pulse train: 4 pulses at 10 Hz (Top) and 8 pulses at 5 Hz (Bottom) under anesthesia). Baseline pupil diameter S1 vs. S2, 0.34 vs. 0.32 mm.
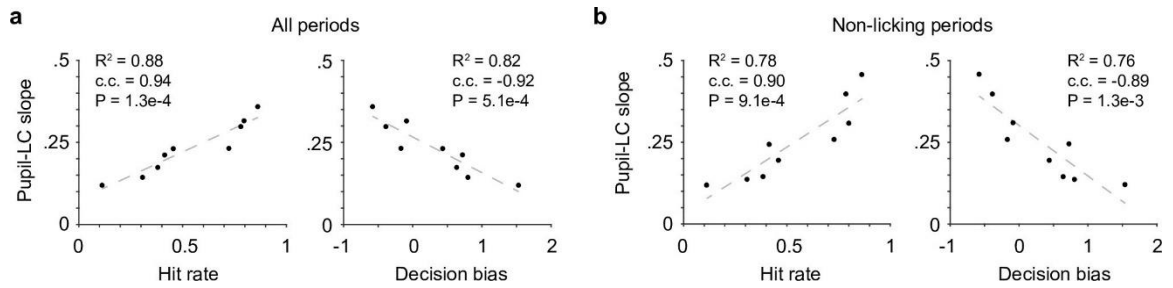
Figure 3.18 Pupil–LC coupling is correlated with decision-bias-related variables.
*(**a**) The variations in the relationship between peak pupil diameter and LC cluster size (linear slopes in Fig. 3.1e) were strongly correlated with Hit rate (left) and decision bias (right, n = 9). c.c., Pearson correlation coefficient. (**b**) The relationships in (**a**) held when pupil–LC slopes were quantified in non-licking periods only.*
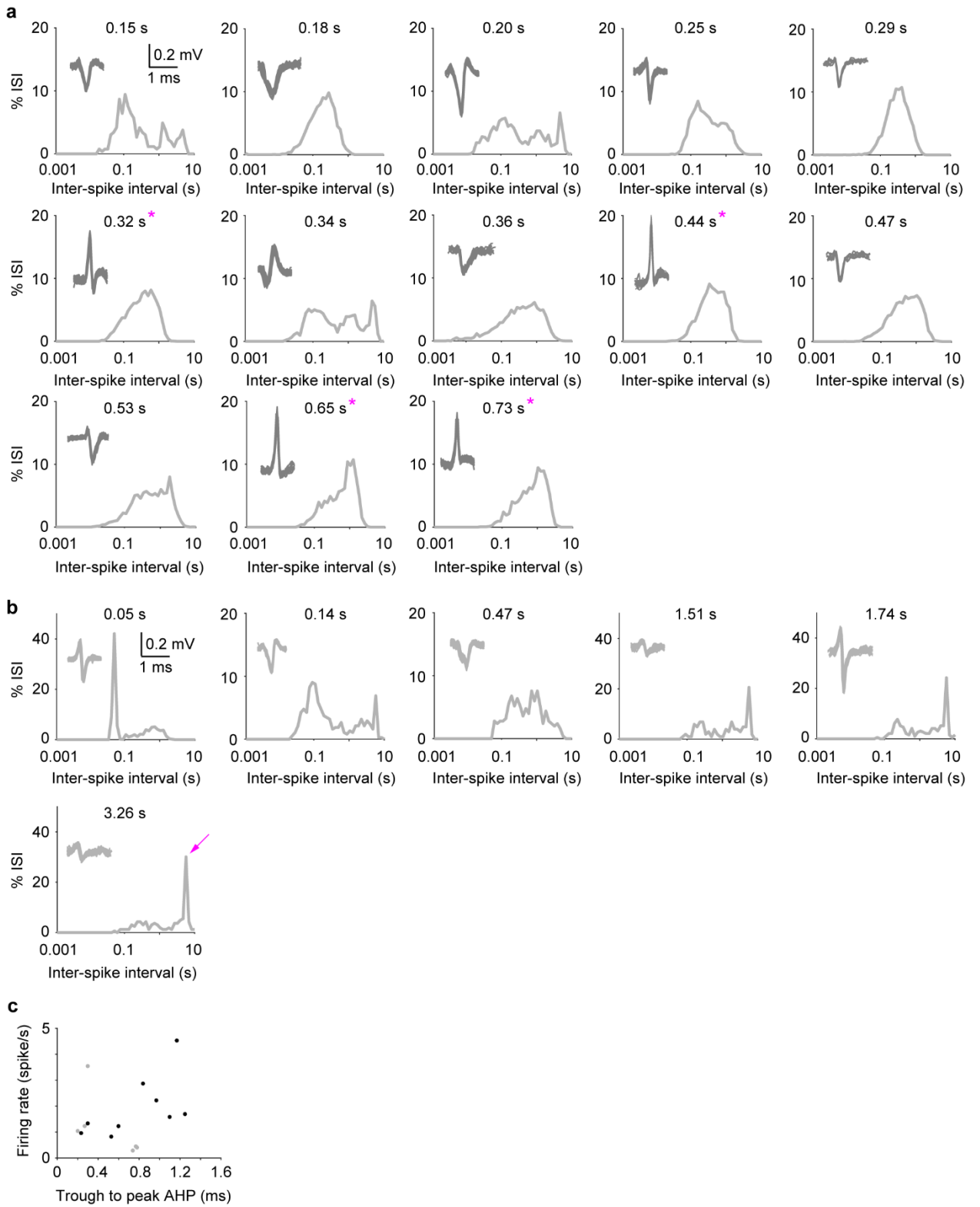
Figure 3.19 Spike characteristics for all LC neurons.

(a-b) ISI distribution and waveform from all recordings, ranked by increasing median ISI. Pupil-LC relationship with $R^2 > 0.6$ (as in Fig. 3.1e) in (a, n = 13), and the remaining in (b, n = 6). All waveforms were plotted on the same scales as shown in the first panel. Each trial lasted 5-6 s, which likely contributed to the peak on the right side of some ISI distributions (e.g., magenta arrow in the last panel of (b)). (c) Average firing rate vs. spike duration (trough to peak AHP). Black dots represent the group in (a), grey dots represent (b). We note that both narrow and wide waveforms were present, supporting recent work (Totah et al., 2018). We did not quantify the width of four waveforms in (a, indicated by *) as their reversed polarity with prominent initial positive deflection indicated that the recording sites were in the more distal axonal or dendritic regions of neurons where mixed-ion capacitive current could become more profound (Gold et al., 2006; Rall & Shepherd, 1968; Sun et al., 2021). Their firing rates were between 1 and 3 spikes/s.